TECHNICAL REPORT STANDARD TITLE PAGE

1. Report No.	2. Government Accession No.	3. Recipient's Catalog No.
FHWA/TX-87/462-1F		

4. Title and Subtitle	5. Report Date
Effects of Repeated Heavy Loads on Highway Bridges	July 1988
	6. Performing Organization Code

7. Author(s)	8. Performing Organization Report No.
Ray W. James, Richard A. Zimmerman, and James H. Loper	Research Report 462-1F

9. Performing Organization Name and Address	10. Work Unit No.
Texas Transportation Institute The Texas A&M University System College Station, Texas 77843-3135	11. Contract or Grant No. Study No. 2-5-86-462
	13. Type of Report and Period Covered Final - September 1985 July 1988
12. Sponsoring Agency Name and Address Texas State Department of Highways and Public Transportation; Transportation Planning Division P. O. Box 5051 Austin, Texas 78763	14. Sponsoring Agency Code

15. Supplementary Notes

Research performed in cooperation with DOT, FHWA.

16. Abstract

A literature study, field study, and a finite-element numerical study were combined to determine the nature and significance of progressive damage due to heavy loads on highway bridges. In the field study candidate bridges and control bridges, identical in design but carrying different levels of truck traffic are compared. Deck damage levels, as indicated by type and density of observed cracking are compared, and to the extent possible, density of observed cracking are compared, and to the extent possible, correlated to the level of truck traffic. In the numerical study, predicted wheel load-induced fracture patterns are identified for various levels of loading.

17. Key Words	18. Distribution Statement
Deck cracking, fatigue, damage, overloads.	No restriction. This document is available to the public through the National Technical Information Service 5285 Port Royal Road Springfield, Virginia 22161

19. Security Classif. (of this report)	20. Security Classif. (of this page)	21. No. of Pages	22. Price
Unclassified	Unclassified	110	

Form DOT F 1700.7 (8-69)

EFFECTS OF REPEATED HEAVY LOADS ON HIGHWAY BRIDGES

by

Ray W. James

Richard A. Zimmerman

and

James H. Loper

Research Report 462-1F
Research Study Number 2-5-86-462

Sponsored by

Texas State Department of Highways and Public Transportation

in cooperation with

U.S. Department of Transportation, Federal Highway Administration

July 1988

TEXAS TRANSPORTATION INSTITUTE
The Texas A&M University System
College Station, Texas 77843

METRIC CONVERSION FACTORS

Approximate Conversions to Metric Measures

Symbol	When You Know	Multiply by	To Find	Symbol
		LENGTH		
in	inches	*2.5	centimeters	cm
ft	feet	30	centimeters	cm
yd	yards	0.9	meters	m
mi	miles	1.6	kilometers	km
		AREA		
in^2	square inches	6.5	square centimeters	cm^2
ft^2	square feet	0.09	square meters	m^2
yd^2	square yards	0.8	square meters	m^2
mi^2	square miles	2.6	square kilometers	km^2
	acres	0.4	hectares	ha
		MASS (weight)		
oz	ounces	28	grams	g
lb	pounds	0.45	kilograms	kg
	short tons (2000 lb)	0.9	tonnes	t
		VOLUME		
tsp	teaspoons	5	milliliters	ml
Tbsp	tablespoons	15	milliliters	ml
fl oz	fluid ounces	30	milliliters	ml
c	cups	0.24	liters	l
pt	pints	0.47	liters	l
qt	quarts	0.95	liters	l
gal	gallons	3.8	liters	l
ft^3	cubic feet	0.03	cubic meters	m^3
yd^3	cubic yards	0.76	cubic meters	m^3
		TEMPERATURE (exact)		
°F	Fahrenheit temperature	5/9 (after subtracting 32)	Celsius temperature	°C

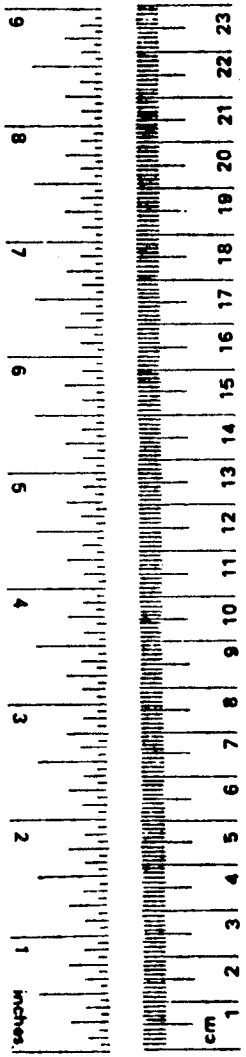

Approximate Conversions from Metric Measures

Symbol	When You Know	Multiply by	To Find	Symbol
		LENGTH		
mm	millimeters	0.04	inches	in
cm	centimeters	0.4	inches	in
m	meters	3.3	feet	ft
m	meters	1.1	yards	yd
km	kilometers	0.6	miles	mi
		AREA		
cm^2	square centimeters	0.16	square inches	in^2
m^2	square meters	1.2	square yards	yd^2
km^2	square kilometers	0.4	square miles	mi^2
ha	hectares (10,000 m^2)	2.5	acres	
		MASS (weight)		
g	grams	0.035	ounces	oz
kg	kilograms	2.2	pounds	lb
t	tonnes (1000 kg)	1.1	short tons	
		VOLUME		
ml	milliliters	0.03	fluid ounces	fl oz
l	liters	2.1	pints	pt
l	liters	1.06	quarts	qt
l	liters	0.26	gallons	gal
m^3	cubic meters	35	cubic feet	ft^3
m^3	cubic meters	1.3	cubic yards	yd^3
		TEMPERATURE (exact)		
°C	Celsius temperature	9/5 (then add 32)	Fahrenheit temperature	°F

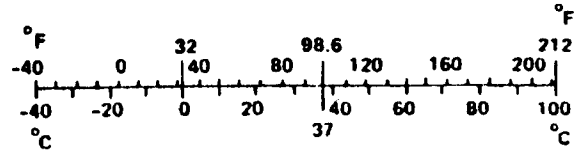

* 1 in = 2.54 (exactly). For other exact conversions and more detailed tables, see NBS Misc. Publ. 286, Units of Weights and Measures, Price $2.25, SD Catalog No. C13.10:286.

TABLE OF CONTENTS

LIST OF FIGURES

LIST OF TABLES

ACKNOWLEDGMENTS

The authors express their appreciation to Mr. Ken Willis of the State Department of Highways and Public Transportation, as well as the many other SDHPT engineers in the various districts who were helpful in planning and accomplishing the field study. Funding was provided by the SDHPT and FHWA, for which the researchers are also appreciative.

The authors are especially endebted to Dr. Howard Furr whose time was generously given and gratefully accepted during the study.

DISCLAIMER

ABSTRACT

A literature study, field study, and a finite-element numerical study were combined to determine the nature and significance of progressive damage due to heavy loads on highway bridges. In the field study candidate bridges and control bridges, identical in design but carrying different levels of truck traffic, are compared. Deck damage levels as indicated by type and density of observed cracking are compared, and to the extent possible, correlated to the level of truck traffic. In the numerical study, predicted wheel load-induced patterns are identified for various levels of loading.

Effects of Repeated Heavy Loads on Highway Bridges

INTRODUCTION

This is a report of a two-year study of the damage caused to highway bridges by heavy truck traffic. As will be discussed, the effects of heavy loading on bridges are most easily observed in the decks, therefore most of the efforts were devoted to the study of progressive damage to reinforced concrete bridge decks. As the primary mechanism of progressive damage to steel bridge superstuctures--fatigue crack growth--is much better understood by bridge designers than are the mechanisms of progressive damage to concrete superstructures, more attention has been given here to the latter problem. The fundamental questions studied are:

1) What types of bridges are most susceptible to heavy load-induced damage?
2) Which bridge components are most susceptible to heavy load-induced damage?
3) What are the manifestations of heavy load-induced damage?
4) What other mechanisms cause damage to bridges, and in what ways do these mechanisms interact with repeated heavy loads?
5) Can progressive damage related to repeated heavy loads be quantified and correlated to the level of overloading?

As will be shown, not all these questions can be answered completely. The results of the present study will, however, provide additional insight into the issues raised by these questions.

REVIEW OF THE LITERATURE

The effects of overloads on bridges are of interest due to: (1) the uncertainty of the exact nature of damage specifically from overloads, (2) the increasing concern over bridge deterioration and maintenance, (3) increasing volume of traffic, and (4) political pressure to increase the maximum legal truck axle and gross weights.

The specific nature of damage due to overloadings is difficult to isolate since there are many other factors which damage bridges and which may interact with overload effects. These may include fatigue or progressive damage caused by repetitive application of legal loads, corrosion, thermal stresses and shrinkage cracking. Even if other factors are eliminated as sources of damage, little is known of the precise mechanisms for the type and degree of deterioration to a bridge by an overload. As the load path through the structure accommodates overstresses, damage may occur in a variety of elements from the bridge deck to the stringers or girders to the pile caps and bents. This damage may appear through increased deck deterioration in cracking and spalling, accelerated crack growth in stringers, floor beams, diaphragms, bearings, expansion joints and other connections, reduced fatigue life of structures, increased deterioration of foundations, and, ultimately, collapse of the bridge. Due to this complex interaction between bridge members and many different sources of damage, it is difficult to correlate the variations of each bridge's construction and an exact load with a specific type and amount of damage as a bridge deteriorates. The goal of this study is to clarify the most probable locations and nature of damage due to overloads and the effects of this damage on bridge service life in order to improve the efficiency of bridge maintenance and design decisions.

Proper bridge maintenance has become increasingly important since the U.S. highway system as a whole is aging, with thousands of bridges requiring significant repair work or replacement. This is a reflection

of the building program in past decades as a rapidly growing number of bridges approach the termination of their service lives. Bridge condition must be monitored, because as bridges deteriorate, their strength may be reduced such that the original design vehicle will cause further deterioration at unacceptable rates. As costs for bridge maintenance also rise, there is an increasing need for efficient allocation of resources which, in turn, requires a better understanding of bridge deterioration to facilitate planning.

The increasing volume of traffic further exacerbates the problems presented by aging and overloads. There may be not only an increasing amount of traffic on a bridge, but also an increasing percentage of overweight vehicles. Bridges are then presented with the problem of carrying greater loads and traffic volumes as they deteriorate.

The effects of overloading or overstressing bridges have been studied for a number of years. A sample study by Kostem of 1277 trucks in Pennsylvania in 1977 found, for example, that overloading is frequent, occurring for up to 20% of the five-axle trucks and extreme overloading occurred for about 1% to 3% of the five-axle trucks. A detailed examination of the five-axle truck data showed that there were violations of legal limits for steering and driving axles by 1.6% of the trucks, of limits for trailer axles by 6% of the trucks, of limits for single axles by 25.2% of the trucks, and of limits for gross vehicle weight by 20.8% of the trucks. Overweight vehicles exceeded legal limits substantially in several different weight categories (Table 1). Even though the legal limits have been raised since this Pennsylvania study was conducted, with current standards the measurements would still be substantial violations of load limits.

Table 1. Comparison of Measured and Legal Maximum Weights

Weight Category	Measured maximum weight kips (kn)	Percent of legal limit	Legal limit kips (kn)
Steering & driving axle	90 (400)	154	58.4 (260)
Trailer axle	70 (311)	194	36.0 (160)
Single axle	45 (200)	250	18.0 (80)
Gross vehicle weight	125 (556)	171	73.0 (325)

According to measurements of truck movements in Texas as reviewed by Cervenka and Walton (1984), the traffic stream contains between 1.4 to 58.2 percent truck traffic with an average of 16.8 percent truck traffic. The percentage of overweight trucks has increased with a large change between 1974 and 1976 in which the percentage of overweight trucks went from 7.75 to 26.33 percent of the truck traffic. Since 1976 the percentage of overweight trucks has remained between twenty and thirty percent of the truck traffic. The increase was observed even though the number of weigh stations was decreased, thus it seems likely that the cause was a combination of several factors. Most importantly, Texas switched from static weighing to weigh-in-motion (WIM) scales. The WIM scales are able to handle much higher volumes of traffic and are more difficult to evade since they are more difficult to detect. Also, fuel costs rose and speed limits fell, raising trucking costs and increasing the economic incentives of overloading. Furthermore, as traffic patterns change, new vehicles may appear (Kostem 1977) which differ from the design vehicle with respect to characteristics such as the total weight and axle spacing. Such vehicles may weigh less than the design vehicle, yet still violate the original bridge design standards because the load is concentrated over a smaller area than originally assumed.

Along with the problems of bridge aging and changing traffic, the continued interest in raising legal load limits to reduce

transportation costs must be considered when evaluating bridge service lives. If new limits are approved, they will necessitate a re-evaluation of most, if not all, current bridges. Even if old bridges will support new legal loads, the safety factor of the original design and its margin for error will be reduced. More bridges will require posting. Increasing legal loads will then lead to a need to more closely monitor bridges with posted load limits, since violation of posted limits will still continue and the probability of damage due to greater loads will increase. Deliberate violation of such posted limits occurs because of driver rationalizations of the inconvenience of a detour from a previously safe route and the "negligible" consequences of violating posted limits. Therefore, because of the continued interest in increasing the maximum axle and gross weights and concern over the impact this might have on our aging transportation network, it would be wise to know the effects of higher loads before implementing greater legal limits.

The current definition of maximum legal load for the nation was established with the Surface Transportation Assistance Act (STAA) of 1982. This act established vehicle size and weight limits for the use of the National System of Interstate and Defense Highways, and as the guideline for state vehicle size and weight limitations in order to maintain compliance with federal funding assistance regulations. STAA requires that the maximum gross weight allowed by any state for vehicles on the interstate highway system, including enforcement tolerances, be 20,000 lbs carried on a single axle, 34,000 pounds carried on a tandem axle, and an overall maximum gross weight on a group of two or more consecutive axles in compliance with the following formula :

$$W = 500 \left(\frac{LN}{N-1} + 12N + 36\right) \qquad (1)$$

...where W is the overall gross weight, L is the distance in feet between the extreme of any group of two or more consecutive axles, andN equals the number of axles in the group under consideration, with the exception that two consecutive sets of tandem axles may carry a gross

load of 34,000 lbs each providing the overall distance between the first and last axles of such consecutive sets of tandem axles is 36 ft or more. This formula governs the weight of vehicles up to a gross weight of 80,000 lbs; any vehicle and load in excess of this limit requires a special permit in accordance with applicable state laws.

Although in 1975 the maximum gross vehicle weight was raised to 80,000 lb, the maximum single axle weight to 20,000 lb, and the maximum tandem weight to 34,000 lb, Texas law was not in full compliance with STAA provisions for observance and enforcement. Effective September 1, 1983, the state legislature brought Texas truck size and weight regulations into full compliance with STAA provisions through House bill numbers 691 and 1114. These bills extended enforcement of the STAA weight limits to state-maintained highways inside incorporated city limits so that the entire state system complied with the STAA. The Texas legislature additionally specified that no vehicle should have a weight greater than 600 lbs per in. width of high-pressure tires or a weight greater than 650 lbs per in. width of low pressure tires concentrated upon the highway surface. Additionally, no wheel should carry a load greater than 8000 lbs on high-pressure tires and 10,000 lbs on low-pressure tires. Also, no axle should carry a load in excess of 16,000 pounds on high-pressure tires and 20,000 lb on low-pressure tires. For the purposes of this study, an overload is thus defined as any load exceeding these legal criteria with interest concentrated on single axle, tandem axle and gross vehicle weights.

Proper assessment of the influence of overloads on bridge damage requires the location of regions and routes likely to be subject to overloading and an attention to changing traffic patterns along those routes. Special-use trip matrices, such as those used by Texas Transportation Institute (TTI), may be used to pinpoint areas where heavy normal or special-permit loads are probable. Of special concern are sources of heavy loads, such as timber, sand, gravel, and other earth materials, which may change as sources are exhausted and opened for use and the destinations of these materials change as major construction areas open and close. Furthermore, attention should be

addressed to special permit loads such as for heavy construction, gas or oil field equipment. These loads may require special conditions to traverse a bridge, such as reduced speed, isolated presence on the bridge, and centering on the longitudinal axis of the bridge rather than in one lane. The matrices make it possible to locate the bridges within the radius of influence of specific industries to select bridges on routes most likely to be traversed by those industries' loads and to determine which bridges may be most susceptible to damage.

Weight data for Texas is collected by a series of permanent and portable weigh stations across the state. The weigh program is changing to reflect changing traffic patterns, with new stations being added to the nine permanent stations in service currently on the Texas highway system. A total of twenty-six stations has been recommended in a report by Maxwell et al. (1986), which also established a distribution of sites across the state to measure truck traffic variations dependent upon region and road classification. Although the WIM system has an error margin of only 1000 lbs, the number of stations required to ensure statistical accuracy of statewide data to that accuracy level was sixty. The selected number of twenty-six weigh stations was based on an error margin of 1500 lbs. The stations are being allocated for each region in Texas according to the percentage of truck traffic and the type and amount of roadway mileage found in each region.

Typical equipment for a WIM site as used by the Texas State Department of Highways and Public Transportation can detect vehicle speed to the nearest mile per hour, axle spacings accurate to the nearest foot, axle weights accurate to the nearest 2000 lbs, and gross vehicle weight accurate to the nearest 2000 lbs. The system can also provide an analysis of the vehicle's conformity to legal load limits for the single axle, tandem axle and gross vehicle weights.

MANIFESTATIONS OF DAMAGE

In attempts to identify traffic-load induced damage, various field

observations and field tests have indicated that bridge damage under loading normally initiates as deck cracking and later may be evidenced by cracking in other parts of the structure.

Slab Damage

One of the primary modes of failure is thought to be flexure, regardless of what type of girder supports the bridge deck, in which the first signs of overload distress appear in the form of flexural cracking in the deck concrete (Kostem 1977, 1978, 1983, 1985). Kostem (1985) concluded that, as a result of observed overload behavior, the best measures of superstructure damage for bridges with prestressed concrete I-beams are cracking of the deck concrete and cracking in the concrete cover over the beam prestressing strands. Overload-induced stress changes in the deck reinforcement and beam prestressing strands were not large enough for use in measurement of the structure's damage. Although transverse cracking often occurs first (Darroch and Furr 1970; Kostem and Ruhl 1982; Kostem 1983, 1985), longitudinal cracking may also occur under wheel loads over beams as deck damage is influenced by the unequal deflection of the beams. Whether cracking initiates in the slab or beam is said to depend on the lateral distribution of the load; the lower the actual lateral distribution, the more likely it is that deck damage will initiate before beam damage (Csagoly et al. 1978; Kostem 1976, 1977, 1983).

The flexural damage may manifest itself as cracking in the deck slab concrete cover over the reinforcing bars under loading. After passage of the load, the cracks close as the beams and slab return to their unloaded state (Kostem and Ruhl 1982). Additionally, longitudinal deck cracking may occur on the lower surface of the slab near the mid-spacing of the beams, possibly initiating near the loading on the upper and lower slab surfaces near the top flanges of the beams (Kostem 1985). Negative bending of the deck slab over the beam flanges was not necessarily where the first cracking occurred (Kostem 1977).

Kostem (1977) explains that after flexural damage begins in the

deck slab, damage may spread over a large area and through the slab depth after the bridge is subjected to additional or heavier loads. In other studies (Kostem 1976) it was determined that, for beams and slabs, critical bridge loading occurred as the midspan of the bridge sustained the maximum bending moment. As loads increase (Kostem 1985), unloaded portions of the deck slab develop more widespread shallow cracking rather than deepening of existing cracks. Only as the level of overloading increases do the initial cracks deepen.

Continuing research which has been incorporated into the Ontario Bridge Design Code has indicated that for reinforced concrete bridge decks, the mode for failure is not flexure but punching shear. It appears that current bridge deck designs are also substantially stronger than necessary, since the punching shear failures occur at loads at least six times heavier than the original design load. In some tests, such as those conducted by Csagoly et al. (1978), failure did not occur until up to ten times the legal load or five times the maximum legal half-axle weight. The explanation for this is thought to be the presence of large in-plane compressive forces due to the restraint of the bridge deck's expansion under loading. These compressive forces may sufficiently increase the flexural capacity of the deck so that the controlling factor becomes punching shear (Csagoly et al. 1978; Beal 1982).

It is suggested here that the mechanisms of progressive damage governing servicability limits are related to deck flexure, even though the ultimate capacity may be governed by shear punching.

Beam Damage

After substantial damage to the deck occurs, beam deterioration begins. This appears as flexural cracking, especially at midspan (Peterson and Kostem 1975; Kostem 1977, 1983), or as shear failure at the interface of the deck and beam. Shearing damage has been found to be a factor primarily in short spans where the controlling parameter is the maximum wheel load and axle spacing, not the gross vehicle weight

or axle weight. In short span bridges with deep beams, beams fail due to the interaction of shear and flexure at high loads (Kostem 1977). In short spans supporting heavy axle loads, Kostem (1976) reported that large shear stresses may result when the axle is near a support. Loads causing this type of shear damage could also cause flexural damage when located at the midspan of a bridge, revealing that the location and magnitude of a load must be examined when determining the type of damage, shear or flexural, which might result. In spans less than 40 ft, Kostem and Ruhl (1982) observed that the initiation of damage was equally likely to result from either interface shear between beams and the deck or cracking of the deck slab. After substantial deck damage, interface shear failure may occur between the slab and beams before flexural cracking of the beams and is most likely to occur near supports (Kostem and Ruhl 1982; Kostem 1977, 1983). In shorter spans of less than 25 ft, it was found that damage could initiate through tension in the beam web at the support as well as by shear at the beam-web interface. Kostem (1984) found that interface shear damage between beams and slabs was rare in comparison to flexural damage. In longer bridge damage the primary type of damage observed was deck slab cracking.

Foundation Damage

The progression of overload damage from the deck and beams to bents and foundations is very uncertain and difficult to quantify. As settlement commonly occurs in all structures over a period of time anyway, the amount of foundation damage specifically attributable to overloading is undetermined. Substructure movements usually result from movement of approach embankments or foundations, poor performance of pile foundations, and horizontal movement of abutments--all problems that may occur due to the dead load of the structure alone (U.S.D.O.T. 1982).

In an examination of arch structures of currugated metal and compacted soil, Kay and Flint (1982) observed that some settlement due

to overloadings is possible. Over half of the permanent deflection of the structure was related to the passage of 77 ton vehicles. No significant damage was observed, with a total permanent deflection of about 65 in. after the opening of the structure. Passage of an additional vehicle weighing 319 tons after the initial settlement period caused a further deflection of only 0.2 inches. While a perceptible deflection was noted, this was not enough to affect the structure's integrity, especially since the damage was uniform over the entire bridge and was not a differential settlement.

In other investigations conducted by Boley and Higginbotham (1984), it has been noted that bridge damage involving pier foundations may have been worsened by the passage of heavy vehicles with respect to the slope stability, but the exact contribution from overloads was unidentifiable.

Hartley et al. (1985) used a finite element model of piers to analyze their cracking in a twenty-three year old, three span continuous steel girder bridge supporting a reinforced concrete deck. Normal dead and live loading and extra heavy live loads were included among the potential causes of damage to be investigated. Even considering two 100 kip concentrated loads applied in one lane, the conclusion was that live loading did not produce the stresses which caused the piers to crack.

Some settlement may be attributable to heavy live loads, but apparently not enough to be significant. Even if overloads cause permanent deflection of foundations, the amount of differential settlement does not appear substantial enough to cause significant damage. Bridge structures may adequately handle one to three inches of differential settlement without severe problems; and, it is uncertain how much, if any, of that may be caused by overloads (Boley and Higginbotham 1984, U.S.D.O.T. 1982).

MECHANISMS OF DAMAGE

Numerous mechanisms may cause deck cracking either individually or

in combination. Each of these may initiate cracking, and, except for shrinkage, each may widen and extend cracks during the bridge's useful service life. The difficulty in specifying the influence of overloading on bridge damage stems in part from this interaction of different mechanisms. Although it is beyond the scope of this study to present a full investigation of each damage mechanism, a brief review will be presented.

Construction

Crack initiation may begin with the original bridge construction as shrinkage cracks form in the concrete. These may provide initial locations for cracking to propogate as initial shrinkage cracks 'breakout' due to stresses from loading, thermal or corrosion stresses.

Poor quality control of construction material and practices will naturally contribute to later damage by creating local defects and weaknesses in the structure. Concrete cracking may occur due to a variety of factors: shrinkage, settlement, incorrect placement of reinforcing steel, improperly mixed concrete, use of reactive aggregates or vibration of recently poured concrete.

Kostem (1985) investigated some of the effects of substandard materials as well as their interaction with damage by aging by examining the effects of the loss of all concrete cover over reinforcing bars and reduced concrete strength. For reduced strength concrete alone, loads initiating and propogating cracks were reduced 12%; the corresponding load levels for beam cracking were reduced 2%. For loss of all cover, deck cracking and penetration through half the slab thickness occurred at 80% of the loads that would cause similar cracking in an undamaged deck. Likewise, beam cracking intiated at 90% of the load that caused cracking in decks with normal concrete cover. The combination of loss of concrete cover and weaker strength concrete (13% below design strength) reduced load levels 30% below that required to initiate and propogate deck cracking in sound decks. In beam analysis, the corresponding beam cracking loads were reduced 12%.

Accidents

Bridge damage sometimes results from accidental impact truck or ship traffic. Bridge girders are frequently damaged by overheight vehicles, resulting in local cracking and spalling of concrete, or plastic deformation of steel members. Traffic accidents may cause severe damage requiring immediate repair or replacement of bridge members, but unattended damage does not appear to be frequent or severe enough to be a major factor contributing to overloading damage.

Flooding

Flood damage to bridges is one of the most significant causes of bridge failures. Although usually not causing deck damage directly, any movement or weakening of the foundations does in turn increase the structure's overall vulnerability to loading damage. In examining cases of scouring, Davis (1984) reported flooding as a prominent problem since about 85% of the bridges in the National Bridge Inventory System span waterways. In studies conducted in the 1970's, scour damage at piers and abutments was found to be the predominant damage resulting from floods, with additional damage to riprap and erosion of abutment slopes also occuring. Annual losses from flood damage were estimated at approximately 75 million dollars. Flooding has not been identified as a major factor contributing to overload damage though, since flood damage often requires immediate remedial action and is not unattended long enough for significant interaction with overload damage to occur. Because of recent failures there is increasing awareness of the danger of scour, which may reduce the capacity of a pier at high flow while leaving no evidence of the danger when the high flow rates subside.

Corrosion

Corrosion is a problem for any steel in a bridge, whether it is the reinforcing steel within the concrete, steel members, connections or bearings. Corrosion of reinforced steel, while reducing the cross-sectional area of the steel, causes the most serious damage to concrete decks because the products of corrosion occupy many times more volume than the steel; and the resulting expansion leads to cracking, delamination and spalling of the concrete cover. Corrosion of steel bridge members also leads to embrittlement and corresponding increased susceptibility to cracking and to increased moments induced in the structure due to freezing of bearings. While an important design factor in providing good corrosion protection is the amount of concrete cover over the reinforcing bars (Csagoly et al. 1978, Leslie and Chamberlin 1980), corrosion of the reinforcement may occur even in uncracked, high quality concrete. The presence of cracks naturally facilitates the entrance of water, oxygen and chloride ions which accelerate corrosion (Leslie and Chamberlin 1980). Cracking due to corrosion can weaken the deck, increasing the possibility of loading damage. Reduced fatigue strength has been associated with corrosion in previous studies (Tilly 1978). As loads extend a crack, this in turn increases the area of reinforcing steel vulnerable to corrosive attack and increases the likelihood of greater corrosion damage.

Thermal

Thermal effects in concrete bridges have been blamed for cracks in bottom slabs and girder stems of box-girder bridges. Imbsen and Vandershaf (1984) have confirmed that this problem is mostly observed in large, prestressed concrete bridges. Stresses have been noted to increase significantly with a small increase in temperature; Tilly (1978) observed that an increase in stresses of 100 percent has been found for a corresponding asphalt temperature increase of 63F (17). Thermal effects have also been associated with cracking at joints, especially in concrete bridges (TRRL 1982).

TRAFFIC-RELATED MECHANISMS OF DAMAGE

Significant bridge damage may result from a wide variety of causes such as those previously cited, but these are only secondary problems in this study. Of primary interest is traffic-induced damage to bridges attributable to overloading. Because traffic also causes damage through dynamic factors and fatigue even when overloads are not a factor, these factors will be briefly discussed along with the problem of overloads.

Dynamic Loads

Dynamic impacts of loads on a bridge are a function of pavement roughness on the approach and on the bridge, vehicle speed, and the presence of other vehicles on the bridge (Wheeler 1984; Peng 1984). Uneven pavement on a bridge approach may essentially 'launch' a vehicle at the approach span of the bridge, increasing damage at the approach joint and span. Dynamic load factors which may relate to the behavior of a bridge "include...vehicle body 'heave' and axle 'bounce' frequency compared to the bridge resonant frequency, the ratio of the vehicle and bridge masses,...vehicle axle spacing, vehicle suspension damping, bridge damping, tire behavior and inflation level." (Wheeler 1984)

Movement at a joint may be related to either traffic or thermal stresses from expansion and contraction. "On composite structures having comparatively low longitudinal deck stiffness, the cracking was induced mainly by traffic loading, but on the stiffer concrete decks, it was mainly due to thermal movement" (TRRL 1982). Deterioration usually starts in the wheel tracks at a joint and then propagates across the roadway. Without repair, the result is multiple cracking and spalling.

Fatigue Loads

Truck traffic has long been associated with bridge fatigue damage

(Fisher and Mertz 1980, 1984; Koob et al. 1984; Fisher et al. 1983). Field observations have revealed fatigue cracking in coverplated bridges supporting a high volume of heavy truck traffic (Fisher et al. 1978). While all types of trucks produce similar patterns of stress variation, the magnitude of the variations changes according to the loading (Fisher et al. 1976).

Under repeated loadings, fatigue crack propogation in steel superstructures may occur at low stress ranges, especially if occasional higher stress ranges also occur (Koob et al. 1984). An increasing incidence of fatigue cracks has been noted for welds on main girders of bridges with concrete decks, with the conclusion that gross vehicle weight is the cause for the damaging stress ranges in main girders (Tilly 1978). Because of the better understanding of repeated loadings on steel structures, the effects of repeated loading on concrete will be addressed here.

Repetitive loadings affect the fatigue life of the concrete slab as well as the steel bridge members. Japanese tests on concrete bridge decks conducted by Okada et al. (1978, 1984) indicate a load carrying capacity greater than three times the design load, yet field observations indicate that service wheel loads are very significant to slab fatigue damage. Design wheel loads of 24.3 kips (108 kN) over an area 7.87 by 19.69 in. (20 by 50 centimeters) were found to cause flexural cracks on the bottom surface of reinforced concrete slabs supported by steel stringers, with load movement causing grid-like crack patterns to form. Application of test loads in this study caused tensile stresses of approximately 157 psi (1080 kPa). After a finite number of loading cycles, the amount of cracking--the crack density--approaches a constant value, and the generation of new cracks declines. Furthermore, after a certain amount of propogation, with increasing cycles, rather than continuing to propogate lengthwise, the cracks extended through the depth of the concrete. Abrasion was also confirmed to occur as, with more load repetitions, the amount of falling material increased and cracks fully penetrated the deck.

Okada et al. (1978) tested seven full-scale slabs with static

loads, central pulsating loads, and moving pulsating loads to study the fatigue failure mechanism of reinforced concrete slabs supported by steel beams. Static load was applied to the point of collapse on a new slab and an old slab which had experienced actual traffic loads. The new slab showed good agreement with the collapse load as predicted by punching shear equations, failing at 97% of the predicted collapse load. The older slab showed a reduction in strength from its previous loadings, with collapse occurring at a load which was only 72% of that predicted for collapse. Under the central pulsating load, cracks initally formed under the load and radiated outward along the slab's bottom surface. As the application of load cycles progressed, crack propogation occurred along the line of the principal moment. With a moving pulsating load, a grid-like crack pattern was formed on the bottom surface of the slab. Results confirmed that abrasion occurred under moving loads as crack surfaces rubbed together. When this opening was penetrated by water, deterioration was accelerated. Crack growth consisted of the initial formation of flexure cracks on the slab's bottom surface under wheel loads, followed by the formation of twisting cracks on the slab's upper surface as loads were removed. Under the pulsating loads comparing the behavior of old and new slabs, only the old slabs collapsed. Work performed by Kato and Goto (1984) indicates that wheel loads great enough to cause abrasion, regardless of whether they initiated or propogated cracks, combine with shrinkage cracks and water infiltration as the primary mechanism of deterioration of concrete bridge decks. Opening and closing of cracks in the deck concrete may involve bond slip of reinforcement. Stress concentrations occur at tips of bending cracks on the neutral plane where transverse shear occurs, and at tops of bending-sections where twisting occurs. Full crack penetration through the slab appears to be due to the alternation of stress concentrations due to transverse and twisting shears (Okada et al. 1984). The Japanese tests on reinforced concrete deck slabs have found further support in U.S. tests by Csagoly et al. (1978), who also observed that hairline cracks may open as a load is applied and subsequently close as the load is removed; and, that as

movement of the load occurs, grid-like crack patterns form.

Crack propogation in steel girders often reflects a cycle of fatigue-brittle fracture, indicating slow growth of a crack due to fatigue, followed by a brittle fracture caused by a particular load or event, followed by continued fatigue growth. This cycle continues until the member is fully cracked, repaired or replaced. Fatigue cracking in steel bridge members frequently initiates due to out-of-plane distortions in a small gap and large initial defects and cracks in the steel members or the weld material, especially low fatigue strength details (Fisher and Mertz 1984). Most fatigue cracks are associated with welds, either at weld toes or weld terminations near a stiffener or other attachment; the location of the detail influences the susceptibility to fatigue (Fisher et al. 1976). Some examples of common locations are the ends of cover plates and at joints and ends of stiffeners, especially in areas carrying tensile stresses or stress reversals (Barsom 1984; TRB 1981). Cracks often initiate within the weld metal and frequently propogate through the base metal into the bottom flanges and girder webs. While the type of attachment may be a factor involved in fatigue due to its nature and location, the length of the weld attachment also significantly influences fatigue cracking (Fisher et al. 1978).

In seeking to identify the traffic causing the fatigue damage in steel girders, a New York Academy of Sciences study (Fisher 1980) found that, if it is assumed that damage occurs when strains are greater than 75% of maximum strain, then about 13% of 5-axle trucks or grouped 3- and 4-axle trucks cause damage. Stress ranges in main girders appear to be caused by gross vehicle weight (Tilly 1978). Results from the AASHO Road Test and lab fatigue tests indicate that the stress range is the only significant factor governing fatigue resistance of cyclically loaded structures (Fisher and Mertz 1980).

In addition to bridge decks and girders, fatigue crack growth has commonly been found in secondary members such as diaphragms. Either wind or traffic loads may cause this damage by inducing resonant vibrations of lightweight attachments (Tilly 1978).

Fatigue is a substantial contributor to overload damage in both concrete decks and steel girders. Once a fatigue crack propagates a finite distance, lower stresses become damaging and may propogate the crack. Stress range appears to be the only significant factor in the fatigue resistance of cyclically loaded structures (Fisher and Mertz 1980).

Overloads

Considerable work has been performed to determine the levels of damage that occur as loads approach the ultimate capacity of a bridge. From field observations it appears that damage associated with loading is clearly related to truck traffic. Damage to decks and beams has been found to be greater under lanes containing most truck traffic (Fisher et al. 1978; Fisher and Mertz 1980). In several studies truck loadings have also been linked to the levels of stress necessary to cause damage (Peng 1984; Kato and Goto 1984; Okada et al. 1978, 1984; Tilly 1978; Fisher and Mertz 1980; Fisher et al. 1976; Kostem 1977, 1985). Fisher and Mertz (1980) found accelerated cracking under truck lanes (i.e. right lane) mainly due to 5-axle trucks or grouped 3- and 4-axle trucks. The fraction of truck traffic causing damage has been noted to involve as little as one to three percent of the truck traffic (Kostem 1977). In further observation of the stresses experienced by bridges supporting this traffic, the average stress was found to be about 1 ksi, confirming that bridges tend to be understressed. However, while stresses were at or below 1 ksi about half of the time, there were recorded stresses of up to 6 ksi.

Jorgenson and Larson (1976) tested a ten year old, three span, cast-in-place, two-lane roadway, reinforced concrete slab bridge by loading it to collapse while measuring deflections under loads. The load causing the first permanent set was found by calculating the slab yield moment, and the collapse load was determined by considering the formation of yield moments along the centerline and over the piers of the bridge for a channel section loaded around the weak axis. Measured

stresses were lower than the calculated concrete stresses. In this test, using the line load for the center span, a load of 375 kips (1668 kn) representing eight HS20-44 trucks at the bridge center caused a permanent deflection, and a load of 950 kips (4226 kn) representing twenty HS20-44 trucks caused collapse. For comparison, a line loading of 94.7 kips (421 kn) produced the same moment in the bridge center as an HS20-44 truck in each lane. Findings showed that the reinforced concrete section will behave elastically until the reinforcing steel reaches yield stress beyond which permanent deflection occurs. Before collapse can occur, yielding and hinges must form under the load and over the two piers.

Gamble (1980) conducted tests on a 1/8 scale three-span continuous prestressed concrete bridge. Girders were precast, the deck was cast-in-place, simple supports were used, and the models were five years old when tested. The loads were applied as an AASHO HS-type vehicle with three axles, with loading positions chosen for flexure with some influence of shear, rather than primarily in shear. The "first test on a given span causes positive moment cracking only after the bottom fiber stresses overcome both the precompression and the tensile capacity of the concrete, while in the second loading of the same beam, only the precompression exists since the tensile capacity has been destroyed by the cracking in the first test." This results in major stiffness loss in the second load test as cracks reopened at considerably lower loadings than those which initiated the cracks. Positive moment cracks appeared at loads approximately equal to 3/8 of the theoretical collapse load in girders due to loads applied in that span. Deck cracking often occurred in adjacent spans. Six loadings were applied, with the last load equal to approximately 7/8 of the theoretical collapse load. After the last load there were large cracks approximately 0.012 in. (3 mm) wide in the deck, and the girder pulled out of its encasement in the pier diaphragm leaving a gap between adjacent beam ends. Negative moment regions suffered serious distress with major cracks 0.16-0.24 in. (4-6 mm) wide over the interior piers. Some bond slip occurred along the bars, but not at the end of the deck

bars. Cracking in beams consisted of flexural, flexure-shear and inclined cracking at the supports in the web only, which might be associated with negative moment deck cracking and web shear cracks. In addition, a long sloping crack in the web along the path of the draped strands indicated that a sliding plane might have been developing. Deck cracking occurred especially at the supports. Negative moment plastic hinges were indicated by cracks at faces of diaphragms, not at the center of the support.

In an attempt to determine the load at which damage initiates, several different formulas have been developed. Kostem's analysis (1976) of decks supported by prestressed concrete beams found the extension of cracks in deck slabs occurring at loads 30%-50% higher than the initial cracking load. Initiation of cracks in beams required loads 80%-200% greater than loads initiating cracks in the deck slabs. Other studies by Kostem (1985) have led to the observation that,

> "When at least 4 wheels per axle and no more than 4 axles per axle group, with axle spacing greater than or equal to 4 feet, at an axle weight equal to 29 kips bridge deck cracking initiates resulting in cracked concrete cover to the top of the rebars and the bottom cover below the bottom rebars. If axle weights are about 56 kips, then the cracks in the deck slab will penetrate one-half the slab depth.

Two proposed formulas for the load causing cracking in the beams are:

$$P = 36.4 + 0.4\ (L) \qquad (2)$$

$$P = 90 - 0.17\ (NW) - 16\ (NA) + 0.47\ (L) \qquad (3)$$

...where, P = the cracking load in kips,
L = span length in feet,
NW = number of wheels, and
NA = number of axles.

Thus, for 100 ft spans, beam cracking is anticipated at an axle weight of 75.6 kips (336 kN). Similarly, for a 70 ft span, the axle weight is 65.6 kips (292 kN), and for a 40 ft span, the axle weight is 51.7 kips (230 kN).

Data has been coordinated with non-linear analysis techniques in several computer programs in efforts to automate the procedure of determining whether a specific load will exceed a bridge's capacity (Johnston et al. 1973; Seible 1982; Cornwell et al. 1983; McClure et al. 1982; Peterson and Kostem 1975; Kostem 1983; White and Minor 1979). The progress of damage has been traced in deck and beam damage. However, the progressive damage to a bridge due to previous overloads is not being considered. An exception by Kostem (1985) which did attempt to look at progressive damage compared axle weights to crack depths and increases in overloads with increases in crack depth as shown in Fig. 1. For example, Kostem reported that if concrete cover already exhibits overload longitudinal cracks that are about one-half to one-third the depth of the thickness of the cover and if new overloads approximately 45 to 50 percent higher than the previous loads are experienced, the new cracking will at least penetrate the full thickness of the concrete cover. Further, if the new overload levels are about twice the value of the initial loads, the resulting cracking will penetrate at least one-half the depth of the bridge deck slab.

More study appears to be required in order to provide a better evaluation of crack development, growth and propogation under constant and varying loads.

Much work has been performed to determine the levels of damage that occur as loads approach the ultimate capacities of a bridge. Data has been coordinated with non-linear analysis techniques in several computer programs in efforts to automate the procedure of determining whether a specific load will exceed a bridge's capacity.

A non-linear method of analysis was developed at the University of California at Berkeley by Seible (1982) in a computer program called NOBOX. This program, developed for multi-cell reinforced concrete box girder bridges, can predict the entire nonlinear response as well as the ultimate failure load and collapse mechanism under stepwise increasing static loads. The program makes no provisions for the interaction of flexure and torsion on ultimate capacities. It also ignores time-dependent effects and geometric nonlinearities, but does

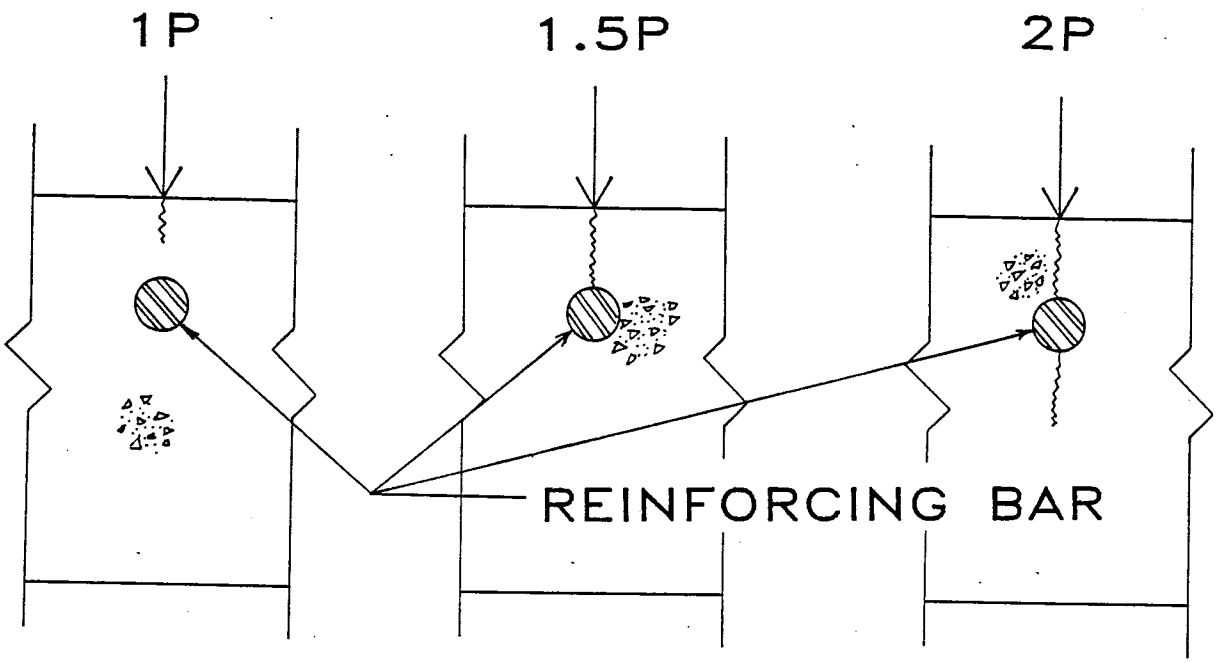

Figure 1.--The effects of increased loads on the depth of deck cracking

consider material nonlinearities such as concrete cracking, reinforcement yielding, and plastic hinge formation. In case studies the program agreed within 5% with the results of actual loading tests. However, NOBOX requires an exact loading history of the bridge in order to be exact.

NOBOX considers nonlinear flexural and nonlinear shear behavior in the longitudinal direction, flexural plastic hinges and shear failure in the longitudinal direction, nonlinear flexural behavior and plastic hinge formation in the transverse direction in the top and bottom of slabs and in the vertical webs, and nonlinear torsional behavior of the box section. The linear-elastic analysis uses a three-dimensional grillage with concentrated loads at coordinates. The nonlinear analysis solves the system, introduces a plastic hinge where maximum moment exceeds the yield moment, resolves the system, and continues the cycle until all hinges have formed. Factors used in the determination of the plastic hinge rotation capacity are (1) ultimate curvature at concrete crushing, (2) plastic hinge length, (3) shift in the effective bending moment diagram due to shear, (4) shear length of the beam expresses by the moment/shear ratio, (5) area of the load application, (6) the steel type, and (7) the longitudinal reinforcement ratio. The program can look at the overall bridge collapse and at local failures of parts of the bridge.

Several investigations have been conducted at Lehigh University of the effects of overloads on individual elements--slabs and beams--as well as on entire bridges. These reports have incorporated field observations as well as extensive computer modeling and have examined a variety of bridge types.

The goal of the program (Peterson and Kostem 1975) was to provide an assessment of damage between the elastic and ultimate loads. This was performed by finding an elastic stress and deflection from the loading, then increasing the load to find the intiation of damage in the form of a cracked layer in the model. Finally, a plastic analysis uses stress and displacement increments to calculate damage progression. This plastic analysis was required because, under dead

loads alone, concrete and reinforcing steel may exhibit non-linear behavior.

The parameters of the computer program BOVAC (Bridge Overload Analysis--Concrete) by Peterson and Kostem (1975) used for both reinforced and prestressed concrete I-beams or rectangular beams are that beams are prismatic and simply supported, with perfect material bonds, failure in flexure, and only strong axis bending, since previous research indicated that minor axis bending and torsional stiffness have minor effects. Slabs are assumed to be planar and rectangular simple spans, with uniform thickness, compression and tension reinforcement, perfect material bonds, failure in flexure, static vertical concentrated and patch loads, and concentrated in-plane loads and moments. Small strain and dislacement fields are assumed, and either full or no composite action may be chosen. Several factors were excluded in the BOVAC analysis. Local buckling and lateral torsional buckling were excluded from consideration through the geometry of deck slabs and beams. Torsional stiffness of beams was neglected. Shear punching failure is excluded because as vehicular loads increase, "more wheels are used to distribute the load over a greater area... Since a substantial area is involved, shear punch failure is not likely to occur (Kostem and Ruhl 1982)." Dynamic effects and impact were also not considered, and diaphragms were excluded, yielding a more conservative approach.

Kostem and Hall (1980) expanded BOVA to incorporate the inelastic analysis of reinforced concrete bridge decks supported by steel girders, with the goal of improving the rating process of bridges and the determination of bridge ultimate load capacity and response to overloads. The program did this by incorporating a layering technique based on displacements which agreed well with previous work. The program assumed small deformations, slippage between the steel beams and the concrete slab, shear deformation of the steel girders, and shear lag of the concrete deck. Along with previous exclusions, the program did not consider torsion of beams or interaction between the steel girders and wind bracings and diaphragms.

The program was further refined by Kostem and Ruhl (1982), involving prestressed concrete girders supporting a reinforced concrete, monolithic deck slab with "full composite interaction between the bridge deck and beams". Beam age was taken into account to include prestressing losses and concrete wear, and slab age was considered by reducing the concrete cover over the reinforcing steel and reducing the concrete compressive strength. Termination checks in analysis of the beams are: maximum concrete strain = 0.002, maximum concrete tension stress = $6\sqrt{f'_c}$, maximum concrete compressive stress = $0.8f'_c$, maximum number of cracked layers = 1, maximum number of crushed layers = 1, maximum prestressing strand strain = 75% yield strain, maximum steel tension stress = 0.75 tensile strength, and maximum allowable flexural shear = $1.7f'_c$. Termination checks in slab analysis for the concrete are: maximum concrete strain = 0.0025, maximum tension stress = $6\sqrt{f'_c}$, maximum compression stress = $0.8\ f'_c$, maximum number of cracked layers = 3, maximum number of crushed layers = 1. For the slab reinforcing steel, the checks are: steel maximum strain = 0.75 yield strain, maximum tension stress = 0.75 yield stress, maximum compression stress = 0.75 yield stress, and maximum number of yielded layers = 1.

In 1977 Kostem studied simple span reinforced concrete decks with prestressed concrete I-beams and found overloading to be a frequently occurring phenomenon. He also concluded that definitions for damage, serviceability and performance criteria are necessary to provide an intelligent and consistent decision process for overload permit applications. This study with Kostem and Ruhl (1982) showed that behavior of the slab and beam when examined separately is different from their behavior when joined together, confirming that analysis of the entire superstructure acting together is required because of the interaction of bridge components. This interaction is not normally fully considered in the design process, and thus complicates the prediction of actual stresses and deformations. Also, the elastic and ultimate strength analyses are not useful for the bridge overload response because parts of the superstructure behave non-linearly.

Damage photographs of field tested bridges confirmed that the primary failure mode of deck slabs and beams is by flexure. If the vehicle load is equally distributed among beams, damage may initiate in the beams or the slab; otherwise damage initiates in the slab. In short span bridges with deep beams, beams fail due to the interaction of shear and flexure at high loads. The first signs of overload distress were found to be cracking to the deck concrete. In 1985 Kostem confirmed that even after substantial cracking in the deck slab, stress levels in the reinforcing steel were not high enough for concern. Beams were found to crack only after substantial deck damage which was due to the unequal deflection of the beams.

Slab inelastic analysis (1977) showed that (1) membrane stresses in the slab substantially affect damage initiation, (2) stresses induced by in-plane forces and biaxial bending must be considered as the significance of material non-linearity and slab damage increases, (3) exclusion of stresses in the direction perpendicular to the plane of the slab does not alter the results, (4) all stress-strain characteristics and failure criteria for concrete can be defined in terms of the 28 day cylinder strength, and (5) large increases in slab strains are noted when wheels are near strain gages, but shear punch failure is not a likely possibility. Additionally, bridge overload response is adversely affected by an increased axle load, increased number of axles grouped together, decreased number of tires on an axle, and decreased spacing between axles--in short, any combination of wheels and axle that concentrates more of the vehicle's weight over a reduced area. Shear stresses in beams were found to be not critical, but could amplify the effects of flexural stresses and thus cause principal stresses in beams to be greater than flexural stresses.

Kostem and Ruhl (1982) found that as the loading is increased above the linear elastic state of stress, damage in the form of concrete cracking usually initiates in the top and bottom surfaces of the slab. With further loading, cracks deepen, new cracks may form and some concrete crushing on the top and bottom surfaces of the deck slab occurs. Skew should not affect applicability of these findings

noticeably, although that was not determined for skew less than 60 degrees. For spans less than 25 feet, damage may initiate in shear through interface deck-beam shear or tension in the beam web at the support. Efforts were made to predict crack width from loading, but due to the wide variability of previous efforts and their extreme dependence on strict quality control, results were inconclusive.

Kostem (1984) stated that observations of "overload case studies have indicated that high stresses due to overloading tend to be more prominent in the vicinity of the details that are prone to fatigue-crack initiation, residual stresses play a nonnegligible role in the inelastic response of primary steel girders, buckling is an important but not a critical phenomenon and damage initation due to overloading can intiate in girders or in the deck, depending on the design details." In bridges consisting of reinforced concrete decks supported by prestressed concrete I-beams, large overloads resulted in cracks forming "partial hinges similar to the formation of the yield lines." For "steel multigirger bridges with reinforced concrete decks...depending on the proportioning of the steel girders, the damage to the superstructure can take place both at the girder as initiation of plastification or web-panel buckling and in the deck slab as cracking of the concrete. In the case of continuous construction, substantial cracking of the concrete over the interior supports takes place before any other damage to the rest of the deck and usually before any damage to the steel components."

Kostem (1985) observed that the transverse positioning of the vehicle on bridges with more than two lanes could noticeably effect the load at which the initiation of damage is observed. The vehicle weight initiating slab concrete cracking approximately 10% higher in spans of 40 ft or less and 5% higher for spans of up to seventy ft when an interior lane was loaded rather than an exterior lane. If slab damage is ignored, then the vehicle weight initiating beam cracking can be increased 15% in both the short and long spans if loading is restricted to an interior lane.

In addition to the vehicle location on the span, Kostem found that

the bridge design, specifically the beam spacing, could have an effect on the capacity of the bridge. For a difference in beam spacing of about 15% (6.5 ft vs. 7.5 ft), it was observed that the load initiating deck cracking was 4% more in bridges with closer beam spacing. If slab damage was neglected, then the load initiating beam cracking was 10% higher for spans with closer beam spacing.

Damage to Skew Bridges

Consideration of bridge skew introduces new factors in the evaluation of the effects of overloads. While there are some advantages to skewed bridge decks, skew also tends to increase the already uneven distribution of shear forces due to additional twisting action. Skew bridges have been found to exhibit shear cracks in exterior girders at obtuse corners. Cracks may also appear at the acute support corners of the span, and transverse cracks appear at midspan (Wallace 1976).

Cope (1985) studied 1/5 scale slab models with skew angles ranging from 30-60 deg and with various reinforcement schemes under loads at obtuse corners. Upon loading near a free edge, the slab between the vehicle and the obtuse corner bearings may incur transverse shear forces several times larger than the average shear force supported across the slab's cross-section, creating a critical loading case.

Service load tests on a slab with 30 deg skew produced cracks of 0.0012 in.(0.03 mm) parallel to the supporting edges on the underside of the slab while the load was applied. Linear analysis proved to be adequate up to the design ultimate flexure load of 50 kN. At increased loads of (80 kN), cracks widened, new cracks formed, and cracking became visible on the upper surface at the obtuse corner bearing. At 130 kN, flexure cracks developed into an inclined shear crack coinciding with the edge of the soffit steel. Testing ended at 150 kN as stiffness was lost. At the highest loads, some local concrete crushing was observed.

Three slabs with 45 deg skew exhibited soffit cracking at service

loads, with upper surface cracking becoming visible at ultimate loads. Slabs did not show significant damage until shear cracks formed. Initial shear cracking in two tests formed at 70 kN loads, with lengthening of flexure cracks in one slab on the top surface at 90 kN loads. In the third test shear cracking became visible at 80 kN loads, and an inclined side crack became visible at a loading of 102 kN. This side crack did not extend to the top or lower surfaces and was shallower than in the other two slabs. Although several different reinforcing schemes were used on the slabs with a 45 deg skew, the ultimate loads were similar. With 45 deg skew, shear cracks occurred at lower loads indicating that limited shear cracking may still transmit considerable load.

On a slab with a 60 deg skew, an inclined side crack appeared at a 35 kN load and extended to both surfaces with increasing loads. Shear displacements became noticeable along a shear crack on the top surface at a load of 60 kN. Top surface cracking was more severe than for slabs with smaller skews, and flexural cracking in the soffit was less than the top surface cracking in the extent and widths of the cracks. Some punching damage formed at 75 kN loads. Cope's investigation showed that the degree of skew may significantly affect the load at which cracking first appears and the mode of failure. As skew angles increase, the slab shear capacity decreases reducing the loads at which cracking and failure occur so that in slabs skewed more than 45 deg, punching shear may control. For the larger skews, punching shear was a potential problem where obtuse corner bearings support most of the load. Although most cracking occurred on the underside of the slab except in the 60 deg skewed slab, cracking also occurred in the slab's top surface as loads increased. Cracking was usually parallel or perpendicular to the supporting slab edge.

Table 2. Cracking and failure loads for slabs with varying skew

	Failure Loads (kip)							
Skew	30			45				60
First visible shear crack	130	80	85	70	70	102	80	35-60
Failure	150	107	100	80	70	110	110	75

Inter-Relationships

Cracking damage has been associated with corrosion, temperature effects, shrinkage and loading. Any cracking is undesirable, since it may allow water and road salts access to the substructure, bearings and reinforcing steel and increase the risk of damage and corrosion. It is clear then, that there are many potential causes of bridge damage, whether through one event or a series of events, which may be completely unrelated to overloads. However, because they work in conjunction to deteriorate a bridge, their effects should be considered. In addition, while it is known that overloads may damage and even cause collapse of bridges, the progressive damage caused by long-term exposure to overloads has not been fully evaluated.

FIELD STUDY

PREVIOUS INVESTIGATIONS

Previous research by Darroch and Furr (1970) has revealed some general trends which are helpful in observing damage. Deck damage was categorized as cracking, spalling, scaling, delamination and surface loss. Cracking ranged in degrees of severity varying from none present, to leaking cracks, to extensive cracking, to tension cracks in the bottom of the deck and cracking throughout the deck resulting in deck failure. Spalling, scaling, delamination and surface loss were all similarly subdivided according to the degree of damage, ranging from no damage to minor, moderate and extensive damage. As more than one form of damage is commonly present in a span, a wide range of damage combinations was allowed for in order to present as full as possible a classification of decks from undamaged to failed decks.

Comparison of different bridge types is presented in Fig. 2, which lists the percentage of bridges of each type exhibiting various levels of cracking. As illustrated, more deck damage is experienced by decks supported by steel I-beams than by those supported by reinforced or prestressed girders. Moderate to extensive cracking involves minor fine cracking to extensive and leaking cracking, extensive scaling or spalling. Severe cracking includes severe spalling and scaling, with extensive delamination, surface loss and loose concrete, with leaking cracks, up to and including deck failure. The degree of deck cracking increases with the type of supporting beam in the following order: prestressed concrete, reinforced concrete, steel I-beam, and steel plate girder. Transverse cracking predominated among the various bridge types, except in pan-formed bridges which exhibit considerable longitudinal cracking. For all bridge types, there was more cracking in wheel paths than in any other specific location. Delamination was

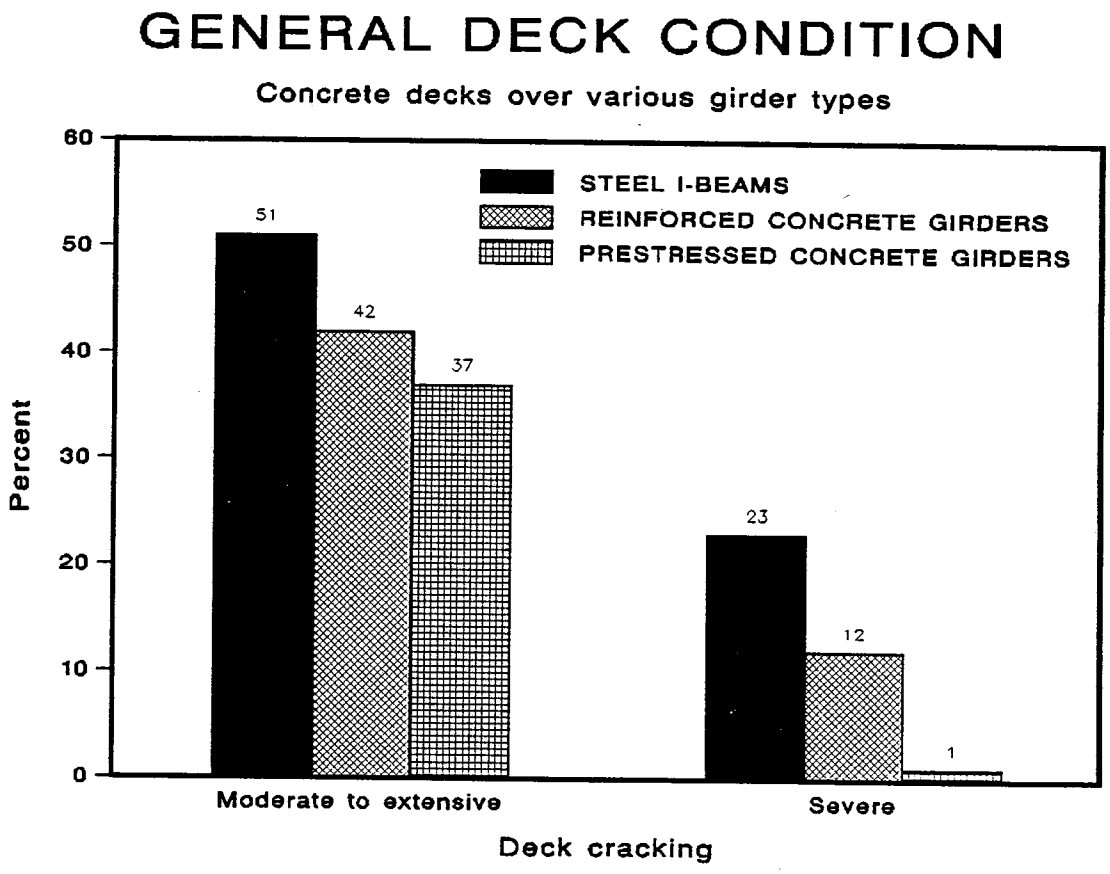

Fig. 2.--Observed levels of deck cracking for various superstructure types

more prevalent in heavily traveled bridges and those designed for heavier loads; but this may be attributable to either the heavier sustained loads or a change in the bridge specifications. Most delamination was either in the wheel paths or scattered over the deck, and visible cracking was commonly found over the delaminations.

In a general study of bridge deterioration in Minnesota by Hill and Shirole (1984), review of over 3500 bridge replacements showed that the major problems of steel structures were found to be corrosion at connections and under leaking joints, and fatigue cracking at or near welds, fire, and accident damage. For steel bridges up to 20 years old, decks, beams and joints have the most problems. After 20 years, steel structures develop problems with bearings; after 31 years, with substructures. Prestressed concrete bridges usually only develop problems with expansion joints after 11 to 31 years. After 31 years, the bridges may also develop problems with beams. Culverts are particularly vulnerable to poor construction and scour damage. Timber bridges are vulnerable to fire, accidents, insects and ice, and after 30 years they may develop problems with their decks.

FIELD INVESTIGATION

To confirm and expand on the findings of the literature survey, a field study was conducted to investigate bridge damage. The goal was to find paired sets of bridges on a route in which one bridge would experience heavy loads due to traffic, while the other bridge would experience lighter loads due to traffic. It was anticipated that the bridge with the more heavily-loaded traffic would show correspondingly greater damage.

In the search for candidate bridges an initial investigation was conducted using the Texas State Department of Highways and Public Transportation's Bridge Inspection file (BRINSAP). It was anticipated that data extracted from the file would reveal relationships between bridge types, traffic levels and bridge conditions, or identify categories of bridges for further study. The file's usefulness was

found to be extremely limited since condition ratings gave only general bridge conditions and were dependent upon the recorder's observations and experience. In particular, the ranges of reported condition ratings were too narrow to be useful in discerning any trends. Consequently, the file was primarily used for obtaining physical data for bridge identification and categorization.

Sampled bridges were selected on a route noted for heavy traffic for over 20 years, based upon the advice of SDHPT personnel. This traffic consisted primarily of aggregate haulers transporting materials to the Dallas-Ft. Worth metropolitan area from quarries northwest of Ft. Worth. This traffic was expected to be the significant, controlling factor providing a noticeable difference in bridge damage, since southbound bridges would experience frequent high loads from loaded trucks travelling to Dallas-Ft. Worth, and northbound bridges would experience lower loads from empty trucks returning to the quarries.

The damage expected was primarily cracking in the underside of the reinforced concrete decks, and in the investigation, this expectation was confirmed. No significant damage to beams was noted. While joints exhibited wear and rust stains, significant damage was not noted. At supports, some fatigue and corrosion cracking of steel diaphragms was also noted. Overall, supports were evidently undamaged and in good working order. No damage was noted to abutments or bents, and no apparent settlement or other foundational damage was evident.

BRIDGE COMPARISONS

In order to evaluate the nature and extent of damage to bridge structures along this route, a wide variety of bridge types and ages were selected and investigated. Twenty-four bridges were examined by three investigators walking along the bridge length to determine any visible damage to the wearing surface, the bottom of the bridge deck, supporting girders and diaphragms, bearings, bents, columns and rip-rap.

Five sites with prestressed concrete deck and girder bridges were found to have little visible damage, except for the skewed bridges. Skewed bridges exhibited some transverse cracking on the top surface along the end of the deck, and in some cases cracking parallel to the skew was observed scattered on the underside of the deck. Although a few cracks exhibited a white exudate indicating full-deck penetration by water, cracks were usually widely spaced, unconnected, and did not appear in consistent patterns.

Two pairs of prestressed concrete box-girder bridges with skew were found to be in generally good condition. The normal damage was minor random cracking parallel and perpendicular to the skew close to piers and on the bottom surface of the deck near the abutments. Cracks perpendicular to the skew exhibited rust stains indicating water leaks, and there appeared to be more damage in the southbound bridges. The only major damage observed was in an outside girder of a southbound bridge in which a major crack with spalls exposing reinforcement extended at least 20 feet along the length of the girder as shown in Fig. 3. Since there was no traffic under this particular span, it appeared that only a heavy load or a significant construction defect could have caused this damage. The bridge had been in service for approximately 10 years.

A flat-slab reinforced concrete bridge without skew and with steel I-beam columns was also found to be in good condition. The only observed damage consisted of minor vertical cracks on the outside edge of the slab at joints connecting continuous slabs.

Four bridges with reinforced concrete decks and r. c. beams were examined and found to be in good condition after decades of service. The only visible damage was some spalling at piers in one bridge and cracks at joints across the deck top on another bridge.

Two unskewed pan girder bridges were found to contain hairline longitudinal cracks between girders and some exposed reinforcing steel on the underside of the deck. One bridge had a transverse crack across the width on the top surface of the joints at the end of the bridge. The other bridge contained small flexure cracks in the bottom of the

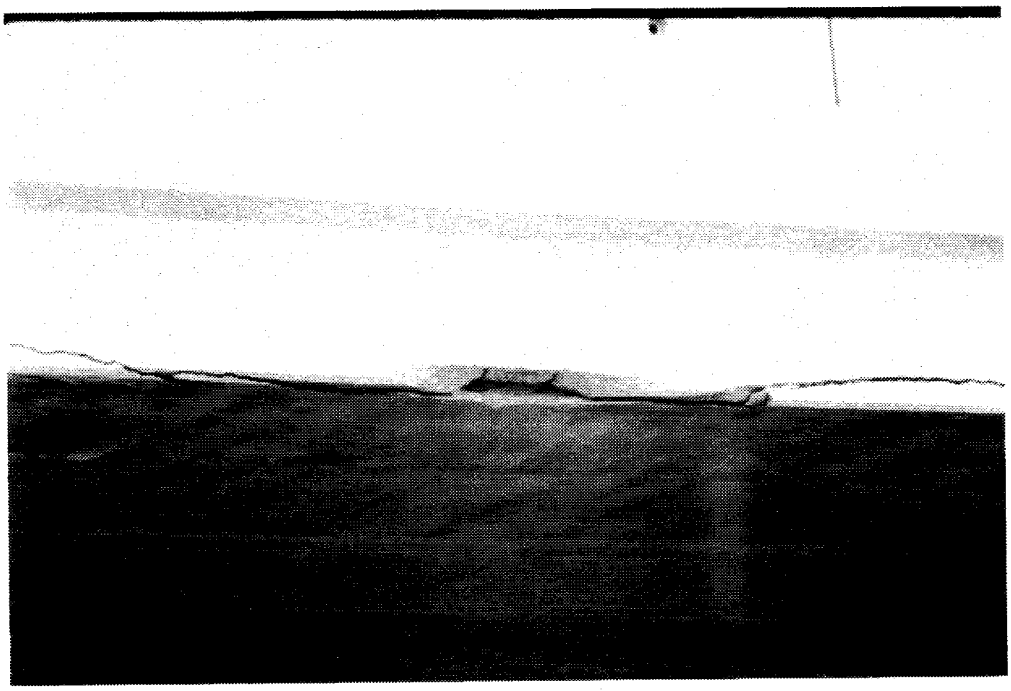

Figure 3. Observed fracture in outer face of concrete box girder

girders and may have had a higher occurrence of cracking in the southbound bridge and the entry span of both bridges. Furthermore, some overheight vehicle damage in the form of minor spalls on girders was noted.

Three pairs of reinforced concrete bridges with steel I-beams were examined and found to contain grid-like crack patterns on the underside of the bridge decks. This damage appeared in both skewed and unskewed bridges. When the approach and exit spans and the northbound and southbound bridges were compared, there appeared to be greater crack densities in the approach spans and in the southbound structures. This difference in damage between the southbound and northbound bridges was accentuated by the evidence of repair to the deck at one southbound bridge on the right side of the traffic flow. Some corrosion damage was noted at connections between beams and the deck, and some large fatigue cracks were observed in welded connections between the steel I-beams. Plastic deformation of the flange of one beam in a northbound span also gave evidence of overheight vehicle impact.

Of the bridges examined during this study, both reinforced concrete and prestressed concrete girder bridges exhibited little damage of any kind, regardless of age. Some transverse cracking and spalling was evident; but the cracking was usually widely spaced, unconnected, and did not appear to follow a consistent pattern. The pan-girder bridges that were examined contained hairline longitudinal cracks and some exposed reinforcing bars between the girders, but they also appeared to be in good condition.

The target bridge type for study thus became steel stringers supporting reinforced concrete decks for several reasons. These bridges had already been consistently described in previous research by Darroch and Furr (1970) and Okada et al. (1984) as most flexible and most cracked in comparison with other bridges. In addition, upon field examination of bridges along routes accommodating large volumes of heavy traffic, it became obvious that the steel stringer bridges exhibited more damage than other bridges with reinforced or prestressed concrete girders or with panformed slabs and girders. Only in

reinforced concrete decks with steel I-beams was any significant damage to the bridges observed. Finally, because heavy traffic was also observed on these bridges, they were selected as most likely to reveal significant differences in bridge damage as a result of overloads.

BRIDGE EXAMINATION

Of the three pairs of bridges supported by steel I-beams, two pairs on US 287 crossing FM 51 and FM 730 at Decatur, Texas, as shown in Fig. 4, were selected for further study. The third pair of bridges was located in the city of Dallas and was not studied due to the comparative difficulty to accurately analyze the traffic crossing it. The truck traffic observed in Decatur, on the other hand, contained a large fraction of aggregate haulers, indicating the desired loading conditions of heavily loaded traffic on one bridge and traffic with lighter loads on the companion structure. Both pairs of bridges in Decatur were constructed in 1961 and were located within two miles of each other. No major routes provided a likely exit for truck traffic between the bridges, so that both pairs of bridges experienced almost identical loading conditions, as well as being of similar age and design. A portion of the span in the US 287 bridge over FM 51 had been replaced, and access to the underside of the deck slab was more restricted at that site. Therefore, most attention was focused on the bridge over FM 730.

The traffic weight data for the bridges in Decatur was collected by a portable weigh-in-motion station, site N-20, located south of the bridge at FM 51. The site was operated for a 22 hr period, and collected data that confirmed a distinct difference in the loading sustained by the bridge pairs.

DAMAGE ANALYSIS

Cracking was determined visually and marked by hand, with each panel clearly labelled to identify its position in the slab. Shaded

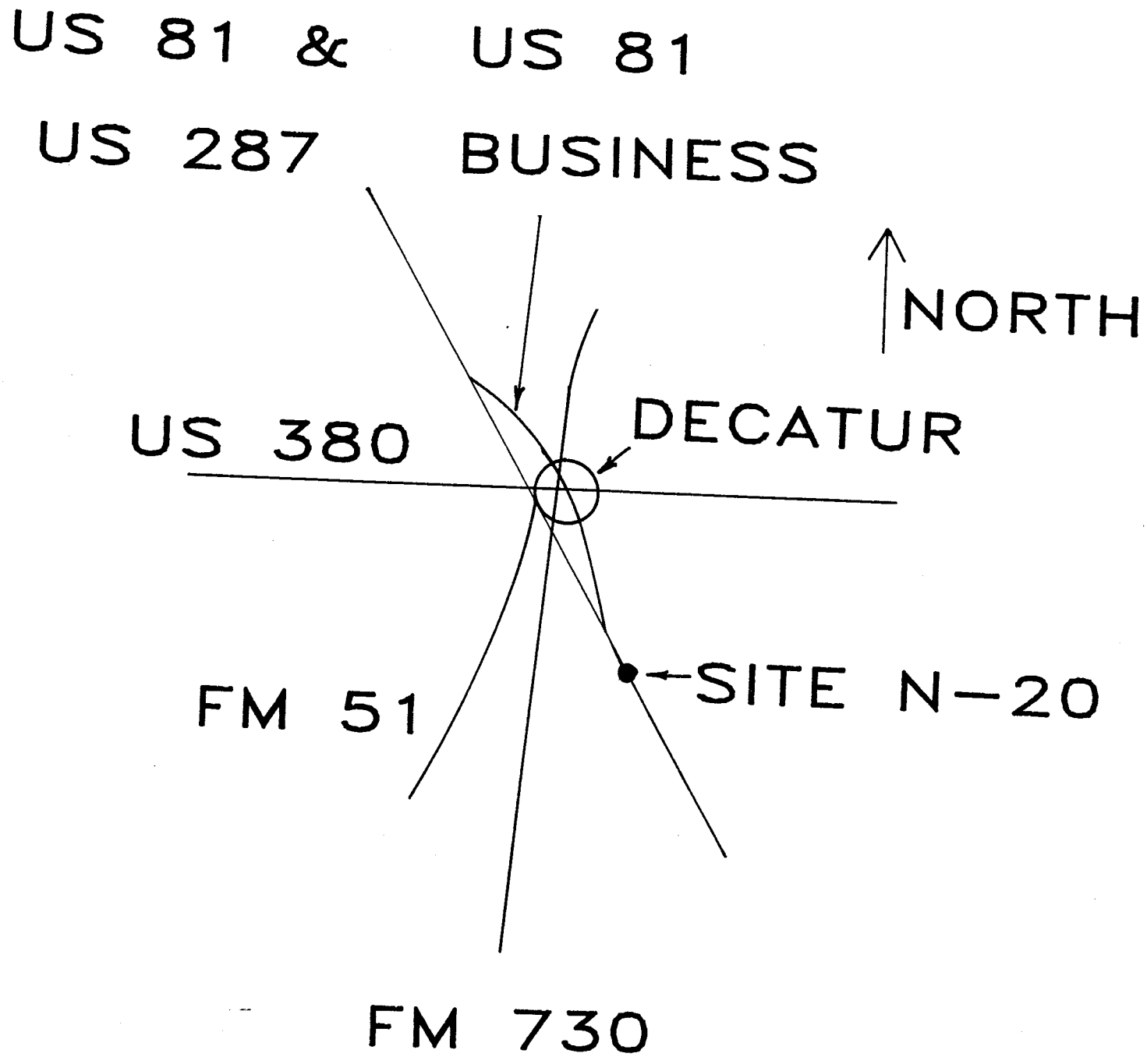

Fig. 4.--Area map showing US 287 over FM 51 and FM 730

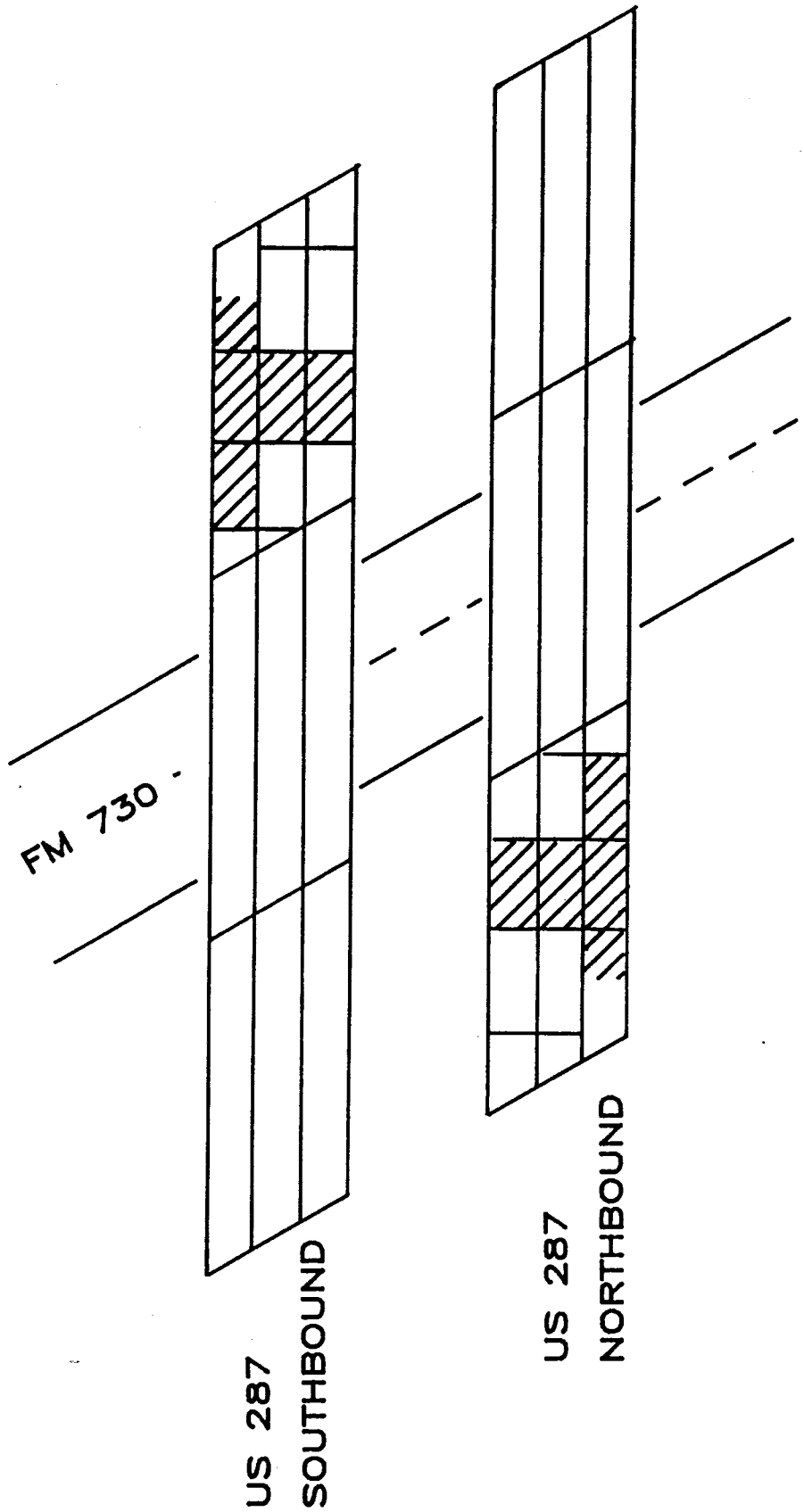

Fig. 5.--US 287 bridges over FM 730 showing areas studied

areas in Fig. 5 denote the marked sections. Categorization of the cracking by severity as well as by location and orientation was desired, but several problems limited this effort. Initially an effort was made to distinguish between hairline and working cracks, denoting cracks roughly 0.1 millimeters or less in width as hairline, and working cracks being any larger cracks, especially those exhibiting crumbling at their edges. Because of the time involved in measuring the width of the large number of cracks and the variation of width along a single crack, a visual estimate of crack widths was attempted with different crack widths marked with different color lumber crayons. After observing the difficulty of consistent classification by eye by separate observers and the inability to clearly distinguish crack coloring in photographs, categorization by widths was abandoned.

In the subsequent analysis of the photographic records, transparencies of each panel were projected onto a wall where a tracing of the panel was made to more conveniently evaluate the crack data. Each crack's location and length were determined and recorded. Cracks within 30 deg of a line perpendicular to the flow of traffic were denoted transverse cracks. Cracks within 30 deg of a line parallel to the flow of traffic were denoted longitudinal cracks. Other cracks were denoted diagonal cracks. The crack density is the sum of the length of cracks in an area divided by the area. Although both bridges are subject to loading, since the southbound bridge subjected to the heavier traffic loads is referred to as the 'loaded' structure and the northbound bridge is referred to as the 'unloaded' structure.

A 12 ft-long section across the width of the approach spans of the US 287 bridges over FM 730 was inspected to investigate the change in cracking across the width of a span. This 12 ft section represented slightly more than 20%. This transverse section began near midspan, 52% of the span length from the approach, and extended to a point 72% of the span length from the approach. This area was divided into nine parts consisting of three panels across the width of the span and three along the length. The sections referred to in the graph titles are 4 ft lengths across the width of the span. Each panel represents a 4 ft-long

area between two of the bridge stringers which were spaced eight feet on center. The designations within the graphs for 'left', 'center', or 'right' panels refer to the area between two of the stringers in relation to the flow of traffic.

In addition to a transverse section, a longitudinal section on the right side of the approach spans of both bridges was marked for investigation. This 35 ft section covered 61% of the span length with one 4 ft-long gap 23 ft from the start of the span. The section extended from 23% to 92% of the span length as measured from the approach. A total of 16 panels were investigated in each approach span involving one-third of the span. Although an examination of the complete bridge was desired, the time involved in the original crack-marking efforts and the inability to access the underside of the entire span limited the study to the approach span which was selected for investigation in anticipation of more damage due to any impact loading.

In summing up the cracking over the entire area of the bridges studied, it is evident that cracking is predominantly transverse, then longitudinal as shown in Fig. 6. The total cracking from both bridges over FM 730 showed that 49% of all cracking was transverse, 36% was longitudinal, and the remaining 15% was diagonal cracking. Comparison of the cracking categories with the total cracking as shown in Fig. 7 reveals some changes across the transverse section. The percentage of transverse cracking decreased from a high of 60% in the left section to a low of 44% in the right section. At the same time, the percentage of longitudinal cracking increased from a low of 24% in the left section to a high of 41% in the right section. These trends were present in both the unloaded and loaded bridges. Diagonal cracking did not exhibit a similar consistant pattern across the cross-section, increasing slightly in the unloaded bridge and decreasing slightly in the loaded bridge as the sections were examined from left to right.

The average total crack density in the center and right sections of both bridges, shown in Fig. 8, was close to 200 in./sq yd, while in the left section the loaded and unloaded bridges respectively contained

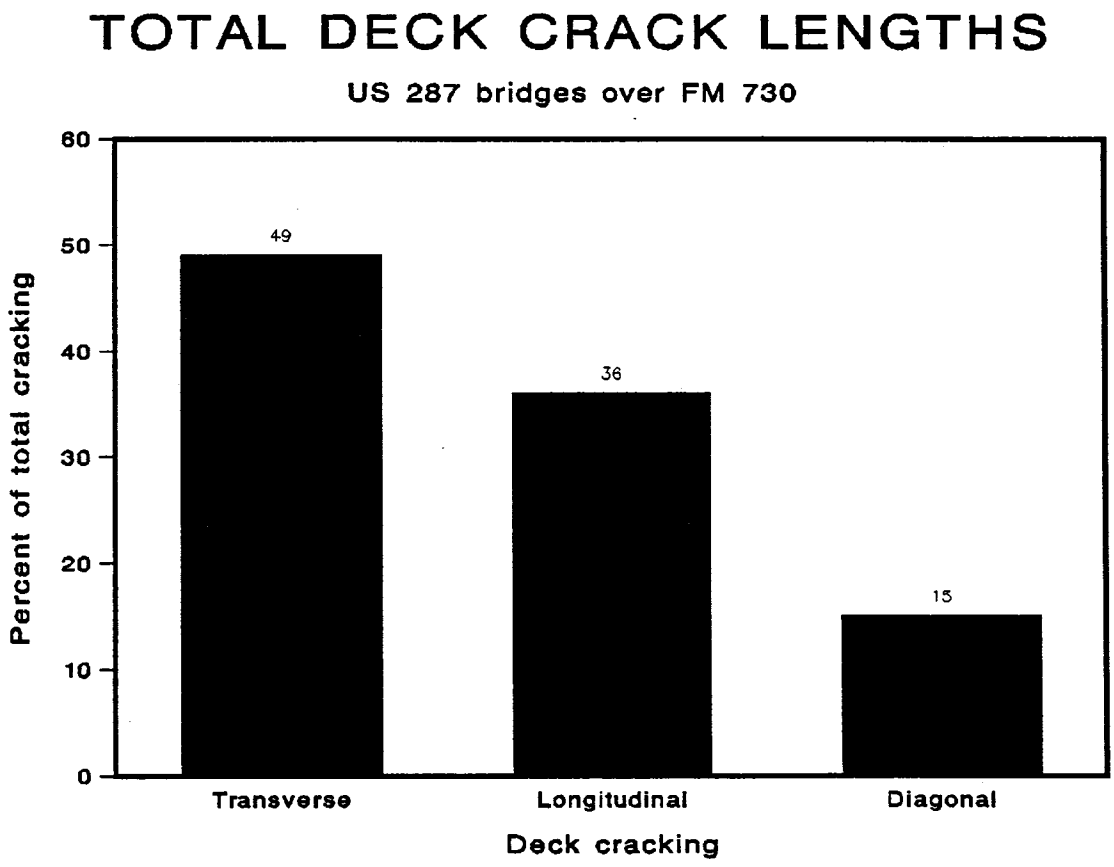

Fig. 6.--Total observed deck cracking

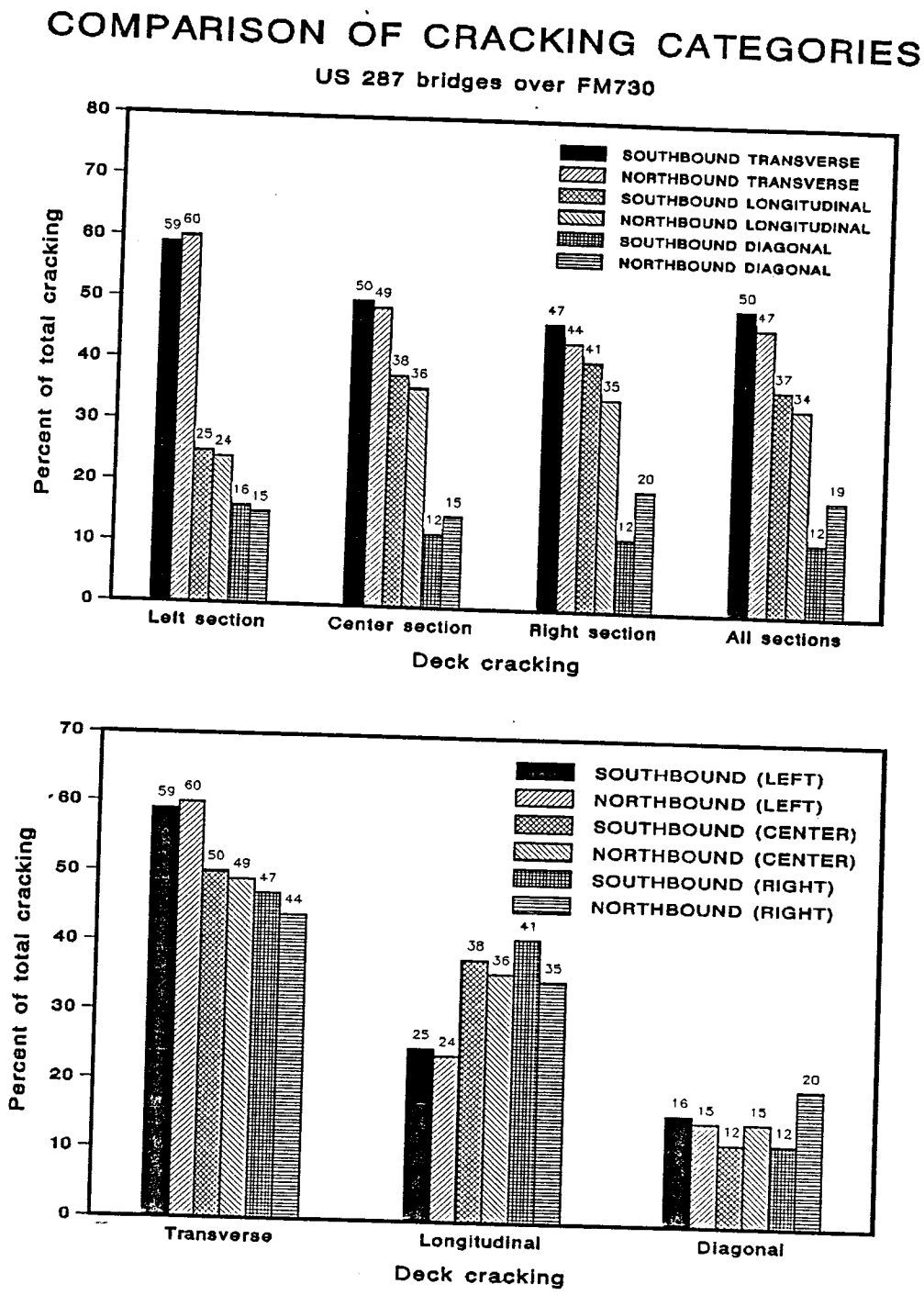

Fig. 7.--Deck cracking by category for loaded and unloaded structures

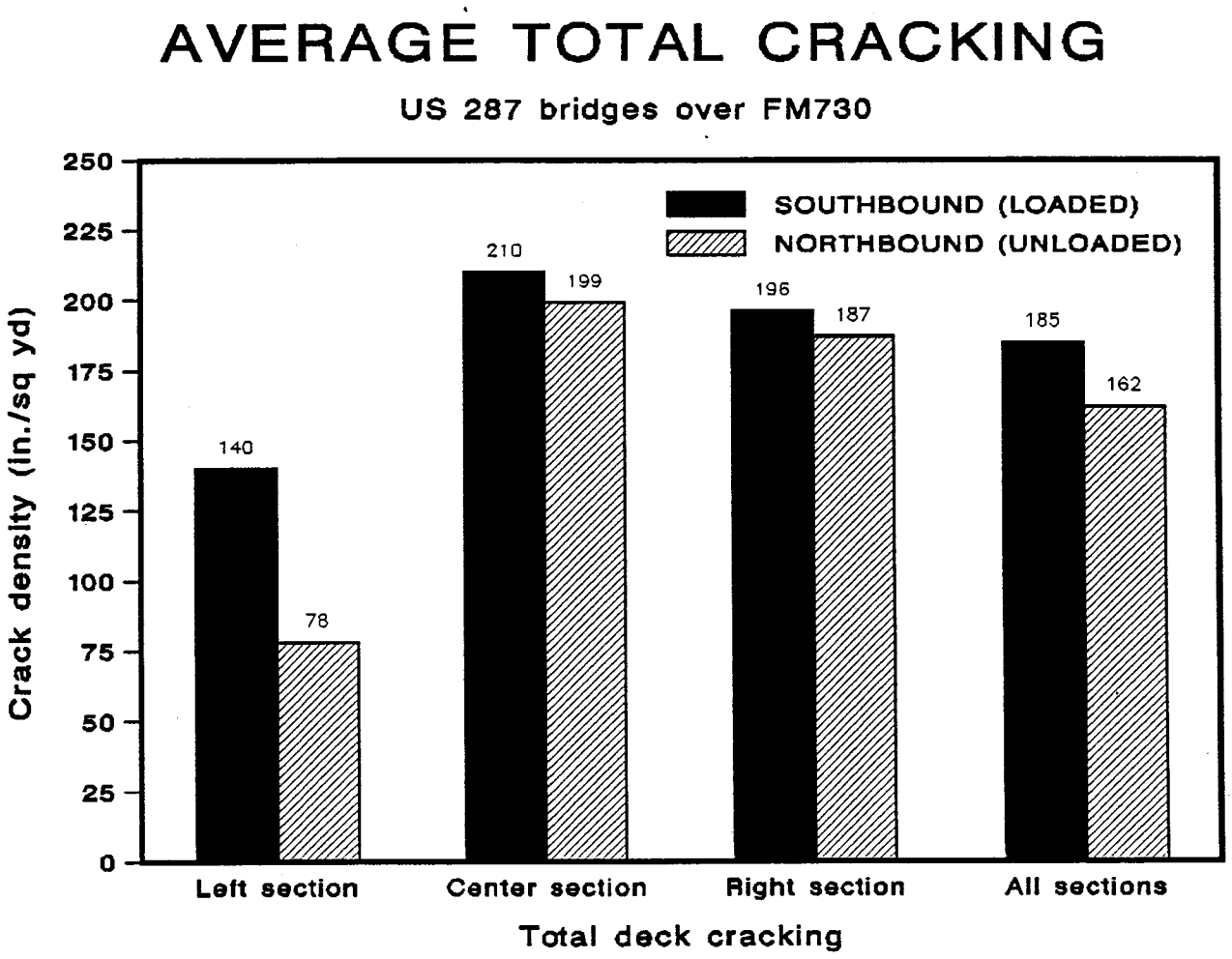

Fig. 8.--Transverse distribution of deck cracking

an average total crack density of 140 and 78 in./sq yd. Of the 16 panels, the loaded span normally displayed more cracking than the unloaded span. The only exceptions to this were two of the nine panels in the right section and one of the three panels in the center section.

LONGITUDINAL SECTIONS

Longitudinal sections along the left, center and right side of the span were examined to determine if any consistent damage patterns might be found such as those which might be attributable to dynamic loading. Data was broken down for transverse, longitudinal and diagonal cracking.

Although along the longitudinal axis and in comparison with other bridges there is too little data to confirm any cracking pattern, there did appear to be areas in the span length of both bridges with greater cracking densities, especially for the transverse cracks. This is evident in Fig. 9, which reveals peaks in transverse cracking near midspan, and for the longitudinal cracking which has fairly uniform crack densities in panels near midspan.

In the left section of the bridge (Fig 10), all cracking categories showed more cracking in the loaded bridge. The difference in cracking between the spans showed no clear pattern, except that differences in the cracking categories were greatest for transverse cracks and least for diagonal cracks. The center section (Fig 11) showed less uniformity in the cracking differences with no apparent pattern. In the right section (Fig. 12) total, transverse and longitudinal cracking were normally greater in the loaded span, and diagonal cracking was greater in the unloaded span.

The average difference in total cracking was highest in the left section and smallest in the center section. Similar but less extreme differences were exhibited by the transverse and longitudinal cracking; but with respect to the diagonal cracking, the right panels exhibited the greatest cracking difference.

The differential in total cracking confirms that the loaded bridge

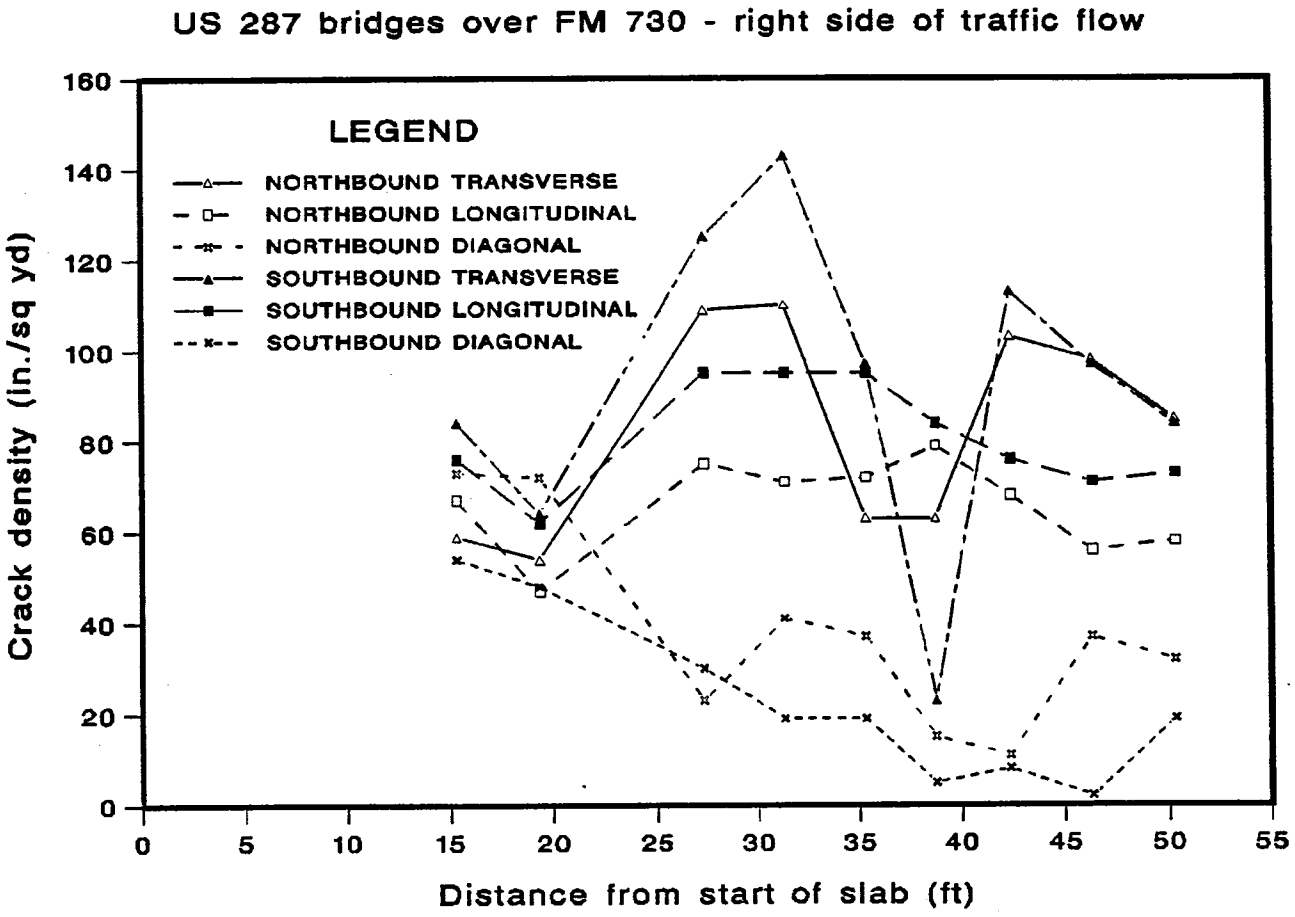

Fig. 9.--Longitudinal distribution of observed crack density

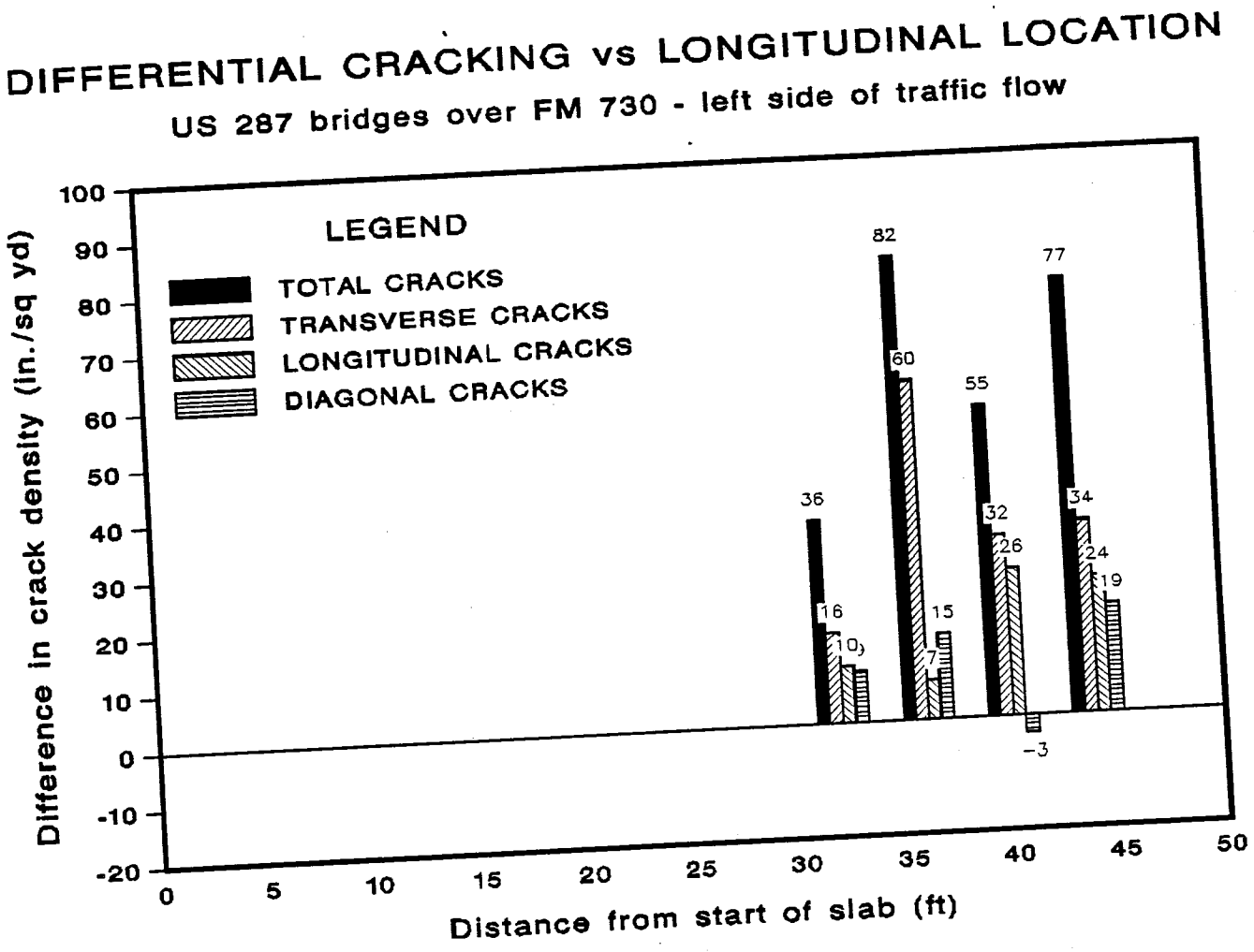

Fig. 10.--Longitudinal distribution of observed crack density on left portion of deck

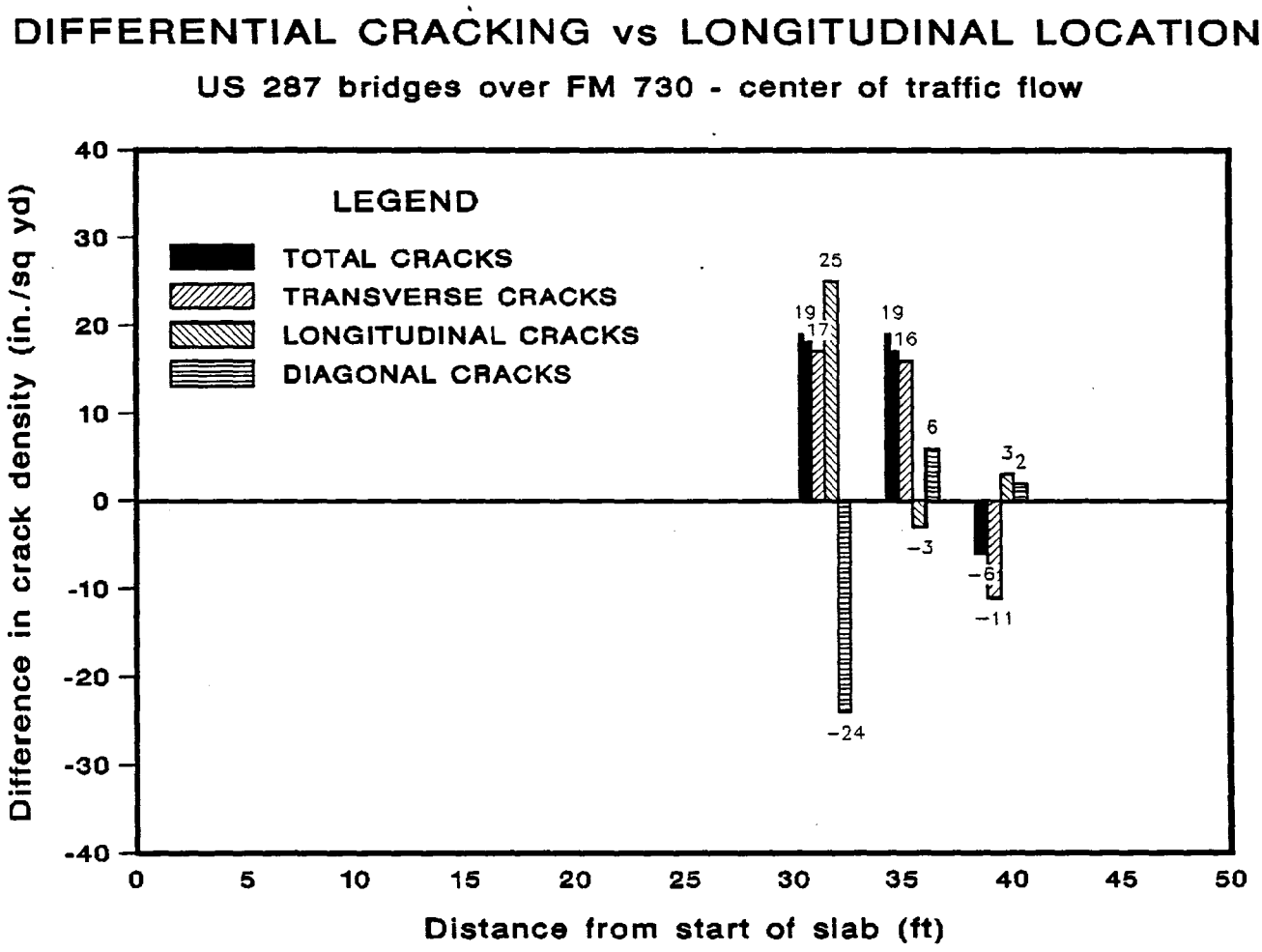

Fig. 11.--Longitudinal distribution of observed crack density on center portion of deck

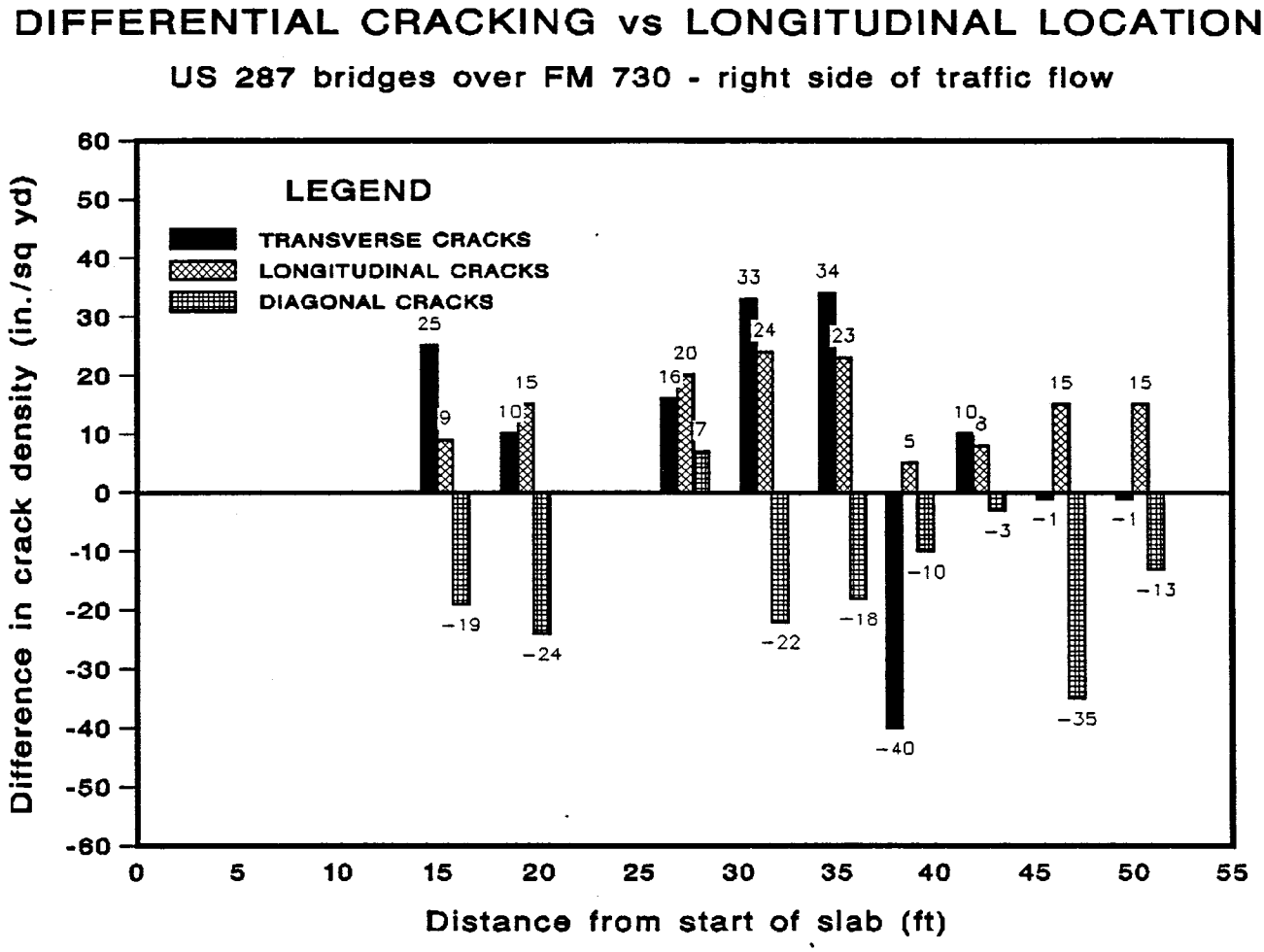

Fig. 12.--Longitudinal distribution of observed crack density on right portion of deck

tends to exhibit more cracking than the unloaded bridge. With the exception of only one panel, longitudinal cracking was greater in the loaded structure. Transverse cracking was usually greater in the loaded structure. Where cracking was greater in individual panels in the unloaded bridge, the margin was smaller than for the panels where cracking was greater in the loaded bridge.

TRANSVERSE SECTIONS

Total Cracking

The loaded bridge usually exhibited more total cracking (Fig. 13) than the unloaded bridge across the span width. In the loaded bridge the left side exhibited greater total cracking by an average of 65%. The center and the right panels usually exhibited more cracking in the loaded bridge, with an average of 6% more cracking for the center panel and an average of 5% more cracking for the right panel.

When directly comparing the panels to each other in both the loaded and unloaded bridges, the center panel exhibited more cracking than the left and right panels in both bridges. The right panel was cracked more than the left panel in the unloaded bridge, averaging 107% more cracking. In the loaded bridge the right panel usually exhibited more cracking than the left, averaging 31% more cracking.

Diagonal Cracking

The loaded bridge usually exhibited more diagonal cracking (Fig. 14) than the unloaded bridge in the left panel by an average of 47%. The center panel was usually less cracked in the loaded bridge by an average of 17%, and the right panel exhibited less cracking in the loaded bridge by an average of 55%.

When directly comparing the panels to each other in both bridges, the center panel usually exhibited more cracking than the left panel. The center panel usually exhibited less cracking than the right panel

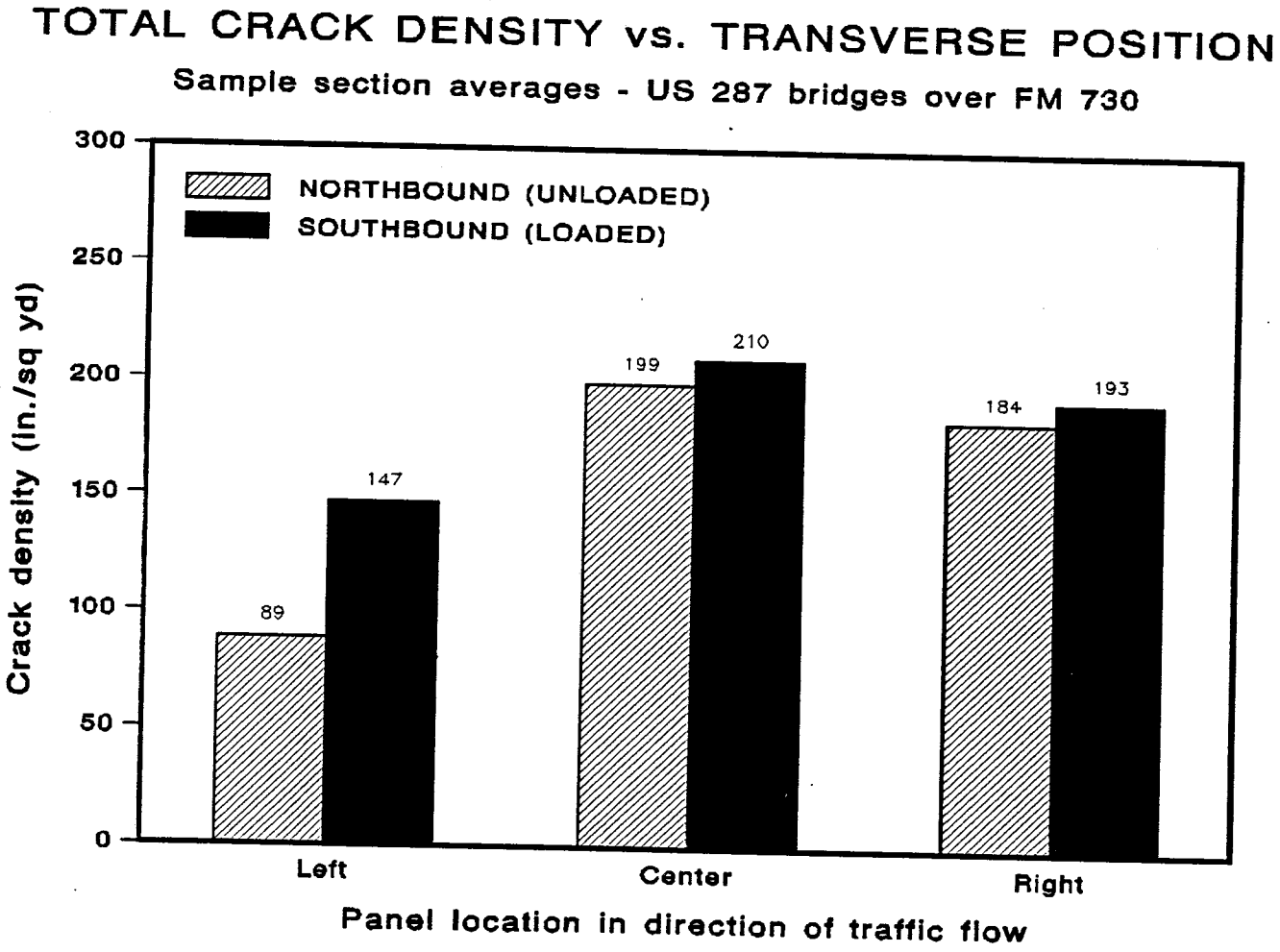

Fig. 13.--Transverse distribution of total crack density

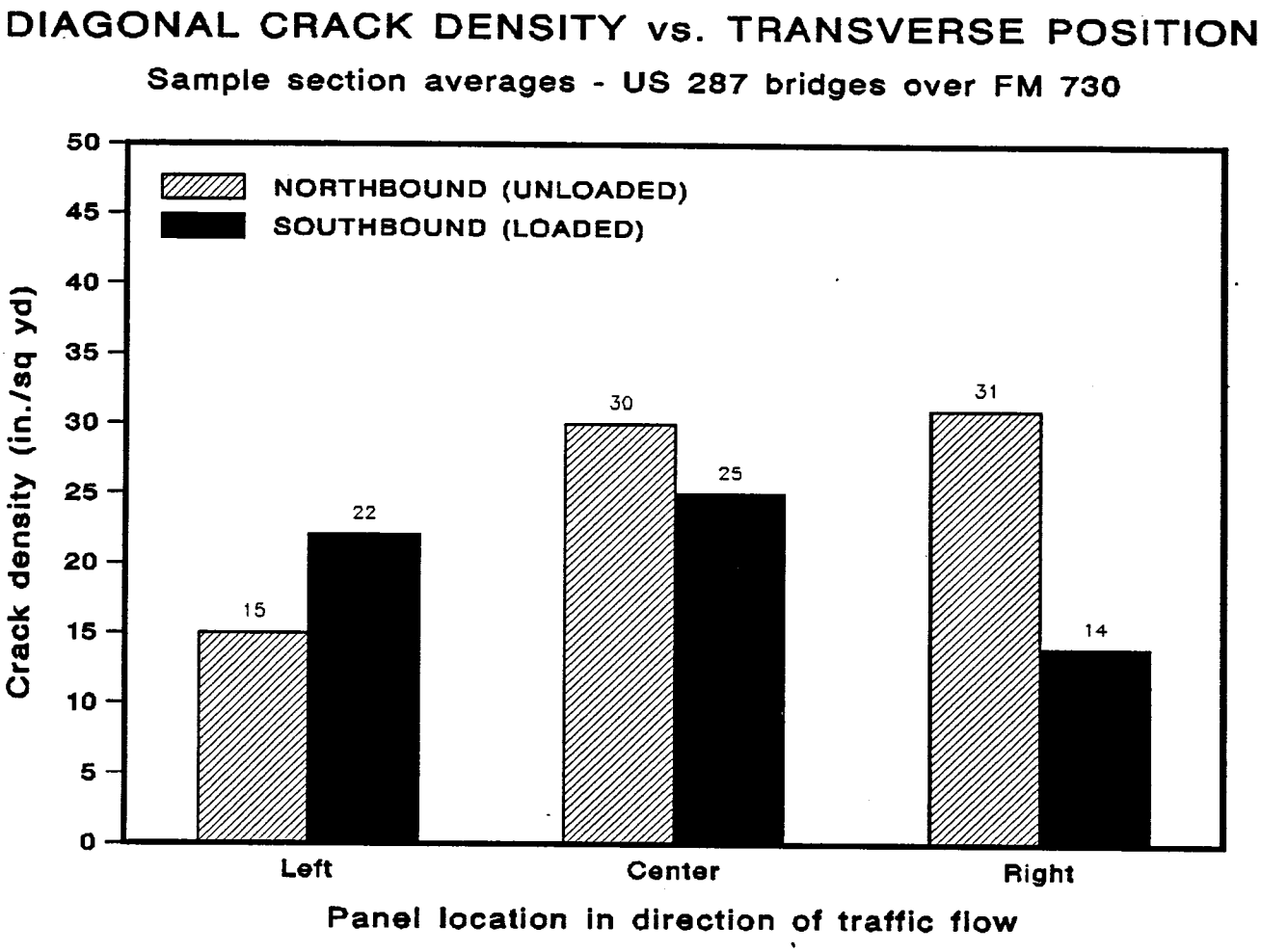

Fig. 14.--Transverse distribution of diagonal crack density

in the unloaded bridge. In the loaded bridge the center panel always exhibited more cracking than the right panel. The right panel always exhibited more cracking than the left panel in the unloaded bridge.

Longitudinal Cracking

The loaded bridge always exhibited more longitudinal cracking (Fig. 15) than the unloaded bridge in the left and right panels. The left panel exhibited an average of 68% more cracking, and the right panel exhibited an average of 23% more cracking. The center panel exhibited more cracking in the loaded bridge by an average of 11%.

When directly comparing the panels to each other in both the loaded and unloaded bridges, the center panel always exhibited more cracking than the left panel. The center panel exhibited less cracking than the right panel in both bridges, and the right panel always exhibited more cracking than the left panel in both bridges.

Transverse Cracking

The loaded bridge always exhibited more transverse cracking (Fig. 16) than the unloaded bridge in the left panel by an average of 71%. The center and right panels usually exhibited more cracking in the loaded bridge by an average of 8% more cracking in the center panel and an average of 11% more cracking in the right panel.

When directly comparing the panels to each other in both the loaded and unloaded bridges, the center panel exhibited more cracking than the left and right panels in both bridges. The right panel always exhibited more cracking than the left panel in the unloaded bridge. In the loaded bridge there was very little difference between the right and left panels.

Comparisons

The difference in crack density between the loaded and unloaded

bridges is far greater on the left side of the bridge deck than for the center or right side. The center and right panel differences between the loaded and unloaded spans are very similar. This relationship was common to the total, transverse and longitudinal crack densities, with the smallest difference between the panels occurring in the longitudinal cracking. Even in the longitudinal cracking, there is a difference in cracking at least three times greater in the left side than in the right or center. In the diagonal cracking, only the left side exhibited substantially more cracking in the loaded bridge. For the center and right side, more cracking occurred in the unloaded bridge. This observation does not apply to the patterns exhibited in the total cracking though, because cracking tends to be predominantly transverse and longitudinal.

In comparing the panels to each other, some other trends became evident. The center panel always cracked more than the left, and the percent difference in cracking was always far greater for the unloaded bridge. This pattern was repeated for each type of cracking.

In both structures the center panel was cracked more than the right for total and transverse cracking, there being similar differences for both bridges. Upon examination of the longitudinal cracking, the center panel was cracked less than the right one with the differences again being similar for both bridges. For diagonal cracking on the unloaded bridge, there was very little difference between the center and right panels; while for the loaded bridge there was far more cracking in the center than in the right panel.

In the comparison of the right and left panels to each other in both structures, more cracking occurred in the right panel except for diagonal cracking in the loaded bridge. The difference between the left and right panels was greater for total, transverse and longitudinal cracking in the unloaded bridge. In the loaded bridge there was little difference in transverse cracking between the right and left sides. For diagonal cracking, there was also far more difference between the right and left panels in the unloaded bridge than in the loaded bridge. However, in the loaded bridge more cracking

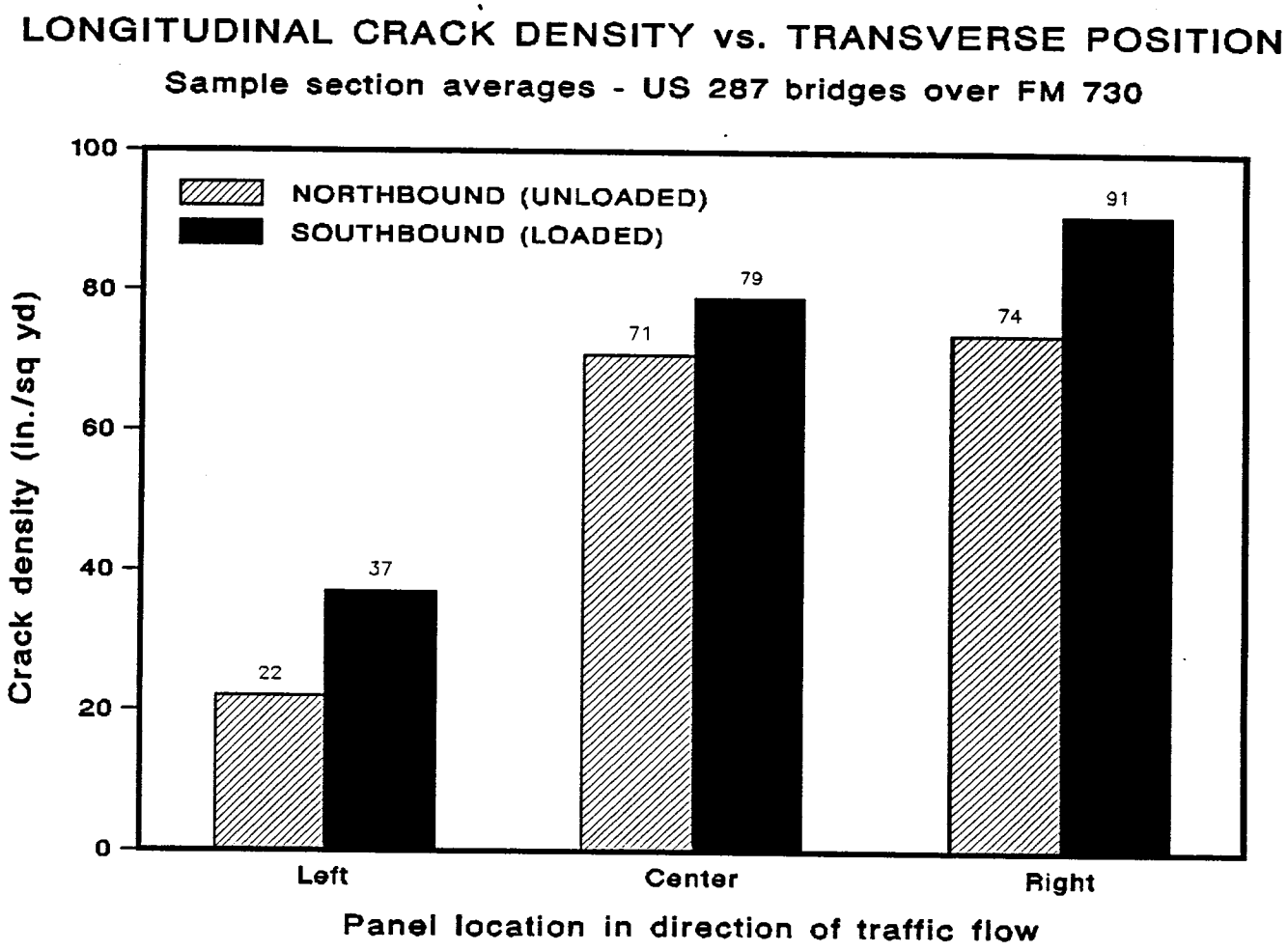

Fig. 15.--Transverse distribution of longitudinal crack density

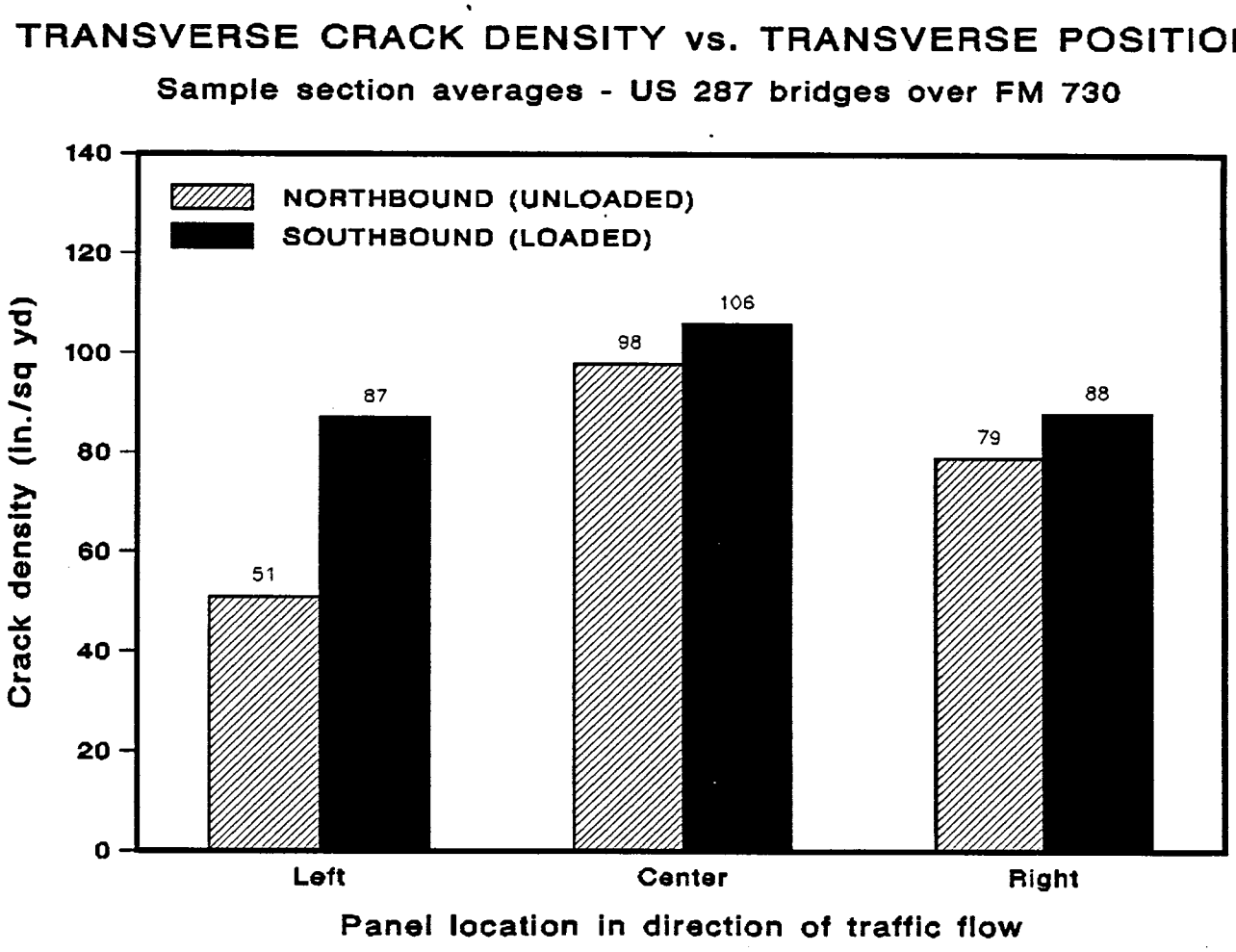

Fig. 16.--Transverse distribution of transverse crack density

occurred in the right panel, while in the unloaded bridge, more cracking was found in the left panel.

Overall, across the transverse section the loaded bridge consistently exhibits more cracking. In addition, whenever a comparison is made between panels in the loaded and unloaded bridges, the differences in the amount of cracking are normally either larger in the unloaded bridge or very similar to the panels in the unloaded bridge.

TRAFFIC EVALUATION

In an attempt to quantify the traffic is causing the observed damage to these bridges, the axle, tandem and gross weight distributions over these bridges were evaluated from data obtained from portable weigh-in-motion site N-20. Because of the presence of a high fraction of aggregate haulers, the traffic patterns on the US 287 bridges indicated a considerable difference between the northbound and southbound traffic. From brief traffic counts, it was evident that there was considerable truck traffic over the bridge with a good probability that much was heavy or overloaded. Five brief traffic counts produced truck counts between 96 and 216 trucks per hour.

Evaluation of the weight data for axle, tandem and gross vehicle weights confirmed that in the southbound traffic a significantly greater percentage of the vehicles contained heavier loads than in the northbound traffic. Data for 2493 trucks was collected from site N-20 near Decatur over 22 consecutive hours in March, 1987. If the total truck count is compared to the estimated daily traffic over the bridges (ADT = 8000), then 31% of the traffic on the bridge is truck traffic.

Fig. 17 shows single axle data for the 11,950 truck single axles weighed during this time period contained a peak of about 39% for the northbound traffic between 6 and 8 kips. This was almost double the traffic at the same weight levels in the southbound bridge. A similar peak occurred with about 19% of the southbound traffic between 12 and 14 kips, almost three times more frequent than the corresponding loads

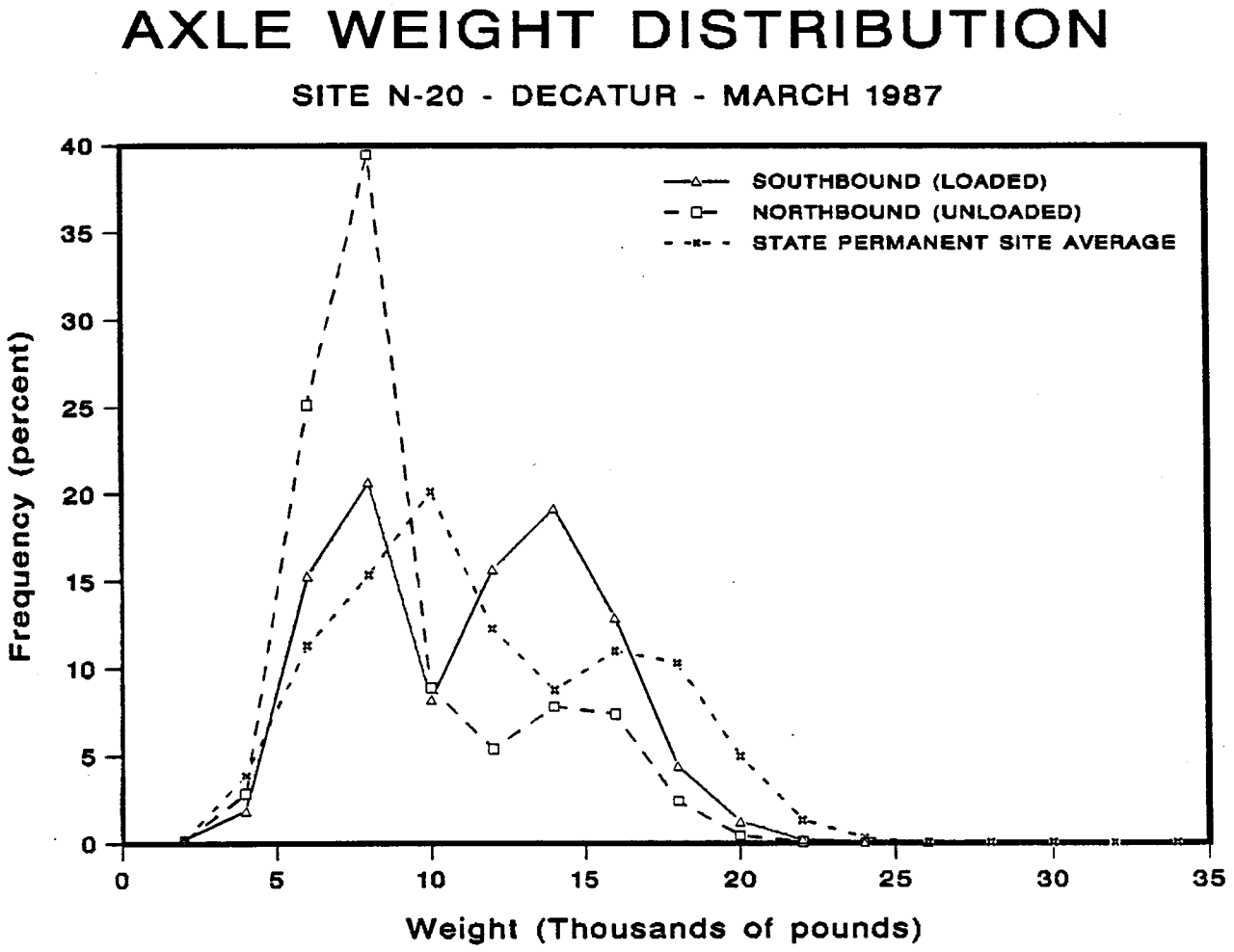

Fig. 17.--Observed frequency of single axles of various weights

experienced in the northbound bridge. The southbound traffic contained a greater maximum axle load of 26 kips; the maximum single axle load in the northbound bridge was 24 kips. The southbound bridge also had a record of 0.24% illegal single axle loads, and the northbound bridge sustained 0.07% overloaded single axles. For both bridges a total of 18 axles, 0.15% of all truck axles, were in excess of the maximum legal load of 20 kips per axle. The average single axle data obtained from the nine permanent WIM sites in Texas was next compared to the data from Decatur. This comparison revealed that while only about 0.15% of the truck single axles over the study bridges represented overloads, about 1.7% of the truck single axles measured elsewhere in the state represented overloads.

Tandem axle data (Fig. 18) for 4415 truck tandem axles measured revealed that between 10 and 13 kips per tandem, there was a peak of 34% for the northbound traffic, three times more frequently than the corresponding southbound traffic. Between 28 and 31 kips, northbound traffic again peaked with 8% of the traffic in that range, while between 25 and 28 kips the southbound traffic peaked at about 25%. The maximum tandem load southbound was 43 kips which was greater than the maximum northbound tandem weight of 40 kips. In Decatur a total of 43 tandem axles, 0.97% of all weighed, were in excess of the legal maximum of 34 kips. The state average tandem data from permanent WIM sites contained an average of 13.7% of the tandem loads above the legal limit.

Similar differences in the gross vehicle weight (Fig. 19) may also be observed, as 44% of the southbound traffic weighed between 55 to 65 kips, and 51% of the northbound traffic weighed between 25 and 35 kips. The maximum gross weight northbound was 80 kips. Only in the southbound traffic were many obvious overloads observed with a maximum load of 100 kips being measured. In Decatur 0.41% of the gross vehicle weights measured were in violation of the maximum legal load, which is less than the 7.33% of gross vehicle weights measured statewide which are overloads.

CORRELATION OF OBSERVED DAMAGE TO OBSERVED TRAFFIC LEVELS

The observed damage can be quantified in several ways, as has been shown. The level of the truck traffic can also be quantified in several ways. The problem of correlating the observed differences in various measures of deck damage to various measures of truck traffic is therefore not an easy problem, nor is it a problem with a unique solution. In spite of these qualifications, the following correlations of damage to traffic level are suggested:

Figure 20 shows the observed transverse, longitudinal and total deck cracking density as a function of the number of passages of vehicles exceeding certain specified gross vehicle weights during the life of the bridge. Since only two structures were examined, the data consists of a pair of points for each specified GVW. The same damage differential is correlated to three measures of vehicle weight--vehicles exceeding 40, 50 and 60 kips, with qualitatively similar results. It is not possible to say conclusively from this data whether the fraction of vehicles having GVWs greater than 40 kips or just those having GVWs greater than 60 kips are primarily responsible for the observed increase in deck damage.

Figure 21 correlates the observed deck damage to the different levels of single axle loads experienced by the two structures. Again, it is not possible to say whether the increase in the number of single axles carrying more than 18 kips is more or less responsible for the observed damage than axles of other weights. The loaded structure carried a heavier spectrum of single axles than the control structure, and a heavier spectrum of GVWs, and experienced a greater level of deck cracking. Further theoretical and analyatical work is required to definitively determine what fraction of the increased level of damage is due to illegal overloads and what fraction is due to increased numbers of heavier but still legal loads compared to the control

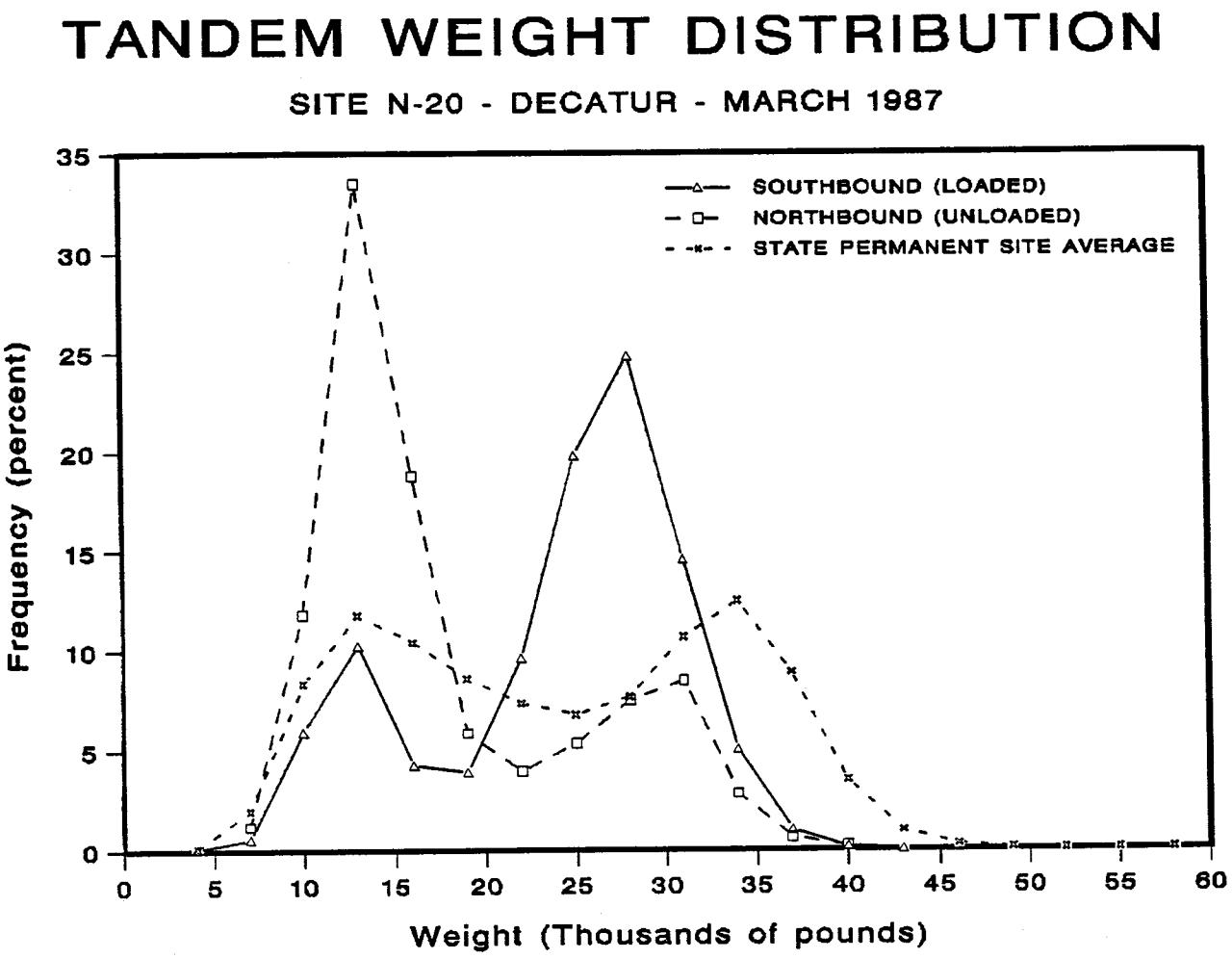

Fig. 18.--Observed frequency of tandem axles of various weights

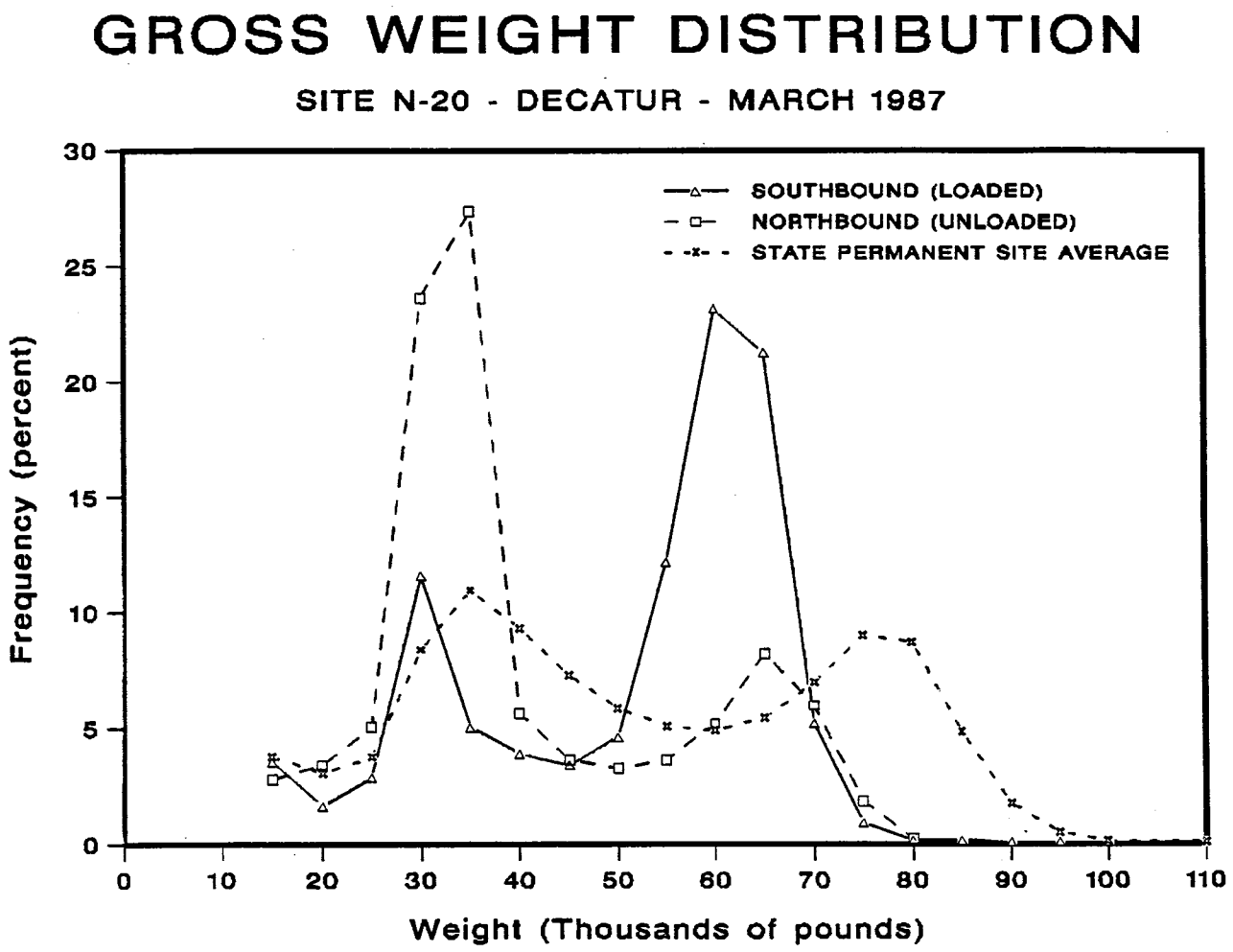

Fig. 19.--Observed frequency distribution of gross vehicle weights

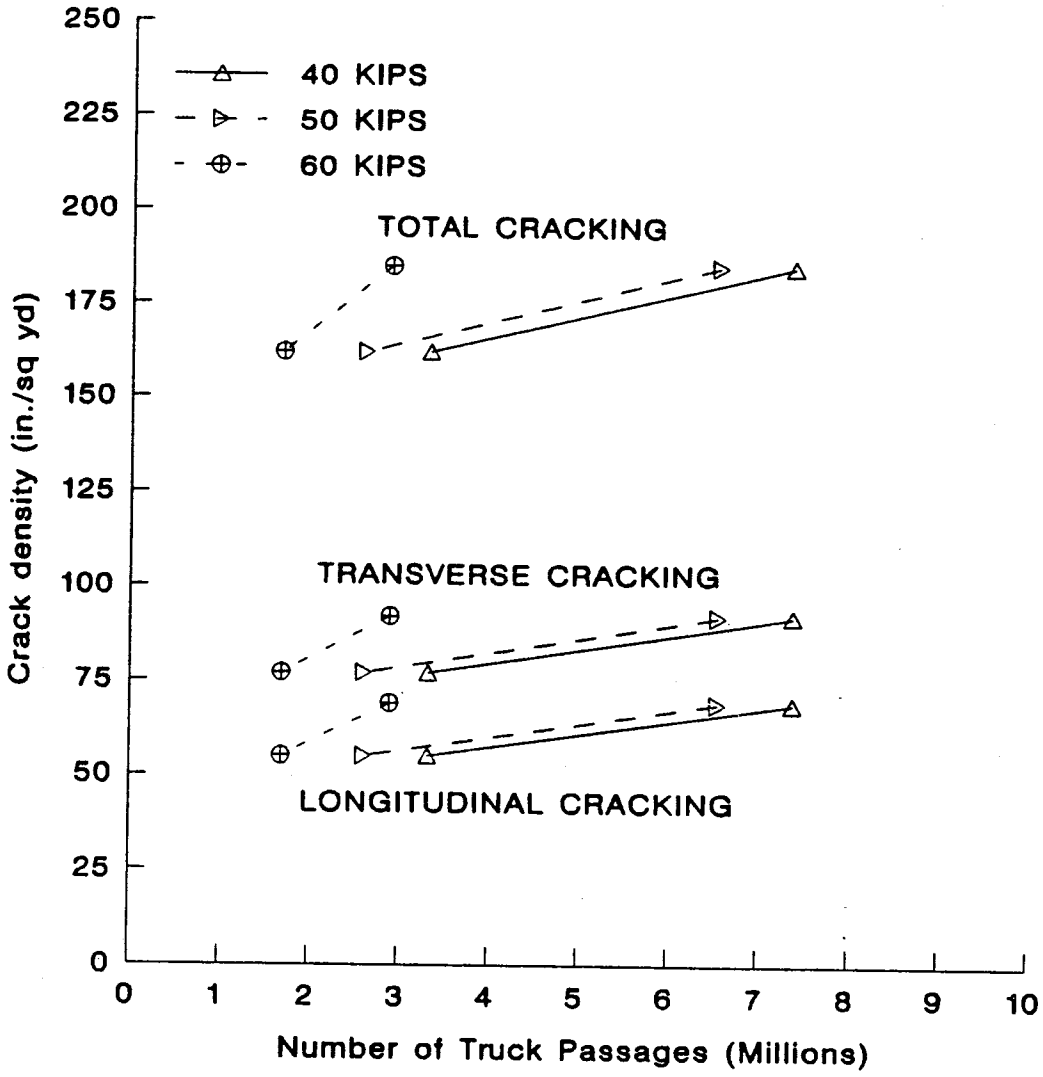

Fig. 20.--Average Deck Cracking Correlated to Total Number of Vehicles Exceeding Certain Specified GVW

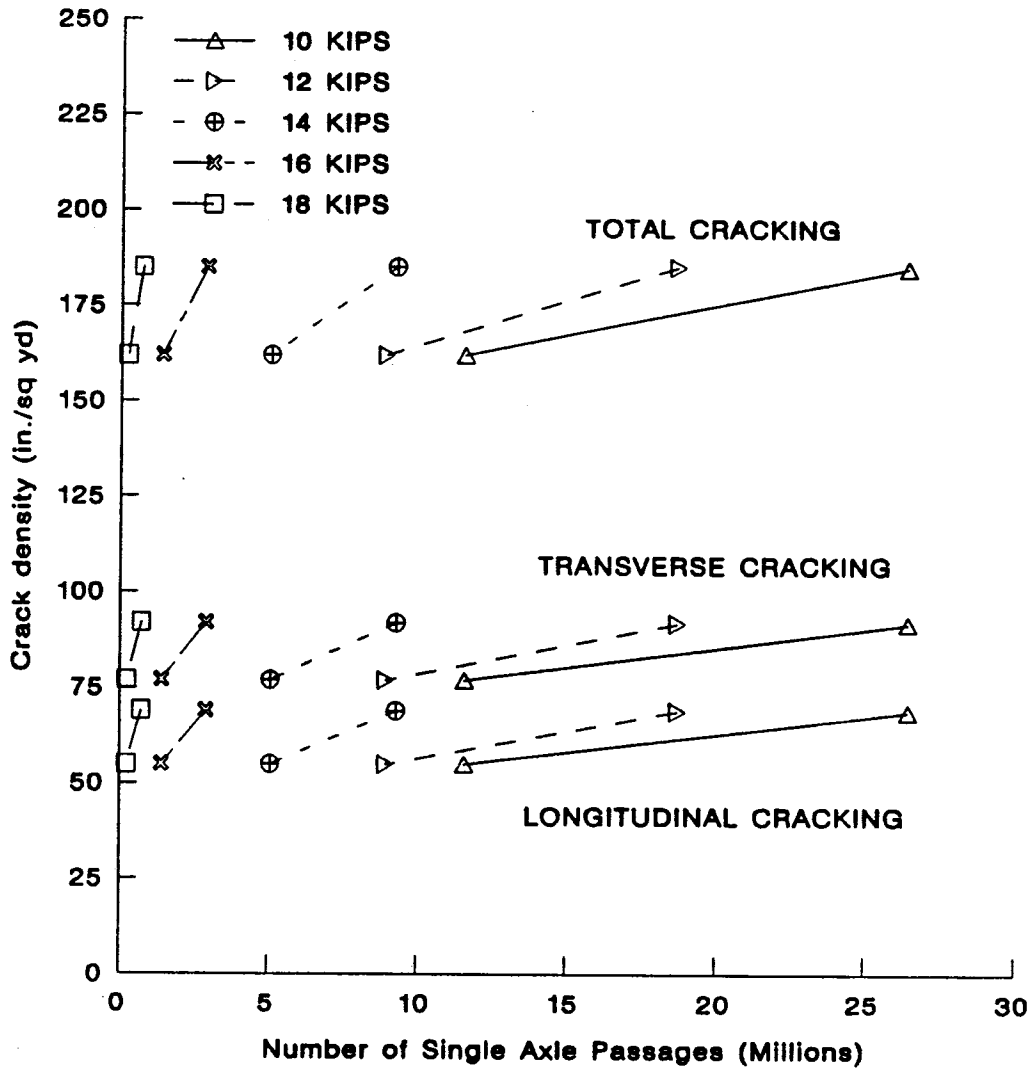

Fig. 21.--Average Deck Cracking Correlated to Total Number of Axles Exceeding Certain Specified Weights

FINITE ELEMENT MODELLING

MODEL OF SKEWED BRIDGE DECK

The objective of this portion of the study is to model the bridge deck of the FM 51 overpass in Decatur, Texas using the finite element program ABAQUS. Specifically, it is desired to determine cracking loads and crack orientations. The geometric layout of the bridge deck model is shown in Figs. 22, 23, and 24. The deck is supported by 2 abutments and 2 bents, and carries two lanes of one-way traffic. The curbs on the actual structure are neglected in the model.

Table 3. FM 51 Bridge Deck Data

Span: 154'-0"
Width: 29'-2"
Skew: 30^{0} right forward skew
2-way slab:
Thickness 6 1/2"
Steel Reinforcement:
Longitudinal : No.4 @ 6" Top and Bottom
2 1/2" Cover
Transverse : No.5 @ 1'-1" Top and Bottom
1 1/2" Cover
Dead Loads
Concrete: 150 pcf
Steel Stringers: 108 lb/ft
Truck loading
Assumed Design Load: HS 20, 3 Axles
Axle Spacing: 14'-0"
Axle Length: 6'-0"
Initial Values of Wheel Loads:
Front Wheels: 4000 lb/wheel

Rear Wheels: 16000 lb/wheel

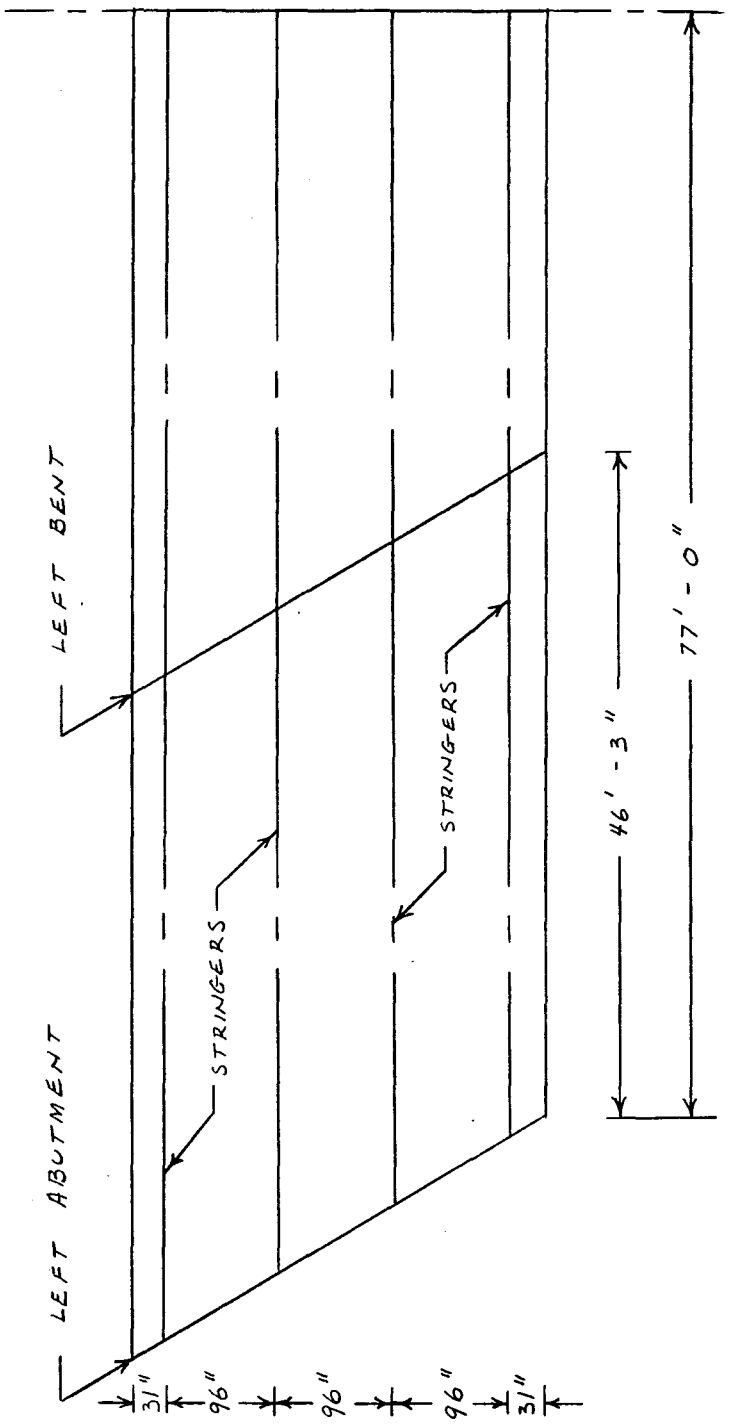

Fig. 22.--South portion of modelled bridge deck

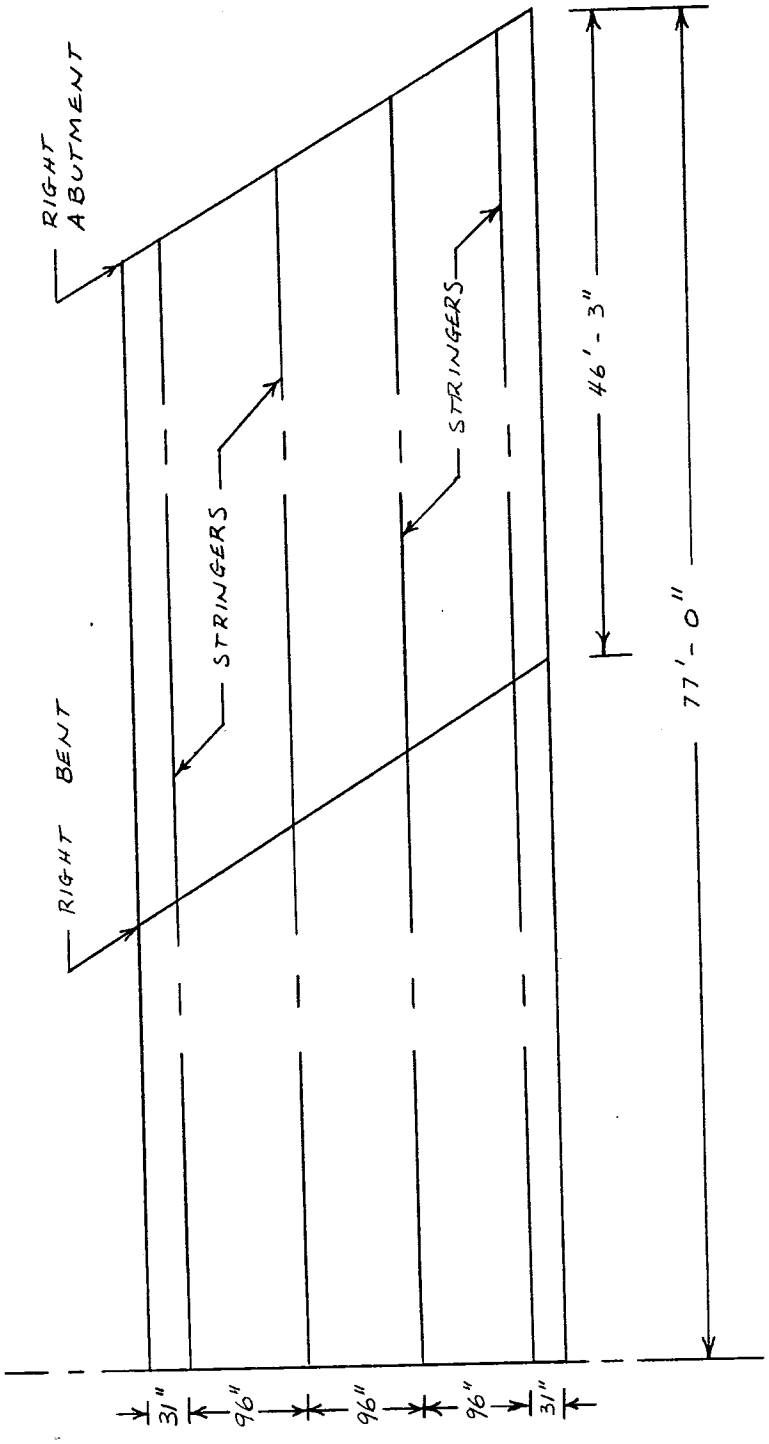

Fig. 23.--North portion of modelled bridge deck

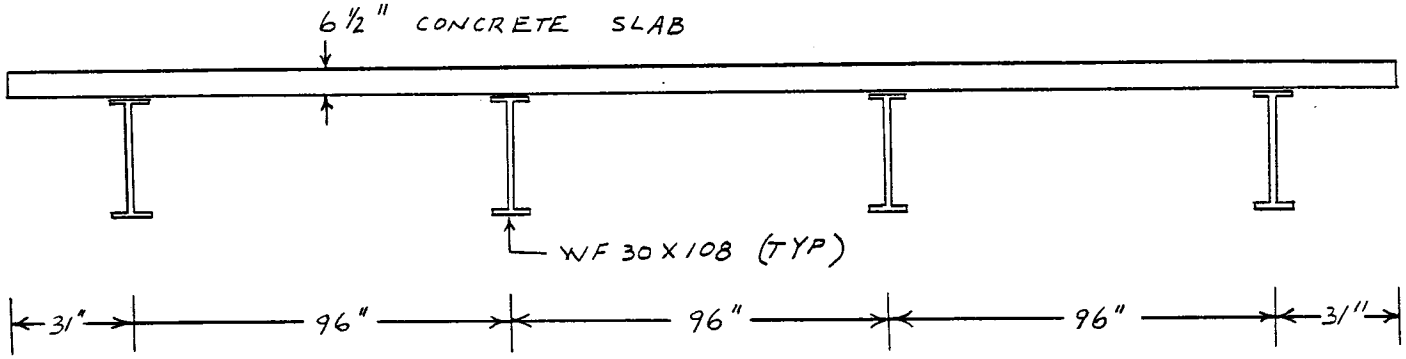

Fig. 24.--Idealized cross section of modelled structure

Fig. 25 shows the truck locations investigated. This loading was chosen to allow study of cracking loads above the interior bents and on the lower surface of the end span slab in positive moment regions.

Geometric Modelling

The entire bridge deck is modelled using a 46 x 11 mesh of 4-node shell elements. The 2 exterior longitudinal rows of elements are 31 in. wide and the 9 interior rows of elements are 32 in. wide. This scheme is used, because the distance from the edge of the slab to the first girder is 31 in. and the interior spacing is 96 in. Each element is approximately 40 in. long. No mesh convergence studies have been performed. Nine integration points are used through the thickness of the concrete, to model development of plasticity and failure through the thickness accurately. The 2-way reinforcement is modelled using the *REBAR option. Boundary conditions are restraint of displacements in the transverse and vertical directions at the left abutment, left bent, and right bent, and right abutment.

The 4 WF30X108 stringers are modelled by 2-noded beam elements. The stringers are connected to the slab using multiple point constraints (MPC). These MPC provide rigid links between beam and slab which cause displacements and rotations of corresponding points in the beam and slab to be compatible.

Material Properties

Table 4 shows the assumed material properties used in this analysis. Of particular interest is the method used by ABAQUS to model the interaction of the concrete and the rebar. After cracking, the stress in the concrete drops to zero as the rebar takes the load. The interaction is modelled by adding a "tension stiffening" effect. To employ this option, the fraction of remaining stress to stress at cracking (σ/σ_{cr}) and the absolute value of the direct strain minus the

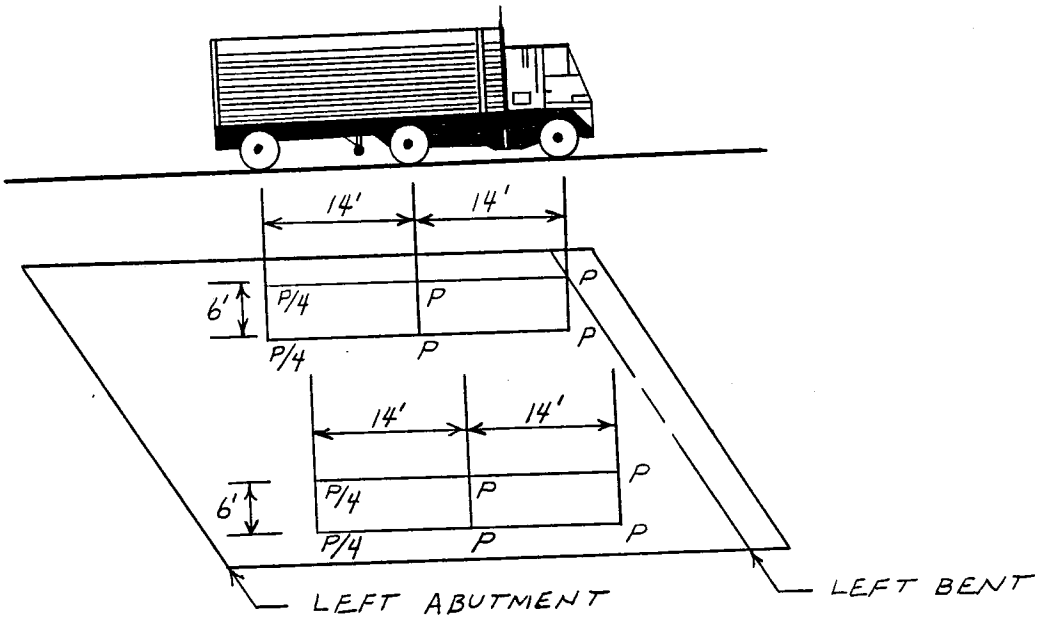

Fig. 25.--HS 20 truck positions investigated

direct strain at cracking are needed (ϵ-ϵ_{cr}). Fig. 26 defines the required parameters.

Table 4. Summary of Assumed Material Properties

Concrete Properties:
- Young's Modulus: 4×10^6 psi
- Poisson's Ratio: 0.18
- Pure Compression Values:
  - Yield Stress: 2670 psi
  - Failure Stress: 4640 psi
  - Plastic Strain at Failure: 1300×10^{-6} in./in.

Steel (rebar) Properties:
- Young's Modulus: 29×10^6 psi
- Poisson's Ratio: 0.29

Note that ϵ_{cr} is the strain at which all of the load is taken by the rebar and stress in the concrete is zero. Values assumed in this analysis are $\sigma/\sigma_{cr} = 0$ and $\epsilon - \epsilon_{cr} = 500 \times 10^{-6}$ in./in. If no tension stiffening is used, then the concrete is assumed to lose all its strength in the direction of the crack after cracking occurs.

Solution Control Parameters

To begin the analysis, front and rear axles are loaded to 4000 and 16000 lb , respectively. Next the loads are incrementally increased to 12000 and 48000 lb , respectively, to simulate overloads. The values of the tolerance measures for the solution for the equilibrium equations at each increment are PTOL = 2000 lb (point loads) and MTOL = 2500 lb-in. (moments). The PTOL value represents about 4% of the actual maximum load.

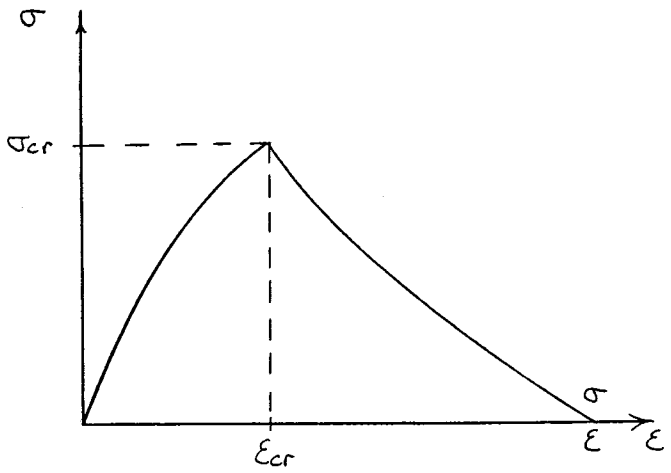

Fig. 26.--Stress-strain curve for concrete in uniaxial tension

Results and Discussion

Fig. 27 shows a summary of cracked elements, the corresponding cracking loads, and the direction cosines of the cracks relative to the local axes. Interestingly, cracking first occurs on the slab's top surface at the left bent. In this area, either the stress or the strain reached critical levels. The critical tensile stress is 417 psi, and the critical plastic strain component is 117×10^{-6} in./in.

The maximum vertical displacement in the slab occurred along the node line parallel to the bents near midspan of the loaded span. Vertical deflections along this node line range form 0.6 in. to 0.8 in. at design HS 20 loading.

As shown in Fig. 27, most of the top surface above the left bent was cracked at 150% of design load. Cracks are expected to initiate at the bottom surface under trucks when loads are increased to 200% or 300% of design load. However, loads of sufficient magnitude to cause cracking at the bottom surface were not obtained due to computational problems.

Under the design load, maximum stresses and strains on the top surfaces of the cracked elements reached about 420 psi and 200×10^{-6} in./in., respectively. Of the 10 elements which cracked, 9 cracked because their strains exceeded the cracking strain value.

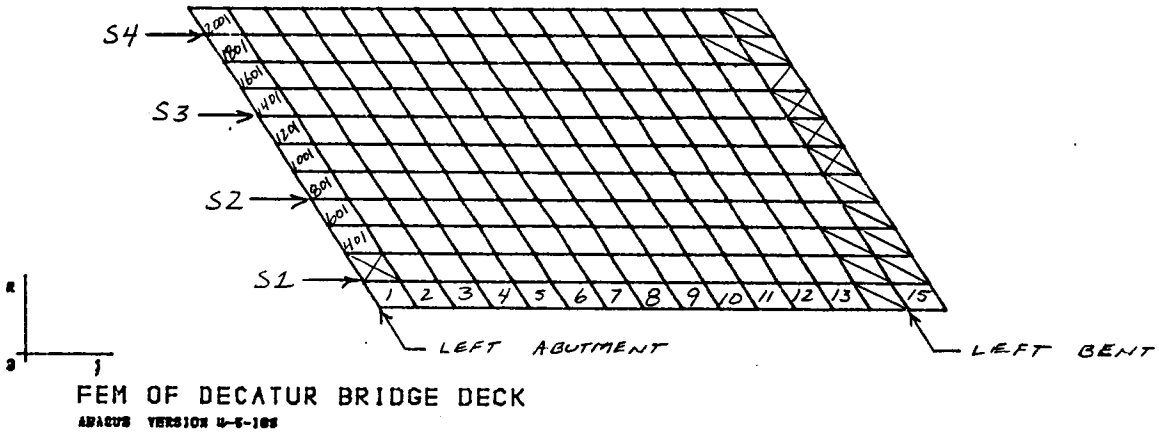

LEGEND :

ELEMENTS CRACKED AT DESIGN LOAD

ELEMENTS CRACKED AT 1.5 * DESIGN LOAD

Fig. 27.--Cracked elements on top surface of modelled slab

Table 5. Cracked Elements

Loads (lb)	Element	Top or Bot	X-Dir cos	Y-Dir cos
4000	14	T	0.995	0.103
16000	214	T	0.972	0.235
	215	T	0.972	0.234
	414	T	0.949	0.315
	415	T	0.959	0.283
	615	T	0.926	0.377
	815	T	0.971	0.240
	1814	T	0.923	0.385
	1815	T	0.887	0.461
	2015	T	1.00	0.003
4400	15	T	0.993	0.116
17500	201	T	0.261	-0.965
	614	T	0.948	0.318
	1615	T	0.934	0.359
5000	1015	T	0.929	0.369
20200	1215	T	0.912	0.411
5500	1415	T	0.992	0.129
22000	1814	T	0.385	-0.923
	1814	T	0.923	0.385

To illustrate the stresses on the slab caused by the design load, contours of largest principal stress were plotted. Integration points 1 and 9 are at the bottom and top surfaces of the slab, respectively. The contours of largest principal stress at the bottom surface are shown in Fig. 28. The highest principal stress contours at the top surface are shown in Fig. 29. The maximum principal stresses occur near the left bent. As a result, elements near the left bent cracked first.

Of more interest are the contours of plastic strain because most of the initial cracking was controlled by the tensile strain. At the bottom surface, tensile strain concentrations appear near the wheel loads, as shown in Fig. 30. These strain concentrations are not

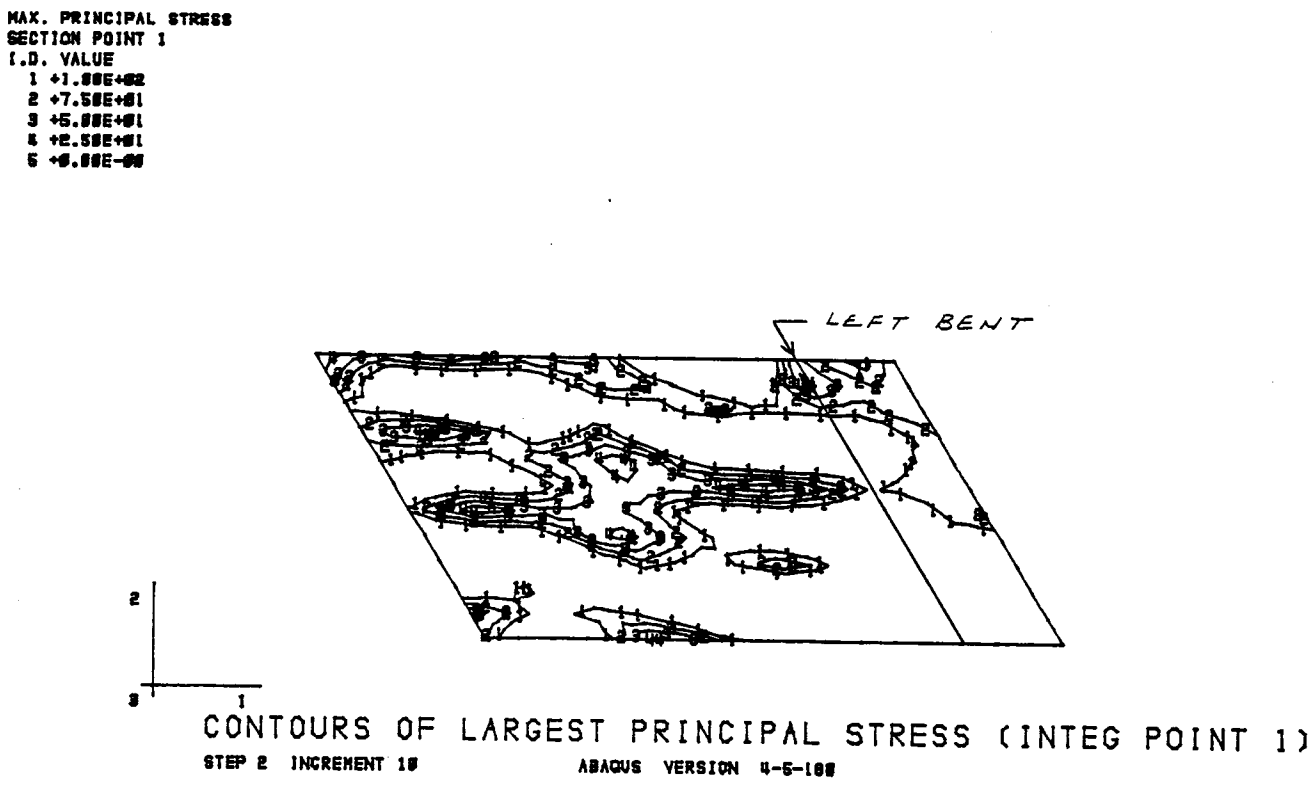

Fig. 28.--Contours of largest tensile principal stress on bottom surface of modelled slab

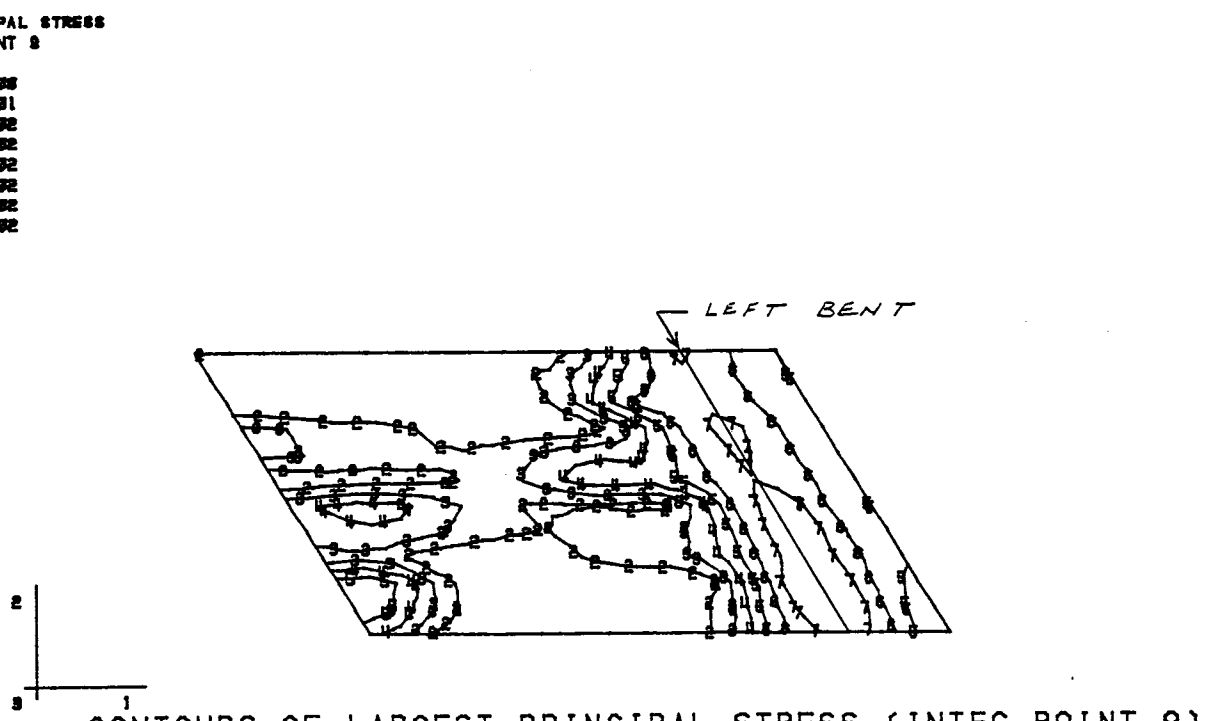

Fig. 29.--Contours of largest tensile principal stress on top surface of modelled slab

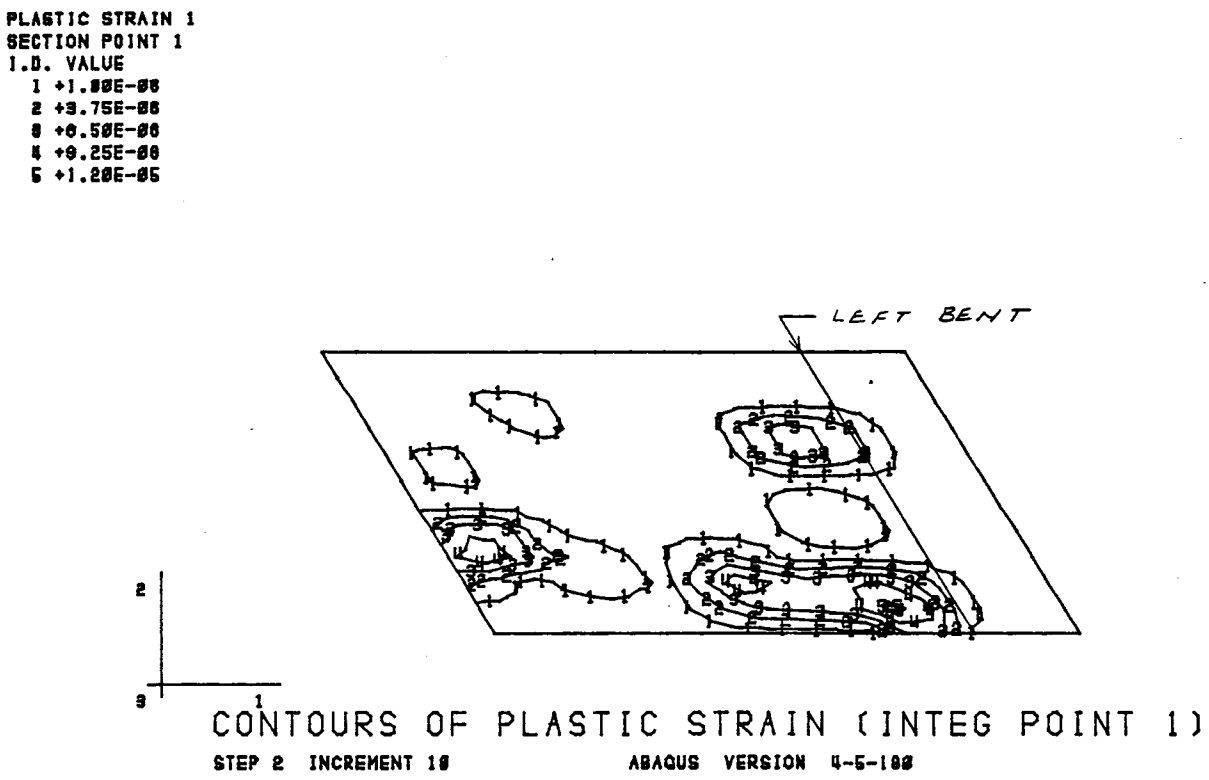

Fig. 30.--Contours of equivalent plastic strain on the bottom surface of the modelled slab

distributed evenly between the trucks, due to the lack of symmetry in the bridge. The plot pinpoints locations of high plastic strain at the design load. As the loads increase, these areas should crack first.

At the slab's top surface, tensile plastic strains are concentrated above the left bent as shown in Fig. 31. As expected, tensile strains only occur in this negative region. Like the contours on the bottom surface, these contours pinpoint the areas where cracking is expected.

Model of Prestressed Concrete Girder

The overload behavior of a prestressed concrete bridge girder reported in National Cooperative Highway Research Program Report No. 280 (NCHRP 280), entitled "Guidelines for Evaluation and Repair of Prestressed Concrete Bridge Members", has been modelled. This analysis utilized the ABAQUS finite element program running on a VAX 8800 mainframe computer. The test specimen described in NCHRP 280 consists of a simply supported 60-ft long type III AASHTO girder topped by a 6-1/2-in. thick, 90-in. wide slab as shown in Fig. 32. Sixteen 1/2-in., 270,000 psi prestressing cables are located in the bottom flange.

The girder and slab are modelled with 8-noded, linear displacement, continuum elements as shown in Fig. 33. Prestressing cables are smeared across the width of the element. Symmetric boundary conditions at midspan as well as along the centerline of the cross section are employed.

The prestressing cable material is modelled with a bilinear stress-strain curve as shown in Fig. 34. An elastic modulus of 29,500,000 psi is used up to 85 percent of ultimate strength, at which point the modulus is reduced to 1,000,000 psi.

The most challenging task of any FEM code for concrete structures is modelling the nonlinear concrete behavior. The behavior of concrete in crushing differs significantly from its cracking behavior. These material nonlinearities introduce geometric nonlinearities during which

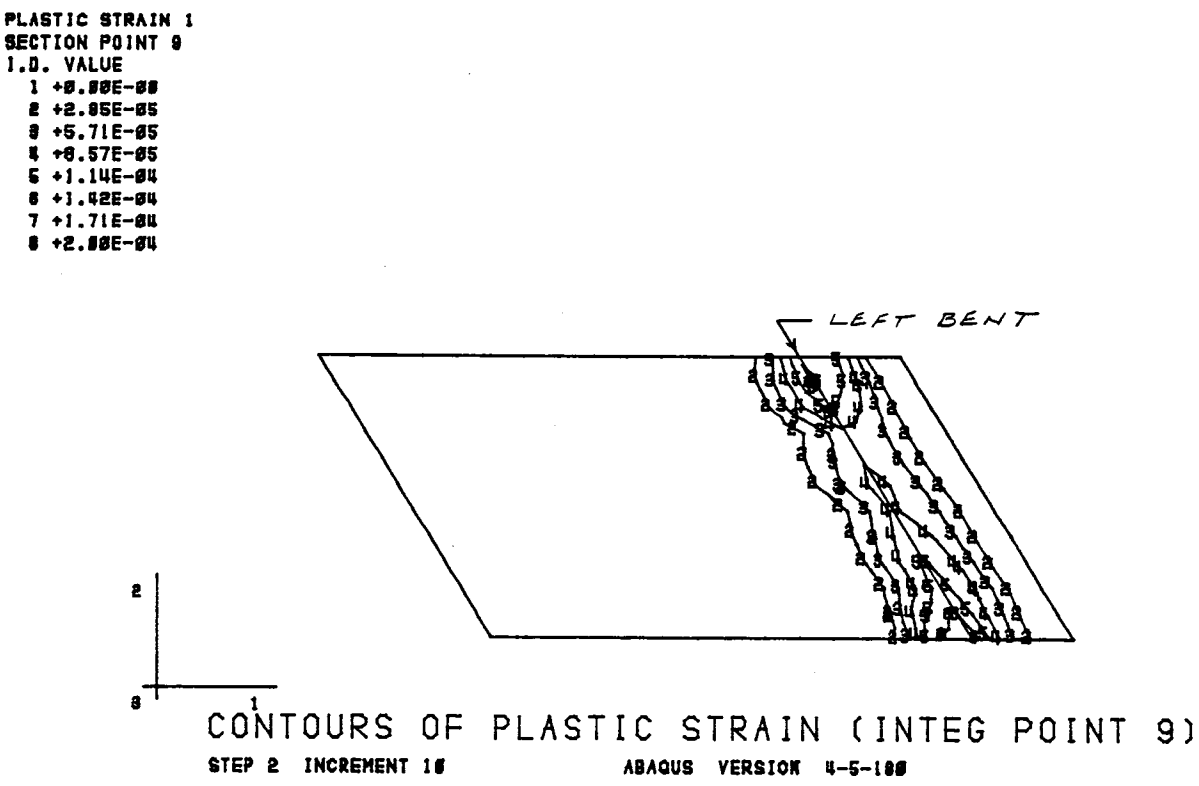

Fig. 31.--Contours of equivalent plastic strain on the top surface of the modelled slab

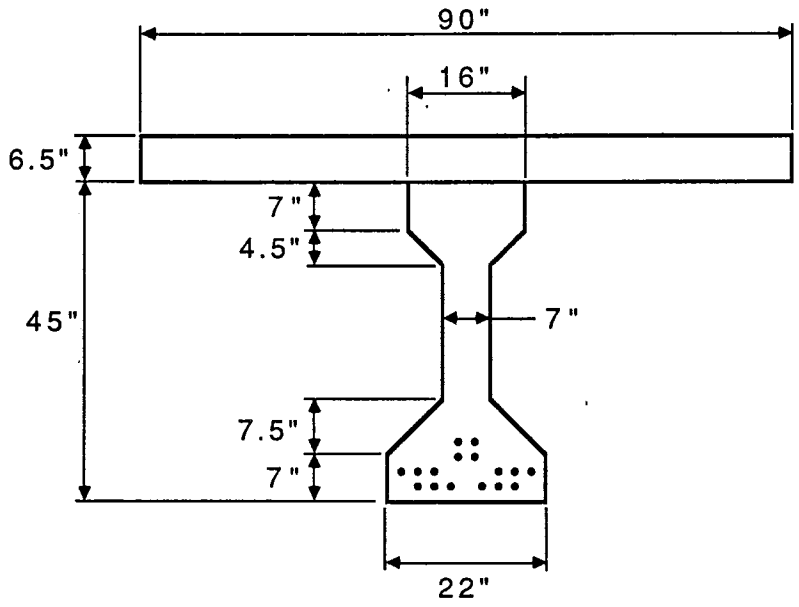

Fig. 32.--Cross-section dimensions of modelled girder

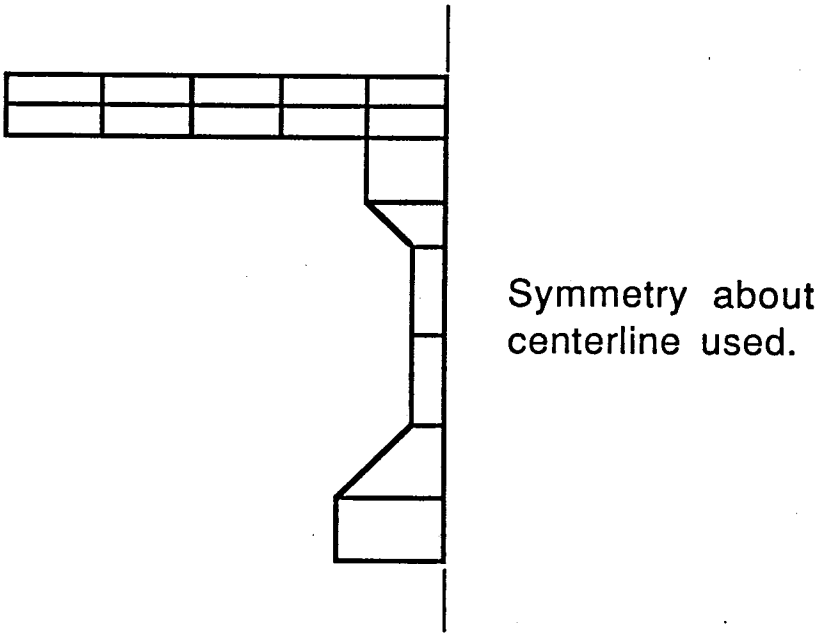

Fig. 33.--Finite element mesh used in model of girder

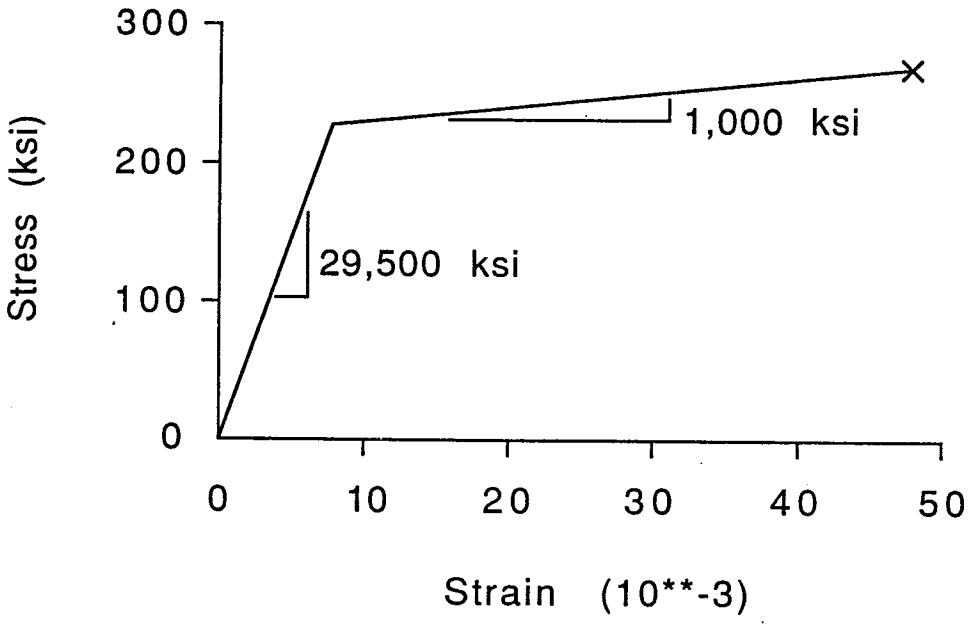

Fig. 34.--Stress-strain curve used for prestressing steel in modelled girder

stresses are being transferred to the steel cables.

The concrete stress-strain relationship in both compression and tension is defined by an initial yield point and a final ultimate strength and corresponding plastic strain. The curve is linear to yield, then utilizes a reduced modulus and isotropic hardening to reach the final stress and strain. Figs. 35 and 36 show the stress-strain curve for compression and tension, respectively, with the latter including the post-cracking strain softening behavior. The model uses a failure surface in biaxial stress space as shown in Fig. 37. The pure compression portion of the surface is parabolic, defined by uniaxial and biaxial compression strengths. The remaining portions of the surface are hyperbolic, defined by unaxial tension and compression strengths. Uniaxial compression and tension strengths are taken as 6030 psi and 300 psi, respectively. A biaxial compression strength of 7360 psi is used.

Initial Stress State

In practice, construction sequence of the girder-slab structure results in all dead load being carried by the girder, and the cured slab being essentially free of dead load stresses, except for stresses due to wearing surfaces, sidewalks, curbs and railings placed later. After extensive trial and error, no convenient method of duplicating this stress state with ABAQUS was found; all attempts induced stresses in the slab. Although the induced slab stresses are small, the resulting stress distribution in the girder is not desirable. For example, since the slab has some effective stiffness, the tensile stress in the bottom girder elements due to dead load is reduced, thus increasing the load required to initiate cracking. An analysis of this model is discussed later. Due to these difficulties, the slab elements were removed from the model. It is believed that the girder alone can be useful in studying the overload behavior predicted by ABAQUS.

Initially, the cables are prestressed to 150,000 psi and the girder elements subjected to gravity loads equal to the combined weight

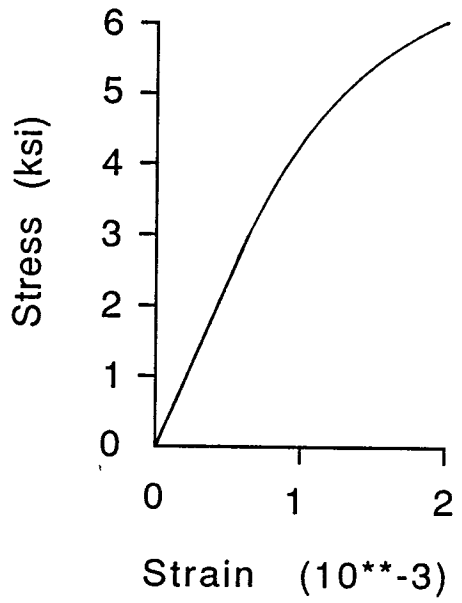

Fig. 35.--Compressive stress-strain curve used for concrete

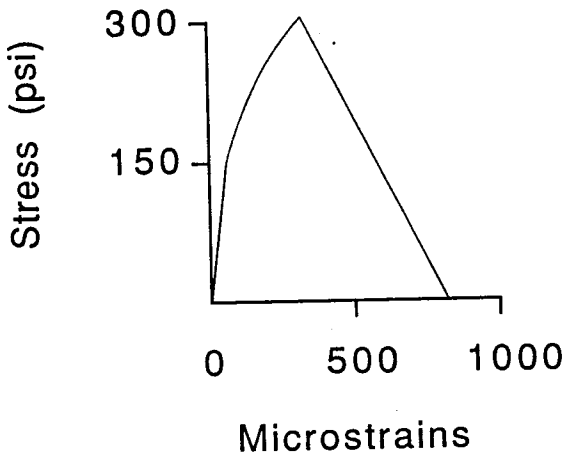

Fig. 36.--Tensile stress-strain curve used for concrete

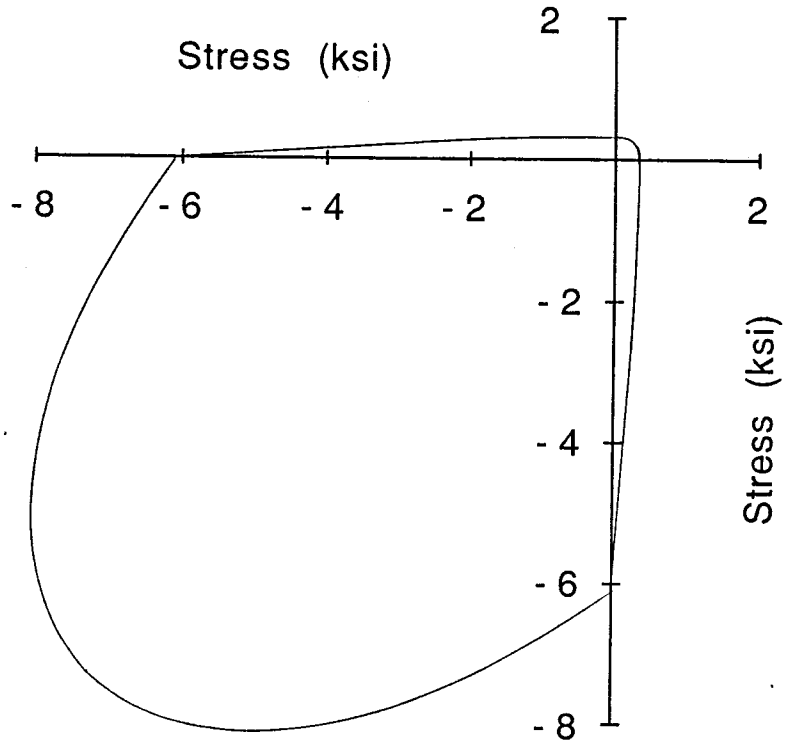

Fig. 37.--Biaxial stress failure surface used for concrete

of the slab and girder. This duplicates the initial stress state of the girder used in NCHRP 280.

Solution Control Parameters

Vertical loads are applied incrementally at midspan at the center of the cross section. The solution after each loading increment is obtained iteratively. Inherent in iterative solvers is the choice of convergence criteria. Although this criteria may be strict for linear analyses or the linear portion of nonlinear analyses, when significant nonlinearities occur, these criteria should be somewhat relaxed. The redistribution of stresses from cracked elements into prestressing cables, which already have large stresses, cause large nodal loads and can result in large force imbalances. Convergence criteria of no less than 5 percent of expected nodal loads is used. Further, ABAQUS provides a means for continuing the analysis even if the convergence criteria has not been satisfied.

The ABAQUS concrete model exhibits convergence problems. The existence of the problems is documented in the literature, and others have developed material subroutines with superior convergence characteristics. The ABAQUS concrete model has also been improved recently, but the improved version was unavailable for this study. For this reason, loose convergence criteria and nonconvergent continuation were utilized.

Discussion

The results of these analyses are presented in Fig. 38, along with test data from NCHRP 280. The NCHRP 280 data indicates an initial cracking load of about 55,000 pounds. Progressive damage causes deteriorating stiffness up to the final test load of 90,400 pounds. An elastic component of deflection is recovered immediately upon unloading. The remainder of the unloading curve generally echos the loading curve, with a residual deformation of about 0.1 in. present

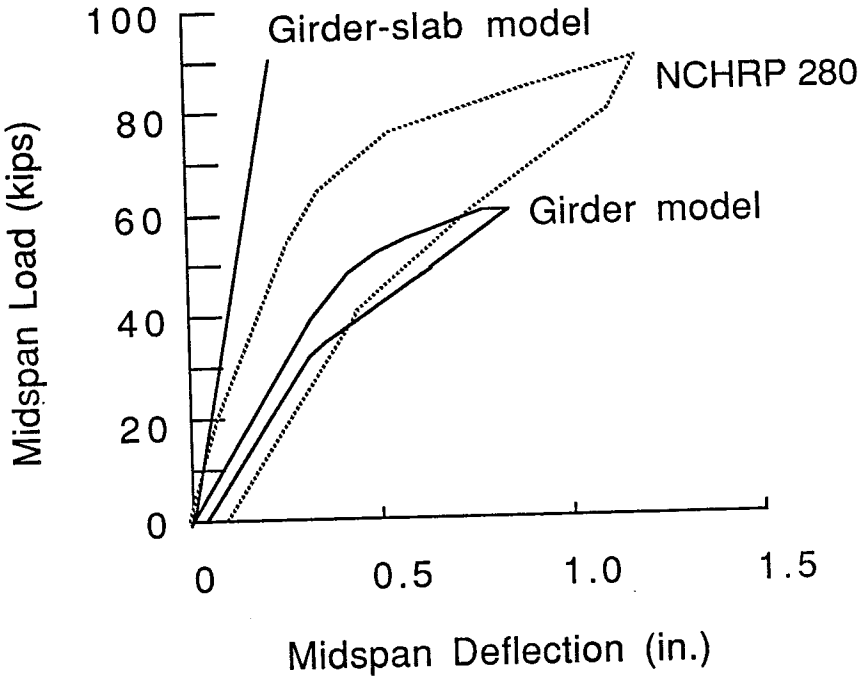

Fig. 38.--Simulated and measured girder response

after complete unloading.

An analysis was performed on the combined girder-slab model; however, as discussed earlier, attempts to duplicate the actual initial stress state of this structure were unsuccessful. All attempts induced net compressive stresses in the slab due to prestress and dead load. This additional stiffness reduced the vertical deflection of the girder, thus reducing the tensile strain components in the bottom elements and increasing the load required to initiate cracking. As shown in Fig. 38, cracking was not initiated at a load of 90,000 pounds, and the analysis was discontinued.

The results of the girder model analysis, presented in Fig. 38, indicate that the girder exhibits less stiffness than the girder-slab structure, as expected. The predicted load-deflection curve is essentially linear to a load of 47,500 pounds, at which cracking is initiated. At this load, the tensile stress in the bottom elements at midspan is 260 psi. Subsequent to cracking, the model exhibits stiffness degradation to the final analysis load of 62,500 pounds.

The predicted unloading behavior is bilinear; first from 62,500 pounds to about 33,000 pounds, then to the totally unloaded state. The predicted residual deformation is about half of that shown in the NCHRP data.

Inspection of Fig. 38 indicates that the girder model predicts the load-deflection behavior better during loading than during unloading. This may be due to the accumulation of concrete particles in the cracked sections of the actual test girder. When the concrete cracks, small pieces of the girder are broken off and displaced. When the cracks begin to close during unloading, these peices become lodged within the section, thus increasing the residual deformation of the girder. This behavior is not modelled by the current ABAQUS concrete model.

Conclusions

The girder model approximates the loading portion of the NCHRP 280 girder and slab load-deflection curve. Particularly encouraging is the

prediction of the rate of stiffness degradation due to progressive cracking through the cross section.

The unloading portion of the curve is not as well predicted by the current model. This may be due to concrete particle accumulation within the cracked sections of the actual girder.

Further work will require a concrete model which better predicts material behavior during crack closure. The revised ABAQUS model may fulfill this requirement. Concrete models for use with ABAQUS have also been developed by others. Lastly, a procedure must be devised for including the slab elements in the model while maintaining the initial stress state of the overall structure.

CONCLUSIONS AND RECOMMENDATIONS

Based on the findings of the field study, the following conclusions and recommendations are offered:

1. Heavy truck traffic, including a measureable fraction of illegally heavy traffic and a substantial average daily truck traffic (ADTT) is carried by the routes studied, US 287 northwest of Ft. Worth, Texas. The performance of the numerous bridges along that route can be used to better understand the influence of heavy truck traffic on highway bridge structures. In particular, the biased traffic flow--southbound traffic containing heavily loaded aggregate haulers and northbound traffic containing empty trucks returning to the quarry--allows comparison of performance of several identical pairs of structures subject to identical average daily traffic (ADT) and ADTT counts, but to ADTTs having different weight spectrums. Any observed difference in structural behavior may logically be attributed primarily to the effect of heavier loads, and not to other factors such as environmental or material or structural differences.

2. Of the various bridge types examined, only the reinforced concrete decks on steel stringers were observed to exhibit different levels of structural damage corresponding to the two different loading spectrums. This result is not surprising, in view of the greater flexibility of the steel stringer construction. Furthermore, the only type of structural damage observed that appeared to be correlated to the loading spectrum was deck cracking. Fatigue cracking in the steel superstructures, particularly at connections of lateral bracing, was observed in both the heavier and lighter loaded structures, but primary interest was focused on concrete damage.

3. Because of the many ways to quantify both the extent of the increased deck damage and the increased level of the loadings, it is not possible to rationally correlate the extent of the increased damage to the increased load level. Several possible correlations are suggested, however. Figures 20 and 21 illustrate how the increased deck damage, measured by three norms, density of longitudinal cracking, transverse cracking and total cracking, correlates to each of several measures of the increased loading, including the number of passages of both single axles and GVWs exceeding certain specified weights. It seems likely that the observed deck damage should be correlated to axle or tandem axle weight, rather than GVW. Support for this is seen in the results of the finite element analysis of the deck, from which it is apparent that the concentrated loads of the individual wheels and the reactions of the pile caps induce local regions of high stress and strain in the concrete deck. While the load positions analysed

were chosen for their severity, the passage of the loads across the span will load other portions of the lower surface in a similar manner.

4. Some deck cracking was observed in all regions of the end spans examined. Approximately one-half of the cracking was observed to be transverse cracking, and more than one-third was observed to be longitudinal. The greatest increased levels of damage are observed in the left panel, that is in the left third of the two-lane deck. In the center and right panels of the regions studied, the difference in damage levels in the heavily loaded and control decks was not nearly so great as in the left panels. Since the right lane is thought to carry the majority of the truck traffic on this route, this observation is interpreted as follows: The increased level of truck traffic (due to the intense aggregate hauling industry) increases the observed damage, but increases it more under the less heavily travelled left lane than under the right lane; increased truck weights appear to cause more widespread damage (deck cracking), rather than more intensive cracking. It is possible that the observed levels of crack density represent some sort of plateau, with additional damage being primarily in the form of deepening or working of existing cracks rather than in increasing the crack density.

5. No significant variation in damage or increase in damage was noted to depend on longitudinal position in the span. Some slight variations observed along longitudinal lines (Fig. 9-12) are considered inconclusive.

It is recommended that further research be directed towards quantifying the correlation between vehicle or axle weights and rate of progressive damage. The observed different levels of damage on the bridge decks studied are clearly attributable to different levels of truck traffic, however it is not possible to say whether the damage is due primarily to the small fraction of illegally overweight axles or tandems, or to the greater numbers of heavily loaded but legal vehicles. Repetitive load tests of reinforced concrete bridge deck specimens appear to be the most feasible approach to the solution of this problem, and only limited test data is presently available in the literature.

It is also apparent that additional study of the costs of increased progressive damage rates is needed. Such data may likely be subjective, from experienced judgement of what levels of fracture density require maintenance.

REFERENCES

Barsom, J. M., "Fatigue Behavior of Weathered Steel Components," TRAFFIC RESEARCH RECORD 950, 2nd BRIDGE ENGINEERING CONFERENCE, Vol. II, 1984, p. 2.

Beal, David, "Load Capacity of Concrete Bridge Decks," TRR No. 871, 1982, p. 70-72.

Beal, David, "Load Capacity of Concrete Bridge Decks," JOURNAL OF THE STRUCTURAL DIVISION, ASCE, Vol. 108, No. ST4, April 1982, p. 814-832.

Boley, Graham and Higginbotham, "Pier Stabilization on Dooker's Hollow Bridge," PROCEEDINGS: FIRST INTERNATIONAL BRIDGE CONFERENCE, June 1984, p. 113.

Cervenka, Kenneth J. and Walton, C. Michael, "Traffic Load Forecasting in Texas," Center for Transportation Research Report 352-1F, 1984.

Cope, R. J., "Flexural Shear Failure of Reinforced Concrete Slab Bridges," PROCEEDINGS OF THE INSTITUTION OF CIVIL ENGINEERS, London, Part 2, December 1985, Vol. 79, p. 559-583.

Cornwell R., Stolleis, R. and Johnson, C. "Structural Evaluation of Bridges for Overload Conditions," Research Report 201-1F, Center for Transportation Research, University of Texas at Austin, August, 1983.

Csagoly, Hoolowka and Dorton, "The True Behavior of Thin Concrete Bridge Slabs," BRIDGE ENGINEERING: VOLUME I - TRR No. 664, 1978, p. 173.

Darroch,, J. G. and Furr, Howard L., "Bridge Deck Condition Survey," Texas Transportation Institute Research Report 106-1F, Study 2-18-67-106, Texas Highway Department Cooperative Research with Department of Transportation, Federal Highway Administration, May 1970.

Davis, Stanley, "Case Histories of Scour Problems at Bridges," TRR No. 950, Vol. II, 1984, p. 149.

Dimillio, Albert, "Performance of Highway Bridge Abutments Supported by Spread Footings on Conpacted Fill (Final Report)," Report FHWA/RD-81/184.

Fisher, J. W., Mertz, D. R. and Zhang, K. "Steel Bridge Members Under Variable Amplitude Long-Life Fatigue Loading," NATIONAL COOPERATIVE HIGHWAY RESEARCH PROGRAM REPORT No. 267,

Transportation Research Board, National Research Council, Washington, D.C., December 1983.

Fisher, John W. and Mertz, Dennis R., "Fatigue and Fracture in Steel Bridges," Fritz Engineering Laboratory, PROCEEDINGS: FIRST INTERNATIONAL BRIDGE CONFERENCE, Engineer's Society of Western Pennsylvania, June 4,5,6, 1984, p. 10-20.

Fisher, John W. and Mertz, Dennis, "Fatigue Cracking in Longer Span Bridges," ANNALS OF THE NEW YORK ACADEMY OF SCIENCES, Vol. 352, New York, N.Y., 1980, p. 193-217.

Fisher, J. W., Pense, A. W., Slockbower, R. E. and Hausammann, H., "Retrofitting Fatigue Damaged Bridges," BRIDGE ENGINEERING: VOLUME I - TRR No. 664, 1978, p. 102-109.

Fisher, J. W., Yen, B. and Daniels, J. H., "Fatigue Damage in the Lehigh Canal Bridge from Displacement-Induced Secondary Stresses," TRR No. 607, 1976, p. 56-62.

Gamble, W. L., "Overload Behavior of One-Eigth Scale Three-Span Continuous Prestressed Concrete Bridge Girders," Report FHWA/IL/UI-182, March, 1980.

Hartley, G., Suter, G., Keller, H. and Marett, D., "Strength Evaluation of the Manotick Bridge Piers," STRENGTH EVALUATION OF EXISTING CONCRETE BRIDGES, American Concrete Institute, Detroit, 1985, p. 1-22.

Hill, J. J. and Shirole, A. M. "Economic and Performance Considerations for Short-Span Bridge Replacement Structures," TRR No. 950, Vol. I, 1984, p. 33-38.

Imbsen, R. A. and Vandershaf, D. E., "Thermal Effects in Concrete Bridge Superstructures," TRR No. 950, Vol II, 1984, p. 101.

Johnston, R., Day, R. and Glandt, D., "Bridge Rating and Analysis Structural System," Vol. I-III, Wyoming Highway Department, FHWA-RD-73-501, September 1973.

Jorgenson, James and Larson, Wayne, "Field Testing of a Reinforced Concrete Highway Bridge to Collapse," TRR No. 607, p. 66-71.

Kato, Takeaki and Goto, Yuji, "Effect of Water Infiltration of Penetrating Cracks on Deterioration of Bridge Deck Slabs," TRR No. 950, Vol. I, 1984, p. 202-208.

Kay, J. N. and Flint, R. C., "Heavy Vehicle Loading of Arch Structures of Corrugated Metal and Soil," TRR No. 878, 1982, p. 34-36.

Koob, Michael J., Hanson, John M. and Fisher, J. W.,

"Post-Construction Evaluation of the Fremont Bridge," TRR No. 950, Vol II, 1984, p. 131-140.

Kostem, Celal, "Assessment of Bridges for Overloads," National Bridge Conference Proceedings, Pittsburgh, Pennsylvania, June 1983, p. 188-195.

Kostem, Celal, "Overloading Behavior of Beam-Slab Type Highway Bridges," Report FHWA/PA/RD-71-12-8, Lehigh University, July 1977.

Kostem, Celal N., OVERLOADING OF HIGHWAY BRIDGES: A PARAMETRIC STUDY, Report FHWA/PA/RD-71-12-7, August 1976.

Kostem, Celal N., "Overloading of Highway Bridges - Initiation of Deck Damage," BRIDGE ENGINEERING: VOLUME I - TRR No. 664, 1978, p. 207-209.

Kostem, C. N., "Overloading of Prestressed Concrete I-Beam Highway Bridges (Final Report 1977-1983)," FHWA Report: FHWA/PA-84/015, January 1985.

Kostem, Celal, "Overloading of Steel Multigirder Bridges," TRR No. 950, Vol. I, 1984, p. 84-88.

Kostem, Celal, "Shear Punching of Bridge Decks," Report FHWA/PA/RD-71-12-4, January 1977.

Kostem, C. and Hall, J., "Inelastic Analysis of Steel Multigirder Highway Bridges," Report FHWA-PA-RD-77-1-1, August 1980.

Kostem Celal and Ruhl, Gregory, "User's Manual for Program BOVAC," Fritz Engineering Laboratory Report 434.1, Lehigh University, April 1982.

Leslie, William and Chamberlin, William, "Effects of Concrete Cover Depth and Absorption on Bridge Deck Deterioration," Report FHWA/NY/RR-88/75, Engineering Research and Development Bureau, New York Department of Transportation, State Campus, Albany, N.Y. 12232, February 1980.

Mancarti, Guy D., "Strengthening California's Bridges by Prestressing," TRR No. 950, SECOND BRIDGE ENGINEERING CONFERENCE, Vol. I, 1984, p. 184.

Maxwell, D. A., Chira-Chaula, T., Nassiri, H. and Mason, J. M., "Evaluation of the Texas Truck Weighing Program," Texas Transportation Institute Research Report 424-1F, 1986.

McClure, R., West, H., and Abdel-Halim, M. "Overload Testing of an Experimental Segmental Bridge," Pennsylvania Transportation Institute Report No. PTI-8211, Pennsylvania State University, July, 1982.

Okada, Kiyoshi, Okamura, Hirokazu, Sonada, Keiichiro, Shimada, Isao, "Cracking and Behavior of Bridge Deck RD Slabs," TRANSACTIONS OF THE JAPANESE SOCIETY OF CIVIL ENGINEERS, Vol. 14, Japan Society of Civil Engineers, March 1984, p. 60-61.

Okada, K., Okamura, H. and Sonoda, K. "Fatigue Failure Mechanism of Reinforced Concrete Bridge Deck Slabs," BRIDGE ENGINEERING: VOLUME I - TRR No. 664, 1978, p. 136.

Peng, S. C., "A Pragmatic Approach in Rating Highway Bridges," TRR 950, Vol. 1, 1984, p. 53-59.

Peterson, William and Kostem, Celal, "The Inelastic Analysis of Beam-Slab Highway Bridge Superstructures," Fritz Engineering Laboratory Report 378 B.5, Lehigh University, Bethlehem, Pennsylvania, March 1975.

"Rehabilitation and Replacement of Bridges on Secondary Highways and Local Roads," NATIONAL COOPERATIVE HIGHWAY RESEARCH PROGRAM REPORT No. 243, Transportation Research Board, December 1981.

Seible, Freider, "Nonlinear Analysis and Ultimate Strength of Multi-Cell Reinforced Concrete Box Girder Bridges," Report No. UCB/SESM-82/02, University of California, Berkeley, California, February, 1982.

THE AASHO ROAD TEST, Proceedings of a Conference Held May 16-18, 1962, St. Louis, Missouri, Highway Research Board, Special Report 73, 1962.

Tilly, G. P., "Fatigue Problems in Highway Bridges," Transport and Road Research Laboratory, TRR No. 664, 1978, p. 93-101.

"Tolerable Movement Criteria for Highway Bridges - Volume I," United States Department of Transportation, Report No. FHWA/RD-81/162, September 1982.

Transport and Road Research Lab, SUPPLEMENTARY-740 - SERVICE PERFORMANCE OF FIFTY BURIED-TYPE BRIDGE EXPANSION JOINTS (FINAL REPORT), 1982.

Wallace, M., "Studies of Skewed Concrete Box-Girder Bridges," TRR No. 607. 1976, p. 50-55.

Wheeler, J. E., "Discussion-Bridge Loading: Research Needed," JOURNAL OF STRUCTURAL ENGINEERING, ASCE, Vol. 110, No. 1, January 1984, p. 190.

White, K. R. and Minor, J., "Evaluation of Bridge Overloads," TRANSPORTATION ENGINEERING JOURNAL, January 1979, Vol. 105, p. 15-21.